Fakultät für Medizin

Institut für Molekulare Immunologie

IKKα links autophagy, ER stress and caspase-12 function in a mouse model of acute colitis

Michaela Alexandra Diamanti

Vollständiger Abdruck der von der Fakultät für Medizin der Technischen Universität München zur Erlangung des akademischen Grades eines

Doctor of Philosophy (Ph.D.)

genehmigten Dissertation

Vorsitzende: Univ.-Prof. Dr. Dr. St. Engelhardt

Betreuer: Univ.-Prof. Dr. F. R. Greten

Prüfer der Dissertation:

1. Univ.-Prof. Dr. J. Ruland

2. Univ.-Prof. Dr. M. Heikenwälder

Die Dissertation wurde am 14.11.2014 bei der Fakultät für Medizin der Technischen Universität München eingereicht und durch die Fakultät für Medizin am 16.02.2015 angenommen.

Abstract

Inflammatory bowel diseases (IBDs), manifesting as Crohn's disease (CD) and Ulcerative colitis (UC), are chronic conditions of the gastrointestinal tract and show a rapidly increasing incidence in industrialized nations. Inhibitor of nuclear factor kappa-B kinase subunit alpha (IKKα), a member of the IκB kinase (IKK) / nuclear factor-kappa B (NF-κB) pathway, is involved in many inflammatory-mediated human diseases. Although the role of IKKβ kinase in IBD has been described, that of IKKα remains currently unknown. Here, the role of IKKα in intestinal homeostasis is investigated. Mice deficient in IKKα kinase activity (*Ikkα*$^{AA/AA}$) exhibit defects in mucosa tissue repair, massive leukocyte infiltration and elevated chemokine production in the colon, resulting in an exacerbated inflammatory response when challenged with dextran sulfate sodium (DSS), causing Ulcerative colitis. Defective IKKα signaling causes enhanced caspase-12 activation leading to the inhibition of inflammasome-dependent IL-18 production by the intestinal epithelial cells (IECs). Loss of caspase-12 or exogenous administration of recombinant IL-18 alleviates the severe colitis phenotype of *Ikkα*$^{AA/AA}$ mice. Importantly, impaired IKKα activation results in defective autophagic protein degradation causing p62 accumulation and elevated endoplasmic reticulum (ER) stress, which is responsible for the elevated caspase-12 activity. The present study demonstrates that IKKα, which might control the autophagic process through its interaction with the Crohn's disease variant, *Atg16l1*, is an essential regulator of inflammatory responses in the large intestine and is required for epithelial regeneration. Thus, IKKα is identified as a novel link between autophagy, ER stress and inflammasome pathway, which are often deregulated in IBD.

Zusammenfassung

Chronisch-entzündliche Darmerkrankungen (CED), die sich als Morbus Crohn oder Colitis Ulcerosa manifestieren, sind chronische Erkrankungen des Magen-Darm-Traktes und zeigen eine rapide ansteigende Inzidenz in Industrieländern. Inhibitor of nuclear factor kappa-B kinase subunit alpha (IKKα), eine Komponente des IκB kinase (IKK) / nuclear factor-kappa B (NF-κB) Signalwegs, ist an vielen entzündlichen Erkrankungen beteiligt. Während die Bedeutung von IKKβ in der Entstehung von CED bereits beschrieben wurde, ist die Rolle von IKKα dabei unbekannt. In der vorliegenden Arbeit wurde die Funktion von IKKα in der Homöostase des Darms untersucht. Transgene Mäuse (*Ikkα*$^{AA/AA}$) mit IKKα-Kinase-Defizienz zeigen gestörte Regeneration der Darmschleimhaut im Kolon, massive Infiltration von Leukozyten sowie gesteigerte Zytokinproduktion. Dies führt zu einer verstärkten Entzündungsreaktion bei Dextran-Sodium-Sulfat (DSS) induzierter Colitis. Fehlregulierte Signaltransduktion von IKKα bewirkt eine verstärkte Aktivierung von Caspase-12 und in Folge eine Hemmung der Inflammasom-abhängigen IL-18 Produktion in Enterozyten. Deletion von Caspase-12 oder Gabe von rekombinantem IL-18 mildert den starken Kolitis-Phänotyp in *Ikkα*$^{AA/AA}$ Mäusen. Die gestörte Aktivierung von IKKα resultiert in defekter autophagosomaler Proteindegradation, welche Akkumulation von p62 und verstärkten ER (Endoplasmatisches Retikulum)-Stress hervorruft. Der gesteigerte ER-Stress wiederum ist ursächlich für die erhöhte Aktivität von Caspase 12. Der autophagische Prozess wird möglicherweise durch Interaktion mit der Morbus Crohn Mutante *Atg16l1* kontrolliert. Die vorliegende Arbeit demonstriert, dass IKKα einen essentieller Regulator von Entzündungsreaktion im Dickdarm darstellt und für die epitheliale Regeneration benötigt wird. Folglich wurde IKKα als neues Bindeglied zwischen Autophagie, ER-Stress und Inflammasom-Aktivierung identifiziert.

Acknowledgements

Acknowledgments

I would like now to thank all those who each in their own special way supported me in this work and without them would have been hard to achieve.

First of all, my sincerest gratitude is extended to my thesis supervisor Prof. Dr. F. Greten for entrusting me with one of his research projects, for his unconditional support, patience, guidance and valuable discussions during the entire course of my Ph.D. Furthermore, I would like to deeply thank him for being instrumental in keeping this project alive, despite the numerous hurdles, and for offering me the chance to publish this work.

I am sincerely grateful to my advisor Dr. M. C. Arkan for her support and inestimable advice and discussions during the entire course of the Ph.D and for her kind collaboration and suggestions concerning this project during the committee meetings.

I am very thankful to my advisor Prof. Dr. J. Ruland for his inspirational supervision, appreciated comments and insights.

Million thanks to my dear friends and colleagues Dr. Özge Canli and Dr. Tiago de Oliveira for teaching and supporting me at the very first steps and course of this 'Journey' and simply for being there for me at tough and joyful moments. Many thanks also to my colleagues, Julia Varga, Dr. Mallika Ramakrishna, Tobias Neumann, Paul Ziegler, Dr. Marina Pesic, Olga Goncharova and Charles Pallangyo for the nice working atmosphere, the joy and excitement we shared and for being wonderful lab mates.

I would also want to thank former members of the lab, especially Dr. Moritz Bennecke for initiating this project, Begüm Alankus, Dr. HsinYu Fang, Dr. Sarah Schwitalla, Dr. Arun Mankan, Dr. Julia Bollrath, Dr. Tim Nebelsiek, and former members of the Arkan group, Dr. Cigdem Atay, Dr. Manon Schultz, Dr. Jessica Heringer and Dr. Franciscka Romrig for their companionship and support.

Acknowledgements

I am really grateful to our technical assistants Natalia Delis, Christine Danneil, Eva Rudolf, Kathleen Moos and former assistants, especially Kerstin Burmeister, one of the nicest person I have ever met, Saskia Ettl and Kristin Retzlaff for their excellent work and honest support.

Moreover, I wish to thank the PhD program coordinator Dr. Katrin Offe and Dessislava Slatanova for excellent PhD program organization and their precious help and guidance.

Special thanks to Dr. Michael Aichler, Dr Jörn Lausen and Dr. Stefan Stein for the conductive instruction during my rotation projects.

I would like to deeply thank my dear friend Dieter Weislmaier for his understanding and support and for always caring for me.

I want to thank my very good friends Nikos Giannakos and Christina Kamilari, Pavlina Gerontari for standing by me all this time and also Sevi Vletsi and Chrysi Petraki for the fun and joy we had together throughout this work.

Last but not least, I deeply want to express my gratitude to my lovely family, my sister Christina Maria Diamanti, my mother Elena Diamanti, my father Zisis Diamantis, my grandfather Radu Cutieru and grandmother Michaela Cutieru for their understanding, encouragement, and patience and for being always there for me. Thank you for believing and trusting me. ‘Σας αγαπάω όλους πάρα πολύ και σας έχω ιδιαίτερη ευγνωμοσύνη.

Table of Contents

Table of Figures

List of Tables

Abbreviations

ASC	Apoptosis-associated speck-like protein containing a caspase recruitment domain
ATF6a	Activating transcription factor 6a
ATG	Autophagy protein
ATG16L1	Autophagy-related protein 16 like-1 protein
BCL2	Pro apoptotic B cell lymphoma 2
Bcl-xl	B-cell lymphoma-extra large
BiP	Binding immunoglobulin protein
CARD	Caspase activation and recruitment domain
CCL2	Chemokine C-C motif ligand 2
CD	Crohn's Disease
CHOP	CCAAT/enhancer-binding protein homologous protein
COX2	Cyclooxygenase 2
CXCL	Chemokine ligand C-X-C motif
DAMPs	Damage-associated molecular patterns
DC	Dendritic cell
DD	Death domain
DEPC	Diethylpyrocarbonate
DMEM	Dulbecco's modified eagle medium
DSS	Dextran sulfate sodium
DTT	Dithiothreitol
ECM1	Extracellular matrix protein 1
EDTA	Ethylenediaminetetraacetic acid
EIF2α	Eukaryotic translation-initiation factor 2
ELISA	Enzyme-linked immunosorbent assay
ER	Endoplasmic reticulum
ERAD	ER-associated degradation
GRP78	78 kDa Glucose regulated protein
HRP	Horseradish peroxidase
IBD	Inflammatory bowel disease
IECs	Intestinal epithelial cells
IFNγ	Interferon γ
IKK	Inhibitor of nuclear factor kappa-B kinase subunit
IL	Interleukin
iNOS	Inducible nitric oxide
IRE1α	Inositol-requiring kinase 1α
IκB	Nuclear factor of kappa light polypeptide gene enhancer in B-cells inhibitor
JNK	C-Jun-N-terminal kinase
LC3	Microtubule-associated protein 1A/1B light chain 3

Abbreviations

LIR	LC3-interacting region
LRR	C-terminal leucine-rich repeats
MAPK	Mitogen-activated protein kinase
MIP	Macrophage inflammatory protein
MMP	Matrix metalloproteinase
mRNA	Messenger RNA
MUC2	Mucin 2
NaCl	Sodium chloride
NF-κB	Nuclear factor kappa-light-chain-enhancer of activated B cells
NIK	NF-κB inducing kinase
NLRP3	NOD-like receptor family pyrin domain containing 3
NLRs	NOD-like receptors
NOD	Nucleotide-binding oligomerization domain-containing protein
PAMPS	Pathogen-associated molecular patterns
PB1	Phox and Bem1
PBS	Phosphate buffered saline
PERK	Eukaryotic translation initiation factor 2-alpha kinase 3
PFA	Paraformaldehyde
PMSF	Phenylmethylsulfonyl fluoride
PRRs	Pattern recognition receptors
PYD	Pyrin domain
RelB	V-rel avian reticuloendotheliosis viral oncogene homolog B
RIP	Receptor interacting protein
ROS	Reactive oxygen species
RT-PCR	Real time-polymerase chain reaction
SEM	Standard error of the mean
SNPs	Single nucleotide polymorphisms
TEMED	Tetramethylethylenediamine
TLR	Toll-like receptor
TNFα	Tumor necrosis factor α
TRAF2	Tumor necrosis factor receptor-associated factor 2
TUNEL	TdT-mediated dUTP-biotin nick end labeling
UC	Ulcerative Colitis
UPR	Unfolded protein response
VEGF	Vascular endothelial growth factor
Wnt	Mouse homolog of wingless
XBP1	X-box binding protein 1
ZZ	ZZ-type zinc finger domain

1.Introduction

1.1 The gastrointestinal tract

The gastrointestinal tract (GI) is a hollow muscular tube that consists of many organs beginning with the oral cavity where food enters the mouth, followed by the pharynx, esophagus, stomach, small intestine, large intestine, rectum and ending with the anus where food is expelled. The primary function of this system is the transport and breakdown of food into basic nutrients that can be absorbed in the body to provide energy. There are various organs, like pancreas, liver, gall bladder that assist in this process by secreting digestive enzymes. The main digestion though takes place in the stomach and small intestine where fat, carbohydrates and proteins are being broken down into their main building blocks [1]. Small molecules pass across the epithelium of the small intestine and then enter the circulation, while reabsorption of excess water, sugar, salts, vitamins and fecal formation takes place in the large intestine. Finally, the undigested material and waste products are excluded from the body [1]. This muscular tube is lined up by a specialized layer of epithelial cells. Despite the fact that each part of the GI system has distinct functions, the entire tract has a similar basic architecture consisting of four layers (*Figure 1.1*).

Serosa: This is the outer layer consisting mainly of fat and mesothelium (layer of epithelial cells). **Muscularis externa**: This smooth muscle layer comprises muscle fibers and neural innervations that control muscle contraction and therefore the mechanical breakdown and peristalsis of the food in the lumen. **Submucosa**: Consists of fat, fibrous connective tissue, vessels and nerves. This layer surrounds the muscularis mucosa. **Mucosa**: The most inner part of the digestive system has specialized epithelial cells, supported underneath by lamina propria, a layer of connective tissue with lymphoid

tissue, blood vessels, nerves and glands. Epithelium can be either stratified (flat) squamous such as in the mouth or esophagus, standing the wear and tear caused by the passing food, or columnar (tall)-like in the stomach and the intestine to help secretion and absorption. Beneath lamina propria is the muscularis mucosa, a layer with smooth muscles that contracts in order to change the shape of the lumen.

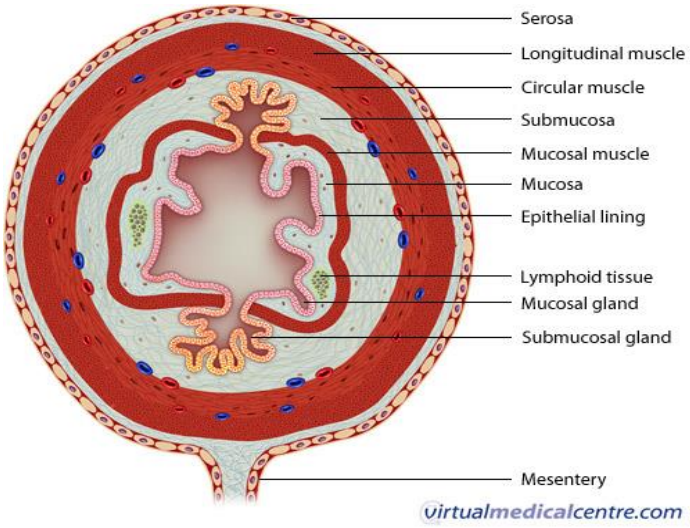

Figure 1.1: Picture depicting the main layers of the GI tract.

1.1.1 Morphology and function of the intestinal tract

The mouse and human intestines share great similarity concerning morphology, physiology and development. The gut is anatomically divided into two parts, the small intestine, which is further subdivided into duodenum, jejunum and ileum, and large intestine/colon. The absorptive surface area of the small intestine is greatly enlarged by finger-like protrusions that point into the lumen, otherwise known as villi. The opposite end of the villi invaginates into the underlying connective tissue, and are referred to as the crypts of Lieberkühn [2]. The crypts comprise the proliferative compartment, while the villi in the small intestine and remainder of the crypt (2/3 of the crypt) in the large intestine, is occupied by transit-amplifying (TA) progenitor cells, which are estimated to

divide twice a day and play a key role in the rapid renewal of the epithelium [3] (*Figure 1.2*). When these TA cells reach the crypt-villus neck they quickly and irreversibly differentiate into functional absorptive or secretory intestinal cells. After their terminal differentiation they reach the top of the villus/crypt, undergo apoptosis and shed into the gut lumen [4].

The constant renewal of the intestinal epithelium (every 4-6 days in both mouse and human) relies on the intestinal stem cells (ISCs) positioned at the bottom of the crypts. Although the identity of the ISCs has been controversial, it is believed that they are the Crypt Base Columnar cells (CBCCs), located between the Paneth cells, or just above them at position +4 (*Figure 1.2*) [4]. The ISCs give rise to the absorptive lineage with the enterocytes and the secretory lineage with goblet, Paneth and enteroendocrine cells (*Figure 1.2*). The enterocytes, the most abundant cell type in both small and large intestines, have a brush border (microvilli) on the apical side and they primarily absorb nutrients. The goblet cells comprise approximately 10-15% of the small intestinal cells and 50% of the colonic cells and their main function is to produce and secrete mucus shielding the epithelium from noxious luminal antigens [5]. 1% of the small and large intestines are composed of enteroenterocrine cells that mainly produce and secrete hormones, like secretin and serotonine [5]. The most unusual differentiated cell type, which is not present in colon, are the Paneth cells. They are unusual because they appear after birth during crypt emergence and migrate towards the base of the crypt where they complete their maturation. They have a role in antimicrobial defense by producing and secreting antibacterial peptides, such as cryptidins, defensins and lysozyme [6]. Some of the lesser known cells found in the intestine are the M cells (Microfold cells) and the Tuft cells. The M cells are restricted to the small intestine in the peyer's patches and are involved in antigen presentation. Tuft cells are found both in small and large intestine and

are believed to be the fourth secretory lineage involved in chemical sensation of luminal antigens [5].

Renewal system and crypt homeostasis are tightly controlled through signaling between the supporting mesenchymal cells and the differentiated epithelial progeny. Wnt pathway has a unique and central role in the (patho) physiology of the intestine, controlling intestinal proliferation and stem cell maintenance, while Notch signaling at the crypt is involved in cell fate determination between absorptive and secretory lineage [3, 5].

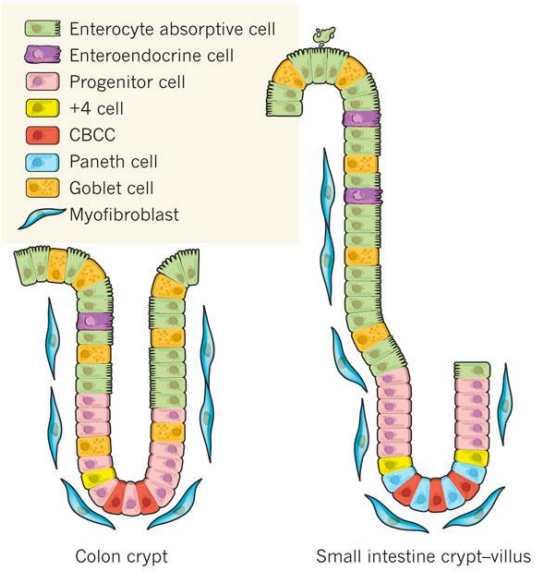

Figure 1.2: Architecture of the colonic crypt and the small intestinal crypt-villus. *Both the colon crypt and small intestine crypt-villus contain a stem cell compartment at the bottom of the crypt. The crypt base columnar cells, located in between the Paneth cells and/or the +4 cells located above the Paneth cells, have been suggested to be the ISCs. Paneth cells are not detected in the colon and they migrate downwards, whereas the other differentiated progenitors migrate upwards [3]. ISC, intestinal stem cells.*

1.2 Inflammatory bowel diseases (IBDs)

The two major clinically defined forms of IBD manifesting as Crohn's Disease (CD) and Ulcerative Colitis (UC), are chronic relapsing inflammatory disorders of the gastrointestinal tract, which are strongly associated with an increased risk of colon

cancer. Crohn's Disease can affect any part of the gastrointestinal tract, especially the ileum and colon, potentially involving all layers of the tissue. Unlike CD, pathology in UC is restricted mainly to the colon and rectum affecting the whole mucosa [7]. Although the primary causative factor for IBD pathogenesis remains unknown, recent research indicates that the *intestinal microbial communities (microbiota), host's genetic susceptibility*, *exaggerated immune responses* and *the external environment* are linked and functionally integrated to the pathogenesis of IBDs [8].

1.2.1 Microbiota

Mammalian hosts have coevolved to exist with the gut microbiota in a mutual symbiotic relationship where the host provides a suitable environment in return for benefits provided to it by the gut *microbiota*. For instance, break-down of indigestible carbohydrates to short chain fatty acids, synthesis of certain vitamins, degradation of dietary oxalates and education of mucosal immune system [9]. The intestinal tract comprises the largest reservoir of microorganisms (Bacteria, Archea, Eukarya and Viruses) in the human body, where their density increases gradually from the proximal to the distal parts of the tract [10]. Commonly identified commensal bacteria include the phyla of Firmicutes (*Lactobacillus, Clostridium, Enterococcus*), Bacteroidetes (*Bacteroides*), Actinobacteria (*Bifidobacteria*) and Proteobacteria (*Escherichia coli and Helicobacter*) [10]. Dysbiosis of the gut microbiota, an alteration of the microbial community structure associated with disease, has been observed in patients with IBD. Many studies have examined the microbiota in UC and CD and found reduced biodiversity in fecal microbiome and higher numbers of mucosa-associated bacteria in IBD patients compared to healthy individuals [11]. For instance, in patients with CD or UC the number of bacteria with anti-inflammatory properties such as, Bacteroidetes and Firmicutes, are

reduced, while a greater abundance of Enterobacteria, mostly *Escherichia coli*, is observed especially in the mucosa and not the fecal samples [11]. The breakthrough finding which implicated the role of gut microflora on disease pathogenesis was that antibiotic treatment or germ-free breeding of several mouse models of IBD including IL-10 deficient or/and other transgenic mice resulted in less pronounced intestinal inflammation [12, 13].

1.2.2 Genetic susceptibility

Both forms of IBD arise in *genetically susceptible* individuals through interplay with poorly comprehended environmental factors [7]. Although both diseases have overlapping genetic factors, hereditability in CD is more important than in UC, as monozygotic twins exhibit 50-75% phenotypic concordance in CD compared to only 10-20% observed in UC [7]. Mutations in autophagy-associated genes (*Atg16l1*, *Irgm*) and NOD-like receptors (*Nod2*) are quite specific for CD, whereas those in loci related to regulatory pathways (*Il10*) and intestinal epithelial (IEC) function (*Ecm1, Cadm2*) appear to be more specific for UC [7]. Polymorphisms in *Atg16l11* and *Nod2* genes interfere with the secretion of antimicrobial peptides by Paneth cells [14, 15], while *Xbp1* variants, present in UC and CD patients, associate with endoplasmic reticulum (ER) stress and affect Paneth cell function [16]. Therefore, patients with mutations in genes involved in autophagy (an innate defence mechanism involved in the elimination of intracellular pathogens), such as *Atg16l1, Irgm* or *Nod2,* in ER stress (*Xbp1*) or innate immunity (*Nod2*) might have altered microbial composition due to defects in defensin secretion [7]. Hence, the genetic variants that confer risk to IBD reflect the importance of autophagy, innate immunity and ER stress in the pathogenesis of these disorders.

1.2.3 Innate and adaptive immunity

Apart from the composition of intestinal microbiota and genetic susceptibility, IBD pathogenesis has been strongly linked to dysfunctions of innate and adaptive pathways that result in aberrant inflammatory responses in patients with CD or UC.

Innate immunity, the first line of defence against pathogens, is mediated by various cell types and is initiated by the recognition of microbial antigens by pattern recognition receptors (PRR) on the cell surface (Toll-like receptors (TLRs)) and in the cytoplasm (NOD-like receptors (NLRs)) [17]. Accumulating evidence suggests that loss of PRR can lead to changes of the microbial composition and intestinal barrier defects allowing microbial invasion of systemic organs. Specifically, deficiency in TLR5, which recognizes bacterial flagellin, leads to the translocation of bacteria to the spleen and liver followed by spontaneous colitis and metabolic syndrome in mice [18, 19]. Furthermore, mice lacking MyD88, a common adaptor for most of the TLR family members, have increased numbers of commensal bacteria in the liver and spleen [20] and specific expression of MyD88 in Paneth cells limits the microbial invasion in those tissues [21]. 30-40% of patients with CD exhibit hypomorphic NOD2 (an intracellular NLR) variants [7] and therefore decreased α-defensin expression [22]. In addition, autophagy is compromised in CD. This can be seen in CD patients who are impaired in their ability to mediate bacterial capture by autophagy due to polymorphisms in the autophagy-related gene *Atg16l1* [23]. Patients with CD and UC display intestinal permeability, which could reflect mucosal barrier defects that allow bacterial translocation through the intestinal mucosa. In healthy intestines, goblet cells secrete mucin glycoproteins (mucus) that generate a two-layer substructure extending up to 150 μm from the epithelium: the outer is loosely adherent, suitable for bacterial growth, while the inner layer is more compact and sterile [24]. The

importance of this mucinous deposit in maintaining the symbiotic relationship with the microbiota is emphasized by the fact that mice deficient in mucin glycoprotein *Muc2*, the most abundant constituent of the mucus layer, ultimately develop spontaneous chronic colitis and colorectal cancer [25, 26]. Likewise, aberrant mucin assembly causes ER stress and spontaneous inflammation that resembles UC in mice [27]. Defects in the mucus composition can also influence the pattern of microbial colonization and maintenance of microbial community and structure [11]. Furthermore, altered function of antimicrobial peptides (including α/β-defensins, lysozyme, C-type lectins (RegIIIγ), cathelicidins and lipocalins) are also involved in IBD [28]. For example, reduced expression of β-defensins by enterocytes or α-defensins by Paneth cells is associated with colonic and ileal CD, respectively [22, 29]. C-type lectin RegIIIγ, secreted by Paneth cells in response to bacterial signals, was found to be a key component in sensing and restricting the bacterial community near the mucosal surface of the small intestine [30], while enhanced secretion of RegIIIγ into the intestinal lumen conferred resistance to *L.monocytogenes* infection via MyD88 signaling emanating from IECs [31].

One of the defence mechanisms of the *adaptive immune system* in sequestering symbiotic bacteria involves the secretion of IgA by B cells. IgA, which is transcytosed through the epithelium [32], was shown to bind to bacteria and regulate their composition and access to the mucosa [33].

Furthermore, it is believed that intestinal inflammation is triggered by imbalances in Th1 (Type 1 helper cells) and Th2 (Type 2 helper cells) cytokine responses that take place in the lamina propria, mesenteric lymph nodes (MLN) and isolated lymphoid follicles (ILFs). CD is mainly mediated by Th1 cells (via IFNγ and IL-12), whereas UC by Th2 cells (via IL-4 and IL-13). Recently, another subset of effector Th cells, the IL-17-producing Th17 cells, was described [34]. This cell type was shown to be induced by IL-6 and transforming

growth factor β (TGFβ) and expanded by IL-23 [35, 36]. The elevated Th1 and Th17 cells in the lamina propria of patients with CD suggested that both IL-12/IFNγ-producing and Th17-associated-IL-23/IL-17 pathways might be involved in disease pathogenesis [37]. However, blockade or genetic ablation of IL-23 demonstrated that IL-23, and not IL-12, is essential in promoting chronic intestinal inflammation via IL-17 [38, 39]. Additionally, antibodies against IL-12p40 (the common p40 subunit of IL-12 and IL-23) induced clinical responses and remissions in patients with active CD [40], demonstrating the prominent role of IL-23/IL-17 in disease development. Contrary to the pathogenic role of Th17, regulatory T cells (T_{reg}) characterized by the expression of the transcription factor FOXP3 and secretion of regulatory cytokines such as TGFβ and IL-10, have been reported to have immunosuppressive functions during intestinal inflammation. This is evident by the fact that both IL-10 [41] and TGFβ [42] deficient mice develop spontaneous intestinal inflammation and co-transfer of T_{reg} in mouse models of T-cell mediated chronic intestinal inflammation rescues the severe pathology [35].

Thus, IBD is a multifactorial complex disorder whose pathogenesis is influenced by the genetic make-up of the individual, the diversity of the intestinal microbiome and the interplay of both the adaptive and innate immune system. This array of factors might be also influenced by the extrinsic environment, such as diet, drugs, social stress, geography, smoking and psychological elements which are also considered as prominent risk factors for IBD [8].

1.3 Nuclear Factor-κB (NF-κB)

One of the most important and devastating consequence of long-term and unresolved inflammation in IBD is the development of colorectal cancer and one of the best studied transcription factors involved in both processes is NF-κB. NF-κB plays vital role in many

biological processes, including development, immune responses, cell proliferation and survival, whereas deregulated NF-κB signaling has been linked to many human diseases, including chronic inflammatory disorders and cancer [43, 44].

In mammals the NF-κB family consists of five related transcription factors, p65 (RelA), RelB, c-Rel, p52 and p50 where they bind as, either hetero - or –homodimers, to κB sites in the target genes and can either activate or suppress gene expression [45]. A hallmark of the NF-κB pathway is its regulation by the IκB proteins, which function as inhibitors for the NF-κB dimers. There are various human IκB proteins such as, IκBα, IκBβ, IκBε, IκBζ, BCL-3, IκBns. In addition the p105 and p100, the respective precursors of the processed p50 and p52 can also function as IκB inhibitors [45]. The prototypical NF-κB complex under steady-state conditions is the p50-p65-IκBα trimer. In the *canonical* or classic pathway IκBα is phosphorylated by the IκBα kinase (IKK) complex, which consists of two catalytically active kinases IKKα/1 and IKKβ/2 and a regulatory scaffold protein NEMO (NF-κB essential modulator)/IKKγ. Phosphorylation of IκBα at serines 32 and 36 targets it for ubiquitin-dependent proteasomal degradation thereby liberating active NF-κB dimers to enter the nucleus and activate the transcription of responsive genes. Target elements of the canonical pathway include genes encoding inflammatory mediators, chemokines, cytokines, inhibitors of apoptosis, proteases and adhesion molecules [43]. The *alternative* or non-canonical NF-κB pathway, on the other hand, is governed exclusively by the IKKα kinase. Activation of IKKα by the upstream NF-κB inducing kinase (NIK) results in the phosphorylation and processing of p100 generating the active p52/RelB heterodimers (*Figure 1.3*). Active p52/RelB dimers translocate to the nucleus where they turn on the transcription of genes involved in lymphoid organogenesis, B cell survival and maturation as well as dendritic cell (DC) activation [46].

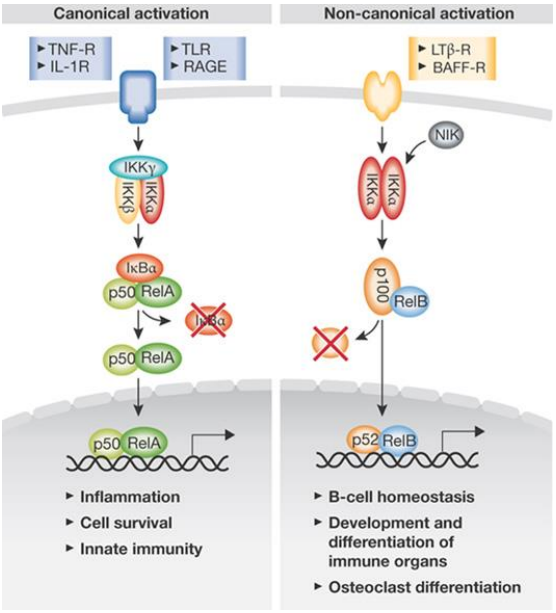

Figure 1.3: Canonical and alternative NF-κB activation. *IKK complex and primarily IKKβ mediate activation of the canonical pathway through phosphorylation and proteasomal degradation of the IκB inhibitors in the cytoplasm. On the other hand, IKKα dimers control exclusively the alternative pathway by phosphorylating and targeting p100 for proteasomal degradation [47].*

1.3.1 NF-κB signaling in IBD

NF-κB, the master transcriptional regulator of inflammation, governs the expression of various cytokines involved in IBDs, such as Tumor necrosis factor α (TNFα), IL-6 and IL-1β. Accordingly, increased NF-κB-dependent expression of TNFα, IL-6 and IL-1β in IECs and macrophages of inflamed mucosa of patients with CD and UC has been reported more than a decade ago [48]. Moreover, rectal or oral administration of p65 antisense oligonucleotides decreased severity of experimental colitis or colitis observed in *Il10* deficient mice [49]. Additionally, deletion of *Ikkβ* in myeloid cells ameliorated chronic colitis observed in *Il10* knockout mice [50], suggesting that targeting NF-κB could be a possible strategy in IBD therapy. However, defective NF-κB activation in the intestinal epithelium, as a result of specific ablation of *NEMO*/*Ikkγ* [51] or *RelA*/*p65* [52] causes spontaneous inflammation and sensitizes the epithelium to radiation-induced apoptosis [53]. Also, loss of IKKβ-dependent NF-κB activation in IECs results in exacerbated DSS-

induced acute colitis due to increased apoptosis and reduced recruitment of inflammatory cells that secreted cytoprotective factors [50, 54]. In addition, epithelial IKKβ can control adaptive immune functions in the lamina propria via distal effects on DCs. More specific, mice lacking *Ikkβ* in the intestinal epithelial cells are characterized by diminished expression of thymic stromal lymphopoietin in the gut and fail to develop specific $CD4^+$ Th2 responses after infection with the parasite *Trichuris muris* [55]. Instead, mucosal DC secrete elevated TNFα and IL-12/23p40 levels and $CD4^+$ cells produce increased amount of IL-17 and IFNγ resulting in severe intestinal inflammation [55].

Thus, inflammatory factors such as NF-κB, can accelerate intestinal epithelial cell proliferation and apoptosis, nevertheless under conditions of impaired replacement of apoptotic enterocytes a breach in the intestinal barrier will allow bacteria translocation that will eventually cause a strong local inflammatory response. It seems that on one hand NF-κB promotes survival of cells by regulating anti-apoptotic genes and on the other hand regulates the expression of many cytokines and other modulators of the inflammatory processes in IBD. Therefore, it is an absolute requirement that NF-κB signaling and the genes induced by this signaling cascade are under tight regulation.

1.3.2 IKKα: a multifunction protein kinase

Despite the fact that IKKα and IKKβ share structural and biochemical similarities the different phenotypes observed in the respective knockouts suggests that they regulate distinct targets and they have non-redundant functions. For instance, *Ikkβ* deficient mice die embryonically due to massive liver apoptosis [56], whereas *Ikkα* knockout mice die soon after birth due to limb and skin abnormalities [57-59]. Interestingly, *Ikkα* knockout mice exhibit normal NF-κB activation demonstrating for the first time IKKβ/γ/NF-κB-independent functions [59]. Another specific function found for IKKα is its involvement

in the alternative NF-κB pathway by phosphorylating the NF-κB2/p100 and generating the active p52 member [60]. The authors demonstrated that the IKKα kinase activity is required for the maturation and activation of B cells as well as for the development of secondary lymphoid organs (Peyer's patches and germinal centers) [60]. Cao *et.al.* presented that IKKα is essential for mammary gland development, and adult female mice bearing an inactive IKKα kinase mutant are deficient in milk production owing to impaired cyclin D1 activation [61]. With this study the authors showed that IKKα activity is required for NF-κB activation in mammary epithelial cells in response to specific signals, such as RANK-L, whereas TNFα-induced NF-κB activation remains intact [61].

1.3.2.1 The anti-inflammatory role of IKKα

IKKα has been suggested as a negative regulator of inflammatory immune responses. It was demonstrated that though IKKα kinase-dead (*Ikkα*$^{AA/AA}$) mutant mice when challenged with bacteria, show better bacterial clearance, they are more prone to septic shock due to elevated inflammatory response [62]. The authors presented that IKKα is important in limiting macrophage activation by preventing prolonged promoter binding of RelA/p65 and c-Rel [62]. Similarly, embryonic liver-derived macrophages deficient in *Ikkα* display elevated production of proinflammatory cytokines and chemokines associated with increased NF-κB activity [63]. Moreover, the role of this kinase in turning off inflammatory pathways was demonstrated by its ability to phosphorylate TAX1BP1 protein in response to TNF and IL-1 stimuli and thus terminating NF-κB signaling [64]. Remarkably, the suggested IKKα-mediated anti-inflammatory effect is not restricted to NF-κB. The alternative mechanism by which IKKα acts to limit inflammation is through phosphorylation and thereby activation of the protein inhibitor of STAT1 (PIAS1). In response to different proinflammatory stimuli, such as TNFα or LPS, IKKα-induced PIAS1

phosphorylation is required for the transcriptional repression of NF-κB/STAT1 dependent genes, with a notable preference for proinflammatory cytokines and chemokines, such as *Mip2, Tnfα, Irf1* and *Iκbα* [65]. A recent study supported the fact that deletion of IKKα in pancreas associates with increased acinar cell death, fibrosis, inflammation and release of pancreatic enzymes, clinical signs resembling those of human chronic pancreatitis [66]. The pathology depended on the protein scaffold p62, as deletion of p62 attenuated pancreatitis [66].

IKKα has acquired a unique role in bridging innate and adaptive immunity. It was demonstrated that IKKα is essential for the induction of genes (*Blc*, *sdf-1*, *Elc* and *Slc*) encoding chemokines crucial for spleen organogenesis and maintenance of tissue architecture [67]. LTβR engagement triggers IKKα-dependent RelB:p52 nuclear translocation and selective recruitment of those dimers to the promoters of genes whose consensus sequence was distinct from that of the classical κB sites. Thus, the authors proposed that IKKα optimizes adaptive immunity through proper organization of secondary lymphoid organs by regulating the production of organogenic chemokines, such as *Blc* and *Elc* [67]. Additionally, IKKα kinase activity is required to limit inflammation while promoting acquired antigen-specific immunity [68]. IKKα kinase-dead mutant mice challenged with the human pathogen *Listeria monocytogenes* display efficient pathogen clearance from the spleen and liver in the acute phase but they are highly susceptible upon secondary infection. This is attributed to the impaired Th1 cell priming and acquired immunity dependent on the development of protective $CD8^+$ memory T cells [68]. *In vitro* assays demonstrated that IKKα activation in DCs is required for T cell priming, whereas the kinase dead mutants ($Ikk\alpha^{AA/AA}$ mice) are unable to prime naïve $CD4^+$ T cells to produce IFNγ [68].

Thus, this protein kinase has the uncommon property of coupling innate and adaptive immunity. It inhibits innate nonspecific immunity and at the same time enhances antigen-acquired immunity making it an attractive molecule to study in inflammatory conditions. IKKα and in general NF-κB signaling have been considered essential regulators in many inflammatory conditions, including IBDs. In addition to NF-κB, three interacting pathways have recently gained more attention due to their implication in IBD. These pathways, which associate with unfolded protein response (UPR), autophagy and intracellular bacteria sensing will be elaborated in the next sections.

1.4 The key players in unfolded protein response (UPR)

An important pathway that has emerged in IBD pathophysiology is the unfolded protein response (UPR), which is induced by endoplasmic reticulum (ER) stress.

The ER in all eukaryotic cells provides a unique environment essential for proper protein folding and post-translational modifications, storage of free calcium and energy and synthesis of lipid and sterols [69]. Since protein folding is a key process for protein function, all cells have evolved sophisticated mechanisms that authorise only properly folded proteins to exit the ER on their way either to the cell surface or other intracellular organelles. Misfolded proteins are retained in the ER lumen bound to molecular chaperones or directed for degradation through the proteasome, a process called ER-associated degradation (ERAD) or through autophagy [69]. Primary-genetic factors (mutated proteins) or secondary-environmental factors (glucose or calcium deprivation) or decreased proteasomal or autophagy function can interfere with the capacity of the ER to fold proteins properly, thus causing ER stress [69]. To sense and respond to ER stress eukaryotic cells activate the UPR signaling cascade which either protects the cell or alternatively promotes cell death. The UPR cascade consists of a group of transmembrane

ER-resident proteins including inositol-requiring protein 1 (IRE1α), PKR-like endoplasmic reticulum kinase (PERK) and activating transcription factor (ATF)-6 (*Figure 1.4*) [70]. This cascade is further regulated by glucose-regulated protein 78 (GRP78), an ER-associated chaperone that binds to all three ER-transmembrane proteins holding them in an inactive state. Binding of misfolded or unfolded proteins to GRP78 releases each of these factors resulting in the characteristic UPR-related behaviours.

The most immediate response, following the release of BiP from PERK, is the homodimerization and *trans*-phosphorylation of PERK, allowing it to phosphorylate the eukaryotic translation initiator factor 2α (eIF2α). Phosphorylation of eIF2α inhibits the assembly of 80S ribosome and consequently leads to attenuation of mRNA translation. ATF6 upon migration to the Golgi becomes transcriptionally active by undergoing proteolytic cleavage of its cytosolic tail by site 1 and 2 proteases. Finally, IRE1α, which governs the most conserved UPR pathway, possesses both kinase and specific endoribonuclease (RNase) activity. When ER stress occurs IRE1α undergoes homodimerization and trans-autophosphorylation turning on the c-Jun N-terminal kinase (JNK) and NF-κB pathways, mediated by its physical and functional interaction with tumor necrosis factor-receptor associated factor 2 (TRAF2) [71, 72]. TRAF2 is essential in regulating ER-induced cell death and its absence reduces NF-κB activation and sensitizes cells to death [73, 74]. Autophosphorylation of IRE1α activates its RNase activity to initiate nonconventional splicing of the *Xbp1* (*X-box binding protein 1*) mRNA, its only known target so far [75]. Only XBP1 protein translated from spliced *Xbp1* mRNA (*Xbp1s*) is transcriptionally active because it contains a C-terminus trans-activating domain, enabling the transcription of target genes encoding proteins that either degrade misfolded proteins or enhance ER-protein folding capacity [75] (*Figure 1.4*).

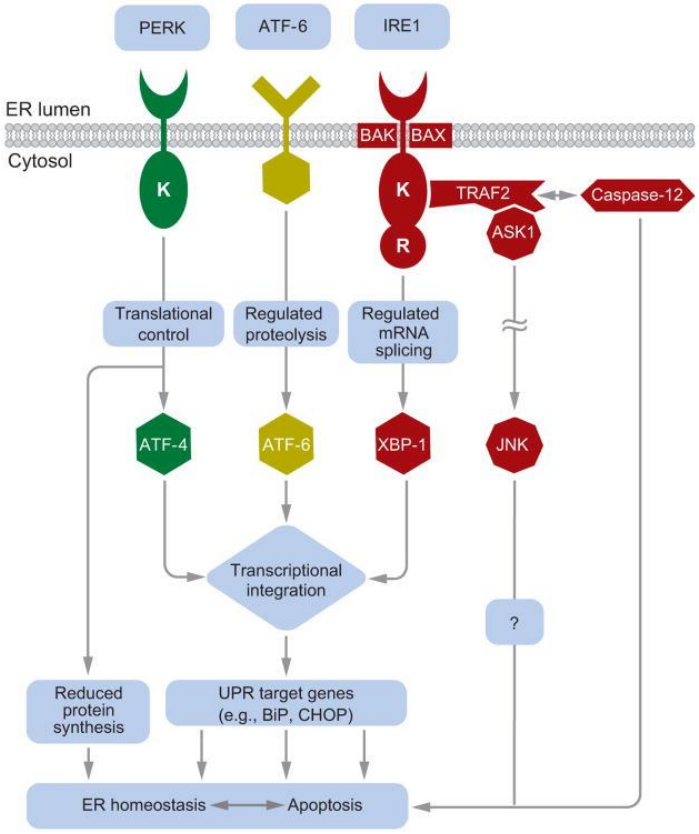

Figure 1.4: Figure depicting the mammalian unfolded protein response (UPR) cascade*. The three transmembrane sensor proteins PERK, ATF6 and IRE1α reside at the ER and with their ER luminal domains sense perturbations in ER homeostasis. In response to ER stress they initiate signal transduction pathways that controls cell survival and death [70].*

1.4.1 ER stress and inflammation

Recent observations suggest that UPR and inflammation can activate each other through various mechanisms, including NF-κB activation, and the interconnection of both processes in specific tissues and/or cells is assumed to be fundamental in the pathogenesis of inflammatory diseases [76].

The significance of ER stress in intestinal physiology is clearly demonstrated in mice lacking nodal components of the UPR signaling pathway. Mice lacking IRE1β, the additional isoform of IRE1, which is expressed specifically in the intestinal epithelium, suffered from severe mucosal damaged induced by DSS [77]. Additionally, the importance of the ATF6 UPR arm in intestinal homeostasis was shown by genetic ablation of ATF6α

and P58^{IPK} ER chaperone, which exacerbated symptoms of DSS-induced colitis due to hyperactivated proapoptotic (IRE1α/JNK) UPR signaling [78]. Recently, Heijmans and colleagues unraveled that ER stress is low in intestinal stem cells compared to transit amplifying cells and ER stress, induced by GPR78 deletion, causes loss of stem cell markers (*Lgr5*, *Olfm4* and *Ascl2*) in a PERK-eIF2α-dependent manner [79]. It was thus suggested, by means of active PERK-eIF2α signaling, that under homeostatic conditions ER stress is both sufficient and critical for stem cell differentiation [79].

Cells employed to secrete high amounts of proteins (plasma cells, hepatocytes, pancreatic acinar cells, plasmacytoid dendritic cells), either for their basal or their induced functions, dependent on a normal UPR and as such are more prone to environmental and/or genetic factors that induce ER stress [80]. Consistent with this, IECs, especially Paneth and goblet cells, rely on an intact UPR for their normal function. The association of XBP1 as a genetic risk factor for IBD originated from a mouse model with partial or complete genetic deletion of *Xbp1* specifically in the intestinal epithelium [16]. These mice develope spontaneous inflammation in the small intestine and increased susceptibility to DSS-induced acute colitis. Deep sequencing in more than 1000 patients with IBD identified rare non-synonymous SNPs (leading to amino-acid exchange) in the *Xbp1* gene that exhibited hypomorphic UPR induction, consistent with the mouse model [16]. Finally, mice with mutations in *Muc2*, develop accumulation of abnormal MUC2 protein in goblet cells, spontaneous ulcerative colitis-like phenotype in association with severe ER stress [27].

These studies indicate the reciprocal interactions between the UPR and innate immunity and suggest that ER stress affects the survival of secretory epithelial cell types, such as Paneth and goblet cells, the composition of intestinal microbiota and susceptibility to IBD.

1.5 Autophagy

Closely intertwined with ER stress and highly implicated in IBD pathogenesis is autophagy. Implication of autophagy in IBD originated from polymorphisms identified in the autophagy-related 16-like protein 1 (ATG16L1) [81] and immunity related-GTPase family M (IRGM) [82] that predispose individuals to CD.

Autophagy (originating from the Greek word for 'self-eating') refers to the cellular degradation pathway involving the delivery of cytoplasmic cargo to the lysosomes. Basal levels of autophagy occurs in all cells as a homeostatic function in the process of macromolecule and organelle turnover [83]. It is substantially elevated in response to starvation (nonselective process), when cells need to produce intracellular nutrients and energy, due to oxidative stress. It is also elevated when cells need to remove damaged organelles (selective process), for instance during infection, or accumulation of misfolded proteins and protein aggregates [84]. Therefore, is not surprising that autophagy is involved in various essential processes, such as embryogenesis, tissue remodelling and immune function (elimination of microbes, antigen presentation via MHC class II etc.) as well as in many disease processes including cancer, neurodegeneration and inflammation [84]. This catabolic process occurs through distinct steps with the aid of autophagy-related proteins (ATG) as depicted in *Figure 1.5*. Autophagy is initiated by the formation of the phagofore or isolation membrane, which in mammalian cells is regulated by the serine/threonine protein kinase, ULK1, and the class III phosphatidylinositol (PtdIns)-3 complex. Additional ATG proteins are required for the elongation step, the growth of the phagofore, such as ATG12-ATG5-ATG16L1 forming complex, ATG7, ATG10, ATG12 and the recruitment of ATG8 (LC3-I) to the phagofore through a membrane anchoring, phosphatidylethanolamine modification of ATG8 (LC3-II). Selectivity of autophagy is achieved by cargo receptors that bind to both substrates and lipidated ATG8 (LC3II)

protein of the elongated phagofore. Closure of the elongated phagofore results in the formation of a double-membrane organelle, called autophagosome. Finally, the maturation step involves fusion of autophagosomes with late endosomes or lysosomes for the formation of the autolysosomes where the substrates are degraded (*Figure 1.5*) [85].

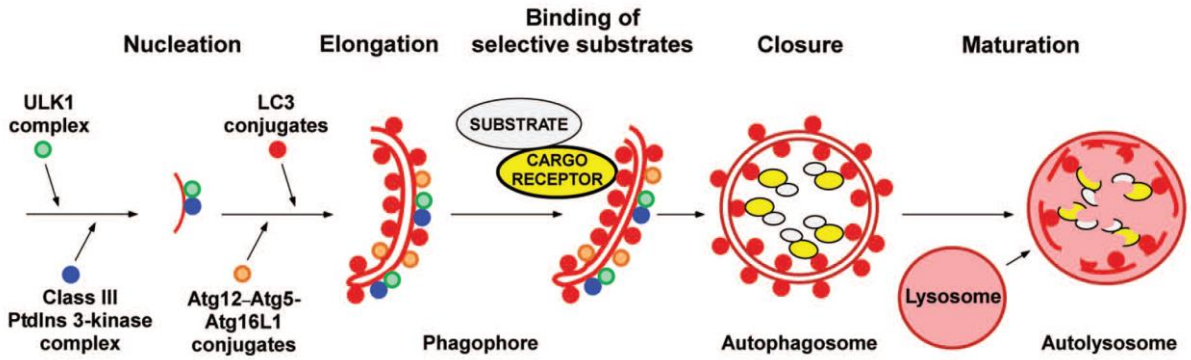

Figure 1.5: Model for autophagy in mammalian cells. *Scheme depicting the main steps and proteins involved in autophagy induction, progression and completion. See text for detailed description [85].*

1.5.1 Role of autophagy in intestinal inflammation

The discovery of a functional polymorphism (Threonine 300-to-Alanine variant) in the *Atg16l1* gene initially described by Schreiber and colleagues [81] brought the autophagy pathway into the spotlight in IBD. The T300A associated risk variant is impaired in its ability to mediate bacteria (*Salmonella*) capture by autophagy, while basal levels of autophagy and dimerization or binding properties to ATG5 remain intact [23]. Recently, it was demonstrated that this risk variant sensitizes ATG16L1 to caspase-3 mediating processing in response to death-receptor activation or starvation-induced metabolic stress, in human and murine macrophages [86]. Furthermore, hypomorphic ATG16L1 expression (resulting in reduced autophagy) in mice causes abnormal Paneth cell

exocytosis [14]. Strikingly, patients homozygous for the *Atg16l1* CD risk allele exhibit comparable Paneth cell abnormalities and a similar distortion was also noted in mice lacking ATG5 in the IECs [14]. In addition, mice expressing hypomorphic ATG16L1 do not develop spontaneous intestinal inflammation but they are more prone to DSS-induced colitis ascribed to overactivation of the NLRP3 inflammasome [87]. These studies suggest a concept that a specific genotype is transformed into a clinically relevant phenotype only when a set of environmental factors are present.

Polymorphisms found in NOD2-encoding *Card15* gene were the first decisive risk factors identified for Crohn's disease [88]. Defects in NOD2 signaling were reported to lead to CD pathology through inefficient induction of autophagy and handling of enteric bacteria [89, 90]. Interestingly, CD-associated NOD2 variants are impaired in their ability to induce autophagy and to recruit ATG16L1 to the bacteria entry sites at the plasma membrane, while their interaction remains intact. The authors suggested a potential mechanism wherein mutant NOD2 impairs autophagy by retaining ATG16L1 to the cytosol suppressing its function [90].

Collectively, autophagy and intracellular sensing of pathogens seems to be part of a major shared mechanism in the development of CD. This is supported by the fact that polymorphisms in *Nod2* receptor (sensing intracellular bacteria) account for the vast majority of genetic heritability of CD and mutations in the *Atg16l1* gene are one of the most prevalent risk factors for CD.

1.6 p62: a multimodule scaffold protein

p62 (also known as sequestosome 1, SQSTM1) is a multimodule adaptor protein implicated in selective signal transduction and degradation of proteins and organelles. The recent generation of p62 knockout mice revealed the role that p62 holds in a number

of cellular functions including, bone remodelling, autophagy, obesity, aging, inflammation and cancer [91]. The structure of p62 shows a high potential for interaction with many proteins consistent with its role as a signaling hub. The main interacting domains are, the PB1 domain (important for oligomerization and interaction with other PB1-containing proteins), the ZZ domain (for interaction with the RIP1 protein kinase), the TB domain (for association with TRAF6), the LIR domain (important for binding to the LC3 protein) and the UBA domain (for association with ubiquitin-tagged proteins and organelles) [92].

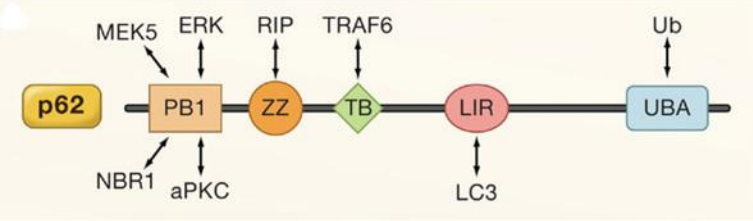

Figure 1.6: The interaction domains of the p62 protein*. The phox and Bem 1 (PB1) domain, the zinc finger (ZZ) domain, the TNFα receptor-associated factor 6 (TRAF6) binding (TB) domain, the LC3-interacting region (LIR) domain and the ubiquitin association (UBA) domain. The interacting partners are depicted in* ***black*** *[92].*

The link between p62 and autophagy was established when it was found that it binds to the autophagic protein LC3/ATG8 and the observation that it accumulates in autophagy deficient mice [93]. Mice lacking *Atg7* are defective in autophagy induction resulting in the appearance of ubiquitinated protein aggregates that colocalize with p62. Deletion of *p62* abrogates the formation of ubiquitin protein aggregates suggesting that p62 plays a structural role in their presence [93]. Accumulation of p62 was also shown to inhibit the ubiquitin-proteasome system (UPS) in autophagy deficient cells [94]. The authors presented that overexpression of the ubiquitin-binding partner, p97, prevents the binding of p62 to ubiquitinated proteins proposing that p62 accumulation may act, at least in part, by preventing ubiquitinated proteins from binding to the machineries that shuttle them

to or into the proteasome [94]. Although p62 is primarily degraded by the autolysosome, a recent study showed that it can also be degraded by the proteasome [95]. The authors demonstrated that cells deficient in the autophagy protein ATG16L1 have enhanced IL-1β signaling due to p62 accumulation and knockdown or overexpression of p62 suppresses or enhances IL-1β signaling, respectively [95].

Apart from being an autophagy target, p62 can determine cell survival or apoptosis. In response to cell stimulation by IL-1 [96], RANK ligand [97] or nerve growth factor (NGF) [98] p62 was shown to interact with the atypical protein kinase C (aPKC) through the PB1 domain and to induce NF-κB activation. Interestingly, in response to those stimuli p62 associates with TRAF6, resulting in NF-κB activation [96, 99]. On the other hand, p62 can promote apoptosis through the extrinsic pathway by interacting with caspase-8 [100]. Recently, a link between p62 accumulation and inflammasome activation was described. Human macrophages infected with *Mycobacterium abscessus* (Mabc) display elevated p62 levels, which result in NLRP3/ASC inflammasome-dependent caspase-1 activation and IL-1β release [101]. Additionally, murine or human macrophages stimulated with monosodium urate (MSU) crystals exhibit impaired proteasome function that causes accumulation of p62 and caspase-1-dependent IL-1β production [102].

Altogether, p62 is a multidomain scaffold protein that not only interacts with the autophagy machinery targeting proteins for degradation but is also implicated in many signaling pathways determining cell fate.

1.7 Microbial recognition by the innate immune system

The presence of microbiota is beneficial for the host immune maturation as it can be viewed that germ-free mammals lack a fully mature immune system and are unable to secrete mucus, antimicrobial peptides and circulating antibodies [28]. The complex

interaction between the intestinal epithelium and commensal bacteria is mediated by innate immune receptors, called pattern recognition receptors (PRRs). They are expressed constitutively by many cells at the front line of defence against infection, such as macrophages, DCs, neutrophils, monocytes, epithelial cells, B and T cells. PRRs include Toll-like receptors (TLRs) and C-type lectin receptors (CTLs) which scan the extracellular milieu and endosomal compartments for microbial components known as pathogen associated molecular patterns (PAMPs). Intracellular PRRs include the nucleic acid sensors, such as the RNA-sensing RIG-I-like receptors (RIGs) and RIG-like helicases (RLHs) and DNA sensors, like AIM2 [17]. According to the PAMP engagement and nature of the responding cell, PRRs can trigger different signaling pathways leading to diverse immune responses. Their signaling cascades converge however, on common inflammatory pathways including NF-κB, caspase-1 and mitogen-activated protein kinase (MAPK) signaling molecules [103]. Another set of PRRs, different from those mentioned above, are the nucleotide and oligomerization domain (NOD)-like receptors (NLRs), which are capable of recognizing PAMPs, such as lipopolysaccharide, peptidoglycan or host-derived endogenous damage-associated molecular patterns (DAMPs), released during cellular or tissue injury [103].

The NLR family is characterized by a central NOD (referred to as NACHT or NBD) domain, flanked by a C-terminal leucine-rich repeats (LRR) and an N-terminal caspase recruitment domain (CARD) or pyrin domain (PYD) [103]. The CARD/PYD domains mediate protein-protein interactions, whereas LRRs determine ligand specificity. NOD/NACHT, which is essential for activation via ATP-dependent oligomerization, is the only domain common to all NLRs. Based on similarities in the NOD domain the NLR family is divided into 3 distinct subfamilies: the NOD (NOD1-2, NOD3/NLRC3, NOD4/NLRC5, NOD5/NLRX1), the NLRP (NLRP1-14 also called NALPs) and the IPAF (NLRC4/IPAF and NAIP) subfamily

[104]. NLRPs, for instance, contain PYD, NOD and LRR domains, with the exception of NLPR10 that lacks LRRs, while NOD1-2 consist of NOD, LRR and CARD instead of PYD domains [104]. Although they are primarily expressed in immune cells, some NLRs are also expressed in non-immune cells and activation of each NLR member is induced by specific microbial or endogenous components. For example, NOD1 and NOD2 recognize products of bacterial cell wall (mesodiaminopimelic and muralmyl dipeptide (MDP), respectively) and, upon ligand sensing, they oligomerize, and through CARD-CARD interactions recruit RIP2 to the complex. Assembly of NOD1-2 signalosome results in NF-κB activation and proinflammatory gene regulation [104]. Contrary to NOD1 and NOD2, which are well studied, the rest of NODs and most of the NLR family members are poorly characterized. However, the diverse functions of NLR members that regulate caspase-1 activity in anti-microbial responses, as well as in multifactorial diseases such as IBDs, have started to be revealed.

1.7.1 Inflammasomes

Inflammasomes are a group of proteins that assemble huge complexes upon recognition of a diverse set of inflammation-inducing stimuli, including PAMPs and DAMPs, and control the production of important proinflammatory cytokines, such as IL-1β and IL-18 [104]. These multi-protein complexes include a sensor protein (NLR family), an adaptor protein (the apoptosis-associated speck-like protein (ASC) containing a CARD domain) and an inflammatory caspase. Activation of the NLR by exogenous or endogenous signals results in direct recruitment of pro-caspase-1 through CARD-CARD interaction or indirectly through PYD domain by means of the adaptor protein ASC, which contains both a CARD and a PYD domain [104]. Activation and assembly of the inflammasome requires simultaneously expression of all 'players' within the same cell type. Caspase-1 and ASC

are usually expressed in many cell types, while the sensor proteins have a more restrictive pattern of expression suggesting cell type-specific mechanisms of sensing tissue perturbation [105]. Many inflammasomes within different cell types, (e.g. epithelial, hematopoietic) display different but often complementary functions during mucosal immune responses. This is more apparent in the intestinal tract where many cell types have to come in contact with the tremendous load of commensal and pathogenic bacteria. A tight regulation of inflammasome signaling is critical to maintain a beneficial level of homeostatic interactions with the gut microflora and inflammasome hyper-activation or absence could be deleterious leading to inflammation and cancer.

1.7.2 Role of the inflammasomes in intestinal homeostasis

It is becoming more apparent that inflammasomes play a crucial role in maintaining intestinal homeostasis and healthy intestinal microflora. NLRP3 is the most widely studied inflammasome which regulates immune responses to microbial infection and auto-inflammatory diseases. NLRP3 is expressed in both hematopoietic and non-hematopoietic cells and requires two signals for its full activation. The priming signal, provided by microbial molecules and cytokines, activates the NF-κB or NOD1/2 receptors resulting in *pro-Il1β* and *Nlrp3* transcriptional induction. The activation signals, potassium efflux, ROS generation, microbial-pore forming toxins or lysosomal membrane damage, trigger inflammasome assembly, caspase-1 activation and subsequent cleavage of pro-IL-1β and pro-IL-18 into their active cytokines [103]. Much attention has been paid to NLPR3 owing to the possible genetic association of the *Nlpr3* locus with IBDs [106]. There are multiple reports on how NLRP3 inflammasome confers protection to the intestinal epithelium upon DSS-induced injury [107-110]. Similarly, *Asc* and *Caspase-1/-11* knockout mice also display high susceptibility to DSS-induced injury. Furthermore,

bone marrow transplantation experiments suggested that NLRP3 expression in the non-hematopoietic compartment, most likely the epithelium, is required for protection. Furthermore, *Asc* and *Caspase-1* knockout mice exhibit reduced IL-18 production by the IECs and administration of recombinant IL-18 protects the knockout mice against colitis (*Figure 1.7*) [107]. NLPR3 was shown to protect the intestinal epithelium from DSS-induced injury by regulating the production of antimicrobial peptides [110]. *Nlrp3* deficient mice exhibit impaired β-defensin production associated with more pathogenic microflora distinct from that of wild-type mice [110]. Additionally, the increased inflammation observed in *Nlrp3* deficient mice results in increased tumor burden in colitis associated cancer that correlates with decreased levels of IL-18 and IL-1β (*Figure 1.7*) [108, 109]. However, despite the proposed role of NLPR3 in the negative regulation of inflammation and inflammation-induced tumorigenesis there is one study showing that *Nlrp3*-null mice are protected against DSS-induced colitis. The protection is related to the decreased IL-1β secretion from *Nlrp3* deficient macrophages, as inhibition of caspase-1 with pranaclasan,a well known caspase-1 inhibitor, results in attenuated colitis [111]. Another group also demonstrated reduced colitis pattern in *Nlrp3* knockout mice [112]. The dissimilar phenotypes of *Nlrp3* deficient mice could be attributed not only to differences in the genetic background of mice or protocols used but most importantly to differences in the gut microbiota.

Recently another inflammasome, NLRP6, was shown to be highly expressed in intestinal epithelial cells and hematopoietic cells regulating colonic homeostasis [103]. In many studies *Nlrp6* deficient mice were shown to suffer from severe inflammation induced by DSS. One of these studies demonstrated that the development of acute colitis and increased AOM/DSS-induced tumorigenesis in *Nlrp6* knockout mice is due to the deficient function of the NLRP6 inflammasome in the hematopoietic cells [113]. A novel role of the

NLPR6 inflammasome as a promising regulator of colonic microbial ecology was recently proposed. Elinav *et.al* revealed that the *Nlrp6* knockout mice are characterized by spontaneous intestinal hyperplasia and develop severe colitis induced by DSS. Interestingly, the microbiota of the knockout mice is distinct from that of the wild-type and more importantly transferrable (colitogenic) to the co-housed wild-type mice. This phenomenon is also observed in *Asc* and *Caspase-1/-11* knockout mice but does not occur in those deficient in other inflammasome components, *Nlrp3*, *Nlrc4* and *Nlrp12* [112]. Additionally, absence of NLRP6 from colonic epithelial cells results in impaired production of IL-18 within the non-hematopoietic compartment and altered micobiota characterized by colonisation of the epithelium by the bacterial phyla Bacteroidetes (*Prevotellaceae*) and TM7 [112]. Recently, a link between autophagy and NLRP6 inflammasome function was described. Wlodarska *et.al* reported that the intestinal epithelium of *Nlrp6*, *Asc*, *Caspase-1/-11* deficient mice is devoid of the inner mucus layer due to impaired mucus secretion. The impaired mucin granule exocytosis renders the NLRP6 inflammasome deficient mice unable to effectively clear colonic and systemic *C. rodentium* colonization resulting eventually in increased pathology [114]. It was further suggested that *Nlrp6* deficient intestinal epithelium exhibits defective autophagy, a critical process required for goblet cell function and mucus secretion in the intestine [114].

1.7.3 IL-1β/IL-18/caspase-1 axis in intestinal homeostasis

The influence of inflammasomes in IBDs received significant attention due to the observation that single nucleotide polymorphisms (SNPs) in the gene encoding the IL-18 and IL-18 receptor accessory protein are associated with both UCs and CDs [115]. In addition, impaired production of IL-1β in patients carrying SNPs in the *Nlrp3* gene

associate with increased susceptibility to CD [106]. These genetic linkage studies designated a role for the inflammasome and IL-1β/IL-18 production in the development of IBDs. IL-18 was found to be elevated in the inflamed intestine of CDs patients, localized in the IECs, macrophages and dendritic cells in the lamina propria [116]. Similarly, decreased production of IL-1β and IL-18 in mice lacking *Caspase-1/-11* during DSS-induced acute colitis related with decreased disease severity [111, 117]. Moreover, mice lacking *Atg16l1* in hematopoietic cells develop increased DSS-induced injury and more importantly antibodies against IL-1β or IL-18 ameliorates disease progression [87]. The anti-inflammatory effect of neutralizing IL-18 was first seen in the lamina propria. In this study the authors confirmed that IL-18 is primarily expressed by macrophages of the lamina propria and depletion of macrophages or neutralizing antibodies against IL-18 prevents TNBS-induced colitis, an intrarectal model directly targeting intestinal permeability [118].

However, recent studies have hypothesized a negative regulatory role of the inflammasome signaling in the development of colitis. DSS-challenged mice deficient in *Nlrp3* [107-110], *Asc* [107-109, 112, 119] and *Caspase-1/-11* [107-109, 112, 119] display increased mortality and colitis as opposed to challenged wild-type mice. It is not really surprising that IL-18 is upregulated in wild-type DSS-treated animals at site of inflammation but not in *Nlrp3*, Asc, *Caspase-1/-11* deficient mice because NLRP3 inflammasome activation is essential for both IL-1β and IL-18 production. IL-18 could be of major significance since disease severity could be reversed by administration of recombinant IL-18 [107, 119]. Furthermore, the main source of IL-18 was proved the intestinal epithelium based on *in vitro* IEC cultures [107, 119]. Additionally, IL-18 production by the NLPR6 inflammasome is critical for the regulation of colitogenic properties of the microbiota and thus disease severity induced by DSS. Again, the main

source of IL-18 production was suggested to be the non-hematopoietic compartment [112]. In addition, *Il18* and *Il18 receptor* knockout mice exhibit severe DSS-induced colitis associated with high lethality and histopathological abnormalities [120]. Finally, IL-18 activation downstream of the NLRP3 and NLRP6 inflammasome was shown to decrease IL-22 binding protein (IL-22BP) expression by dendritic cells and thus protecting the intestinal mucosa from DSS-induced injury [121].

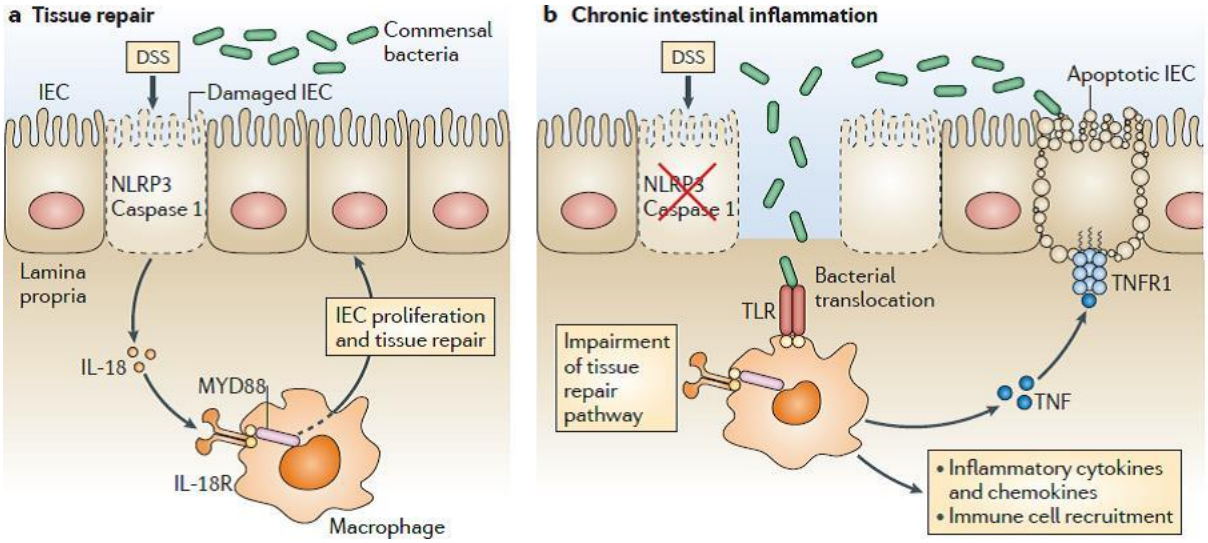

Figure 1.7: The inflammasome-IL-1β-IL-18 axis mediates tissue repair in the intestine. a) *Upon tissue damage (with DSS) the NLRP3 inflammasome assembles in IECs. This results in the production of IL-18 at the mucosal sites, which binds to its cognate receptor IL-18R, expressed by myeloid cells in the lamina propria. IL-18, which signals through the myeloid differentiation primary response protein 88 (MyD88), induces compensatory proliferation of IECs and tissue repair.* ***b)*** *When this innate pathway is compromised, such as when NLRP3, caspase-1/-11, ASC, IL-18, IL-18R are absent, insistent tissue damage allows bacteria translocation to the submucosa stimulating resident immune cells through TLRs or other pattern recognition receptors (PRRs) [122].*

Collectively, the studies so far suggest that IL-18 production downstream of NLPR3 and NLRP6 inflammasomes within the IECs is essential for maintaining intestinal homeostasis and barrier integrity and thereby limiting bacteria translocation (*Figure 1.7*a). In remarkable contrast, activation of IL-18 by the NLRP3 inflammasome in the immune cells

of the lamina propria seems to be proinflammatory and thus promoting intestinal inflammation (*Figure 1.7b*). Therefore tight control of the caspase-1/IL-1 axis of inflammation is the key to achieve immune tolerance in the intestine and deregulation of this pathway contributes to the development of IBDs.

1.8 Caspase-12 expression and activation

Caspases are cysteine proteases that initiate or execute cellular programs causing inflammation or cell death. All caspases are produced in cells as inactive zymogens and then undergo proteolytic processing upon activation. They are categorized, according to the cellular program they are involved in, either as proinflammatory or proapoptotic. The proinflammatory caspases comprise caspase-1,-11,-12 and -1, -4, -5 and -12 in humans, and they are called so due to their ability to regulate the production of the proinflammatory cytokines IL-1β and IL-18 [123]. They share a conserved common structure composed of a CARD-containing prodomain found at the N-terminus, a large and a small subunit at the C-terminus. Furthermore, they are able to segregate their large and small subunits through autoproteolysis which also serves to remove their N-terminal prodomains [124].

Caspase-12 is expressed in many tissues at the RNA level with the highest expression observed in the lung, small intestine and stomach [125]. Its constitutive protein expression is restricted to the brain, heart, skeletal muscle, eye, liver, testis [126] and in intestinal epithelial cells [127]. Although its expression is low in the liver, thymus and spleen [126] it can be highly induced by IFNγ and bacterial components in various cell types [126, 127]. Moreover, caspase-12 was found to localize at the cytoplasmic site of the endoplasmic reticulum (ER) [128, 129].

Several mechanisms have been postulated for the processing and activation of caspase-12. Calpains [130], calcium-activated cysteine peptidases, or caspase-7 [128] in response to ER stress process caspase-12 at first at the N-terminus, between the prodomain and the large subunit. This is followed by autoprocessing of caspase-12, between the large and small subunits. Another mechanism proposes that caspase-12 is released from TRAF2 during ER stress and then is autoprocessed via oligomerization [131]. Also, caspase-12 was suggested to be activated by tunicamycin, an ER stress stimulus, by inducing its processing at the N-terminal and C-terminal region [132]. Unlike the other inflammatory caspases, caspase-12 is unique in the respect that it is catalytically competent but its specificity is highly confined to the cleavage of its corresponding pro-enzyme [133].

1.8.1 The role of caspase-12 in inflammatory responses

Human and murine pro-caspase-12 were reported to have the highest homology (68% sequence identity) among all human and murine members of the interleukin-1β-converting enzyme (ICE) subfamily of caspases [125]. Initial studies in *Caspase-12* deficient mice have shown that caspase-12 is involved in ER stress-induced apoptosis [129]. Similarly, other *in vitro* studies are in agreement with a role of caspase-12 in ER stress mediated apoptosis [128, 130, 132]. Although activation and proteolysis of caspase-12 is a hallmark of ER stress its role in ER stress-induced apoptosis is challenged. More recent studies suggest that *Caspase-12* deficient cells, in both humans and mice, are as sensitive to ER stress-induced apoptosis as *Caspase-12* proficient cells [126, 127, 134-136].

Despite the high sequence identity between human and murine caspase-12, in the majority of human population caspase-12 is truncated due to a single nucleotide polymorphism that introduces a premature stop codon [136]. However, 20% of

individuals of African descent have a point mutation that replaces the stop codon resulting in the synthesis of the full length caspase-12. African individuals diagnosed with severe sepsis are homozygous for the SNP encoding the full length variant and consequently this mutation correlates with increased mortality rates compared to the individuals harboring the stop codon mutation. The full length caspase-12 is associated with attenuated cytokine production (IL-1β, IFNγ, TNFα) in response to endotoxin and decreased NF-κB activation in response to TNFα, strongly suggesting that human caspase-12 functions as dominant regulator of inflammatory responses and innate immunity [136].

Likewise, murine caspase-12 appears to have an inflammatory role as human caspase-12. *Caspase-12* deficiency in mice results in enhanced parasite clearance during blood-stage *Plasmodium* infection and hyper-production of NF-κB and IFNγ [137]. This response is NF-κB and IFNγ-dependent as systemic inhibition of NF-κB or neutralizing antibodies against IFNγ reversed the increased resistance of the knockout mice to malaria infection. Mechanistically, caspase-12 was proposed to associate with the IKKα/β kinases, thus preventing IKKγ from binding to the complex and ultimately inhibiting NF-κB signaling [137]. Moreover, mice lacking *Caspase-12* were shown to be more resistant to polymicrobial sepsis than wild-type mice due to more efficient bacterial clearance [127]. Mechanistically, caspase-12 dampens the production of proinflammatory cytokines (IL-1β and IL-18) by associating with and blocking caspase-1 activation concomitant with the downregulation of downstream cytokine production [127]. Nevertheless, the inhibitory effect is independent of caspase-12 catalytic activity, since catalytically inactive caspase-12 associates and as well blocks caspase-1 activity [127].

Furthermore, caspase-12 has been proven to be an important modulator of intestinal mucosa immunity. *Caspase-12* proficient enterocytes are blunted in their ability to activate NOD and downstream NF-κB signaling and therefore cannot produce

antimicrobial peptides and cytokines in response to bacterial infection [138]. *Caspase-12* ablation results in efficient bacterial clearance and less severe pathology, independently of caspase-1 activity [138]. Thus, in addition to its role in inhibiting caspase-1 activity in macrophages, in the intestinal epithelium caspase-12 functions as negative regulator of defensin and cytokine production by suppressing NOD signaling [138]. Lastly, caspase-12 is critical for the induction of inflammation in the gut after injury [119]. *Caspase-12* deficient mice are more resistant to acute and chronic colitis induced by DSS and show exaggerated epithelial cell compensatory proliferation. However, the increased inflammation and tissue repair renders them more vulnerable to colitis-associated cancer induced by AOM/DSS [119].

Overall, the presence of caspase-12 is linked to immunosuppressive responses to pathogenic bacteria and parasites rendering both mice and humans prone to infection. However, in the intestinal tract and under conditions that trigger chronic inflammation and inflammation-associated tumorigenesis, caspase-12 is required to restrict excessive inflammation and proliferation in the colon and thus to maintain intestinal homeostasis

Aim of Study

Inflammatory bowel diseases (IBD), including Crohn's Disease and Ulcerative Colitis, are chronic inflammatory conditions of the gastrointestinal tract and are strongly associated with the development of colorectal cancer. A large amount of evidence corroborates the existence of a major influence of innate immunity, proper activation of PRRs, autophagy and UPR pathways in the development of IBDs. NF-κB pathway is the key regulator of inflammation and is strongly associated with IBD. IKKα, one of the core elements of this pathway, has been shown by several independent studies to suppress inflammation in response to a variety of stimuli. This study aimed to investigate the role of IKKα in colonic inflammation by using a mouse model where IKKα is inactive. It demonstrates that IKKα activation is required to suppress excessive inflammation in response to chemical factors, such as dextran sodium sulfate, that induce colon injury.

To functionally examine the role of IKKα activation during inflammatory conditions in the colon, the response of *Ikk*α kinase-dead ($Ikk\alpha^{AA/AA}$) knock-in mice to DSS-induced colitis was studied. To investigate the cell type specific functions of this kinase tissue specific *Ikkα* knockout ($Ikk\alpha^{\Delta IEC}$ and $Ikk\alpha^{\Delta mye}$) mice were used.

2. Material and Methods

2.1 Materials

2.1.1 Mouse models

$Ikk\alpha^{AA/AA}$ Knock-in mice

A targeting vector was designed to place a neomycin resistance cassette flanked by loxP sites (floxed, fl) into the exons 176 and 180 of the *Ikkα* gene [61]. Serines 176 and 180 were converted to alanines and the targeted vector was introduced into ES (Embryonic Stem) cells. Cre-expressing vector was brought into the $Ikk\alpha^{AA}$ positive clones to disrupt the neomycin cassette and such clones were injected into female's blastocysts to generate chimeric mice. These females were then crossed with males to give rise to heterozygous $Ikk\alpha^{AA/+}$ mice that were then intercrossed to obtain the homozygous $Ikk\alpha^{AA/AA}$ mutants.

$Ikk\alpha^{fl/fl}$

Mice harboring a loxP flanked *Ikkα* allele were created by inserting a neomycin cassette fragment with loxP sites into the exons 6 and 9 of the gene [139]. The neomycin cassette was deleted by introducing a Cre-expressing vector and thus following Cre recombination the exons 6 to 8 were deleted resulting in a frame shift for *Ikkα*.

***NfκB2*-deficient mice**

These mice were generated by replacing the exons 1b to 9 of the *NfκB2* gene, which contains the translation site and part of the Rel homology domain, with a targeting vector containing a phosphoglycerate kinase-promoter neomycin resistance cassette [140]. The

resulting vector was introduced into ES cells and clones containing a single copy insertion of the neomycin cassette were used to generate independent knockout lines.

Villin-Cre

The Cre recombinase is expressed under the control of the mouse *Villin 1* promoter [141]. Intercrossing with a strain harboring a loxP-flanked gene of interest results in Cre-mediated recombination and enterocyte-specific deletion of the targeted gene.

Lysozyme M-Cre

Mice expressing Cre in myeloid cells were generated by targeted insertion of a vector expressing the Cre cDNA into exon 1 of the *M Lysozyme* locus [142]. When crossed with mice harboring loxP site flanked gene of interest Cre-mediated recombination results in excision of the trageted gene in the myeloid lineage (monocytes, macrophages and granulocytes).

***Caspase-12*-Knockout mice**

Caspase-12 knockout mice were generated by targeted replacement of exon 2 of *Caspase-12* gene by a cassette consisting of the β-galactosidase gene and the neomycin resistance gene [127]. The resulting vector was introduced into ES cells and clones obtained with the disrupting allele were injected into blastocysts to generate chimeric mice.

2.1.2 Chemicals and reagents

All chemicals and reagents used are listed in the *Appendix A.1*

2.2 Methods

2.2.1 Animal experiments

Induction of experimental acute colitis

In order to induce acute colitis in mice dextran sulfate sodium (DSS, MP Biomedicals) was administrated in the drinking water at concentrations between 2.5 and 3.5 % (w/v). The mice were subjected to the DSS treatment for 5 days followed by 5 additional days of normal drinking water.

IL-18 treatment

For IL-18 rescue experiments, recombinant IL-18 (MBL International) was injected intra-peritoneally at a concentration of 0.5 g/mouse, dissolved in cold PBS (Invitrogen), every day during the whole acute DSS treatment. 25 g of lyophilized IL-18 were reconstituted with 250 µl of ice-cold distilled water on ice.

Bone marrow isolation

For isolation of the bone marrow donor mice with the same genetic background as the recipient mice, were sacrificed and femoral bones were removed carefully and placed in cold PBS. Then under sterile conditions, bones were cut on the top and bottom, flushed with sterile PBS using a 25 G needle, resuspended and filtered with a 70 µm strainer to get rid of the skeletal parts and stromal cells. Total cell number was counted and then the cells were pelleted by 5 minutes centrifugation at 500 g 4°C. Resuspension was done in the appropriate buffer according to the purpose of the isolation.

Irradiation and transplantation

For the transplantation to be accomplished, recipient mice were irradiated with a lethal dose of 9 Gy to get rid of the immune cells and were injected with $4*10^6$ cells in 100 μl PBS in the tail vein. The transplanted mice were given broad spectrum antibiotic (Ciprobay, Bayer) at a concentration of 1 mg/ml for two weeks in the drinking water, in order to avoid possible infections. After two weeks, the antibiotic water was replaced with normal drinking water and the intestinal microflora of the transplanted mice was reconstituted by placing feces from other mice into the cages, two weeks before the start of experiments.

Blood serum (culture media supernatant)

For determination of secreted cytokines blood serum was used. The blood was collected from the heart, left in room temperature for 10 minutes to clot and then centrifuged in EDTA-free tubes for 5 minutes at 10.000 g to precipitate the blood cells. The upper layer containing the serum was then collected, aliquoted and stored at -80 ˚C until use.

Genotyping of mice

For the genotyping of mice a very small piece of tail was obtained and digested in 95 μl tail lysis buffer (*Table 2:1*) with additional 5 μl of Proteinase K (Qiagen) overnight at 60˚C.

Tail Lysis Buffer	
Tris HCl (Roth)	100 mM (PH 8.5)
NaCl (Sigma)	200 mM
SDS (Roth)	0.20%
EDTA (Roth)	5 mM

Table 2:1 Tail lysis buffer recipe

The following day, the tails were heated for 10 minutes at 95 ˚C, for proteinase K inactivation, then diluted with 900 µl of distilled water and subsequently centrifuged for 15 minutes at 13.2 Krpm. Supernatants were then used for Polymerase Chain Reaction (PCR). The general PCR recipe is as following (*Table 2:2*):

PCR reaction mix	
10X PCR buffer	2 µl
50 mM $MgCl_2$	0.6-0.8 µl
100 mM dNTP mix	0.4 µl
20 pMol forward primer	0.5 µl
20 pMol reverse primer	0.5 µl
Taq polymerase (5 U/µl)	0.15 µl
DNA	1-1.5 µl
Distilled water	13.45-14.15 µl
Total volume	20 µl

Table 2:2 General PCR reaction mix recipe

All above reagents were obtained from Invitrogen. All reaction conditions for each gene are given in the *Appendix A.2.*

Each sample was loaded into a 2 % agarose gel (*Table 2:3*) containing 2.5 % ethidium bromide and the bands were visualized under UV light.

Agarose Gel Buffer 50X	
Tris (Roth)	2 M
Acetic acid (Sigma)	5.71%
EDTA (Roth)	50 mM

Table 2:3 Agarose gel buffer recipe

2.2.2 Primary cell isolation and culture

Intestinal epithelial cell (IEC) isolation

After the mice were sacrificed, the intestine was divided into 4 parts (duodenum, jejunum, ileum and colon) and the part/s of interest was/were cleaned from feces with PBS. The intestinal parts were then cut-open longitudinally and divided in half. One half was used for histological analysis, the other was rolled up to make a 'swiss-roll' [143], fixed over-night at 4˚C in 4 % paraformaldehyde (PFA), dehydrated and embedded in paraffin, while the other half was used for epithelial cell isolation. For the cell isolation, the half of the intestine was further cut in small pieces, incubated in 8 ml of pre-warmed HBSS (Invitrogen) supplemented with 30 mM EDTA (Roth) and shacked for 10 minutes gently at 37˚C in order to remove epithelial cell physically. Next, the 50 ml falcon tube containing the above tissue was strongly vortexed for 30 seconds, to detach epithelia and lamina propria, and placed directly on ice. After 30 seconds approximately, lamina propria was precipitated while epithelial cells remained in the supernatant. Supernatant was slowly removed and transferred to a new 15 ml falcon tube for further centrifugation for 5 minutes at 1.5 Krpm at 4˚C. The pellet was resuspended in cold 2 ml PBS and divided into three 1.5 ml tubes that were subsequently centrifuged at 5 Krpm at 4˚C for 5 minutes. Washouts were discarded and pelleted epithelial cells were frozen in liquid nitrogen and stored at -80˚C until use.

For further analysis whole parts of intestinal mucosa (mostly distal part of each intestinal part) were cut in small pieces, schock frozen in liquid nitrogen and stored as the epithelial cells at -80˚C.

IEC isolation from colons and overnight culture

Following mice sacrifice, colons were removed and washed with RPMI1640 (GIBCO) supplemented with penicillin/streptomycin and 50 μg/ml gentamicin. Colons were then cut in small pieces and incubated at 37˚C for 30 minutes with gentle shaking in pre-warmed RPMI medium supplemented with penicillin, streptomycin, 50 μg/ml gentamicin, 5 mM EDTA pH:8, 3 % FCS, 0.145 mg/ml DTT (Sigma) (reffered as full RPMI medium). Next, colons were vortexed for 30 seconds, to detach epithelia and lamina propria, placed on ice for 30 seconds, to allow lamina propria to precipitate while the epithelial cells remained in the supernatant. Supernatants were then filtered with 100 μM strainers directly into a 50 ml falcon and centrifuged at 1.5 Krpm for 5 minutes at 4˚C. IEC pellets were then resuspended in 30 % Percoll (GE Healthcare), for efficient density separation, and centrifuged at 500 g for 5 minutes at 4˚C. The top layer containing the IECs was removed carefully and washed 2 times in full RPMI medium to remove remaining Percoll. Finally, pelleted IECs were resuspended in RPMI medium supplemented with 10 % FCS, penicillin, streptomycin, gentamycin, L-glutamine, and 10 % FCS, counted and plated on 96-well plates pre-coated with collagen type I (GE Healthcare). 100.000 epithelial cells were plated and left overnight in the incubator (37˚C and 5 % CO_2).

For coating 96-well plates with collagen type I (GE Healthcare), collagen was diluted to a concentration of 10 μg/ml in 0.02 N acetic acid and 5 μg of collagen per cm^2 was required for the coating. The collagen-coated plates were left at 37˚C for 30 minutes and then washed 2 times with PBS. Supernatants and cells were collected 24 hours later and analyzed by ELISA or immunobloting.

Isolation of lamina propria cells

For isolation of lamina propria cells, the remaining colon pieces (after IEC isolation) were recovered and incubated with RPMI supplemented with penicillin/streptomycin, + 0.1 mg/ml liberase TL (Roche) + 0.05 % DNase (Roche) for 30 minutes at 37˚C with gentle shaking. Supernatants were then filtered with 70 µm strainers and washed two times with RPMI supplemented with penicillin/ streptomycin and 10 % FCS. Cells were then sorted with BD FACS Aria into different cell populations.

Flow cytometry assisted cell sorting (FACS)

For cell sorting cells were washed in FACS buffer (5 % FCS/PBS). Before staining for the cell surface markers, cells were blocked for unspecific binding with FcR block (diluted 1:100 in FACS buffer) for 10 minutes at 4˚C and then washed once with PBS and pelleted at 500 g for 5 minutes. Then cells were stained with the desired antibodies (*Appendix A.3.3*) in FACS buffer at 4˚C for 20 minutes, in the dark. Cells were washed 2 times in PBS, pelleted at 500 g for 5 minutes, resuspended in FACS buffer and subjected for sorting with BD FACS Aria.

Cell counts

Cells were harvested with 0.25 % Trypsin/EDTA (Invitrogen) and counted with a hematocytometer in the presence of 1 % trypan blue (Sigma). Cells that were not stained blue were considered alive.

2.2.3 Histology

Hematoxylin & Eosin (H & E) staining

For closer examination of tissues H & E staining was performed. The organ/s was/were isolated, fixed in 4 % PFA dehydrated and embedded in paraffin. The paraffin embedded tissues were then cut 3 µm thick, fixed on glass slides (Thermo Scientific) and dry out either over night at room temperature either at 37˚C for 2 hours. The slides were rehydrated following the procedure below (*Table 2:4*):

Rehydration Procedure	
2X xylol (X-TRA Solv, Medite)	10 min each
2X 100% ethanol	2 min each
2X 96% ethanol	2 min each
2X 80% ethanol	2 min each
2X 70% ethanol	2 min each
2X 50% ethanol	2 min each
PBS	5 minutes

Table 2:4 Rehydration procedure

Slides were stained with ready to use Haematoxylin (Vector Laboratories) for 1 minute and washed well with distilled water. Next, slides were stained with Eosin (Sigma) for 10 seconds, rinsed twice in distilled water and dehydrated with the following procedure (*Table 2:5*):

Dehydration Procedure	
1X 50% ethanol	30 seconds
1X 70% ethanol	30 seconds
1X 80% ethanol	30 seconds
1X 96% ethanol	30 seconds
1X 100% ethanol	30 seconds
2X xylol (X-TRA Solv, Medite)	5 minutes each

Table 2:5 Dehydration procedure

Afterwards, slides were air-dried, mounted with mounting medium (Vector Laboratories) and then covered with cover slides.

Eosin solution: 1 % Eosin + 15 drops of acetic acid in 200 ml of dH_2O

DNA fragmentation Assay

This assay is based on Terminal deoxynucleotidyl Transferase (TdT)-mediated dUTP nick-end-labeling (TUNEL). This enzyme catalyses the incorporation of fluorescein labelled dUTP at the free 3'-OH end of fragmented DNA. The fluorescein labelled DNA can be visualised by fluorescence microscope equipped with FITC filters. The staining was carried out using ApoAlert®DNA Fragmentation Assay (Clontech) *in situ* in tissue sections. Tissue sections were deparaffinised and rehydrated as described in H & E staining section. Sections were incubated for 5 minutes in 0.85 % sodium chloride solution and afterwards washed with PBS. Then, the sections were fixed in 4 % PFA in 0.1 % Diethylpyrocarbonate (DEPC) (Sigma) distilled water for 15 minutes in room temperature. After one more wash with PBS, samples were incubated in 4 % DEPC in distilled water for 30 minutes at 4˚C followed by a step of proteinase K (20 µg/ml) digestion for 5 minutes at room temperature. Following PBS wash, tissues were incubated with equilibration buffer for 15 minutes followed by another incubation with the enzyme/buffer/nucleotide mix (30 µl equilibration buffer, 3.3 µl nucleotide mix , 0.33 µl TdT enzyme), in the dark at 37˚C for 1 hour. The reaction was stopped with 2x SSC buffer for 15 minutes, in the dark and washed twice with PBS. Samples were then covered with DAPI containing mounting medium (ProLong Gold, Invitrogen) and stored at 4˚C in the dark.

Immunohistochemistry

After slides were deparaffinized and rehydrated (*Table 2:4*), permeabilization protocol followed. For nuclear and cytoplasmic stainings the slides were heated up in the microwave for 20 minutes in unmasking solution (VectorLab), cooled down to room temperature and washed in PBS. Blocking of endogenous peroxidases was achieved by incubating the slides in 3 % H_2O_2 / PBS for 5 minutes at room temperature. The slides were then blocked with 3 % BSA / PBS + streptavidin (VectorLab) for 30 minutes at room temperature in order to avoid unspecific binding of the primary antibody. After blocking the slides were incubated with the primary antibody + 3 % BSA/PBS + biotin (VectorLab) in different conditions (*Appendix A.3.2*). Subsequently, slides were washed 3 times in PBS, 5 minutes each washing step, and then incubated for 30 minutes at room temperature with the appropriate secondary antibody conjugated with biotin molecule. Following 3 washing steps in PBS, slides were incubated with ABC (VectorLab) complex containing 2 drops of Avidin DH (Reagent A) and 2 drops of its paired biotinylated (horseradish peroxidase) enzyme (Reagent B) for 30 minutes at room temperature. After washing with PBS colour reaction with DAB kit (VectorLab) followed. The reaction was done by mixing the three components of the kit (2 drops of buffer + 2 drops of hydrogen peroxide solution + 4 drops of DAB (3, 3'-diaminobenzidine)) just before starting the developing. The colour reaction was observed under the microscope and was stopped with distilled water. Nuclei were stained with haematoxylin for 1 minute (counter staining). After extensive washes with distilled water sections were dehydrated (*Table 2:5*), air dried, mounted with mounting medium (VectorLab) and covered with cover slides.

Immunofluorescence

For immunofluorescence staining sections were first deparaffinized, rehydrated and then tissues were permeabilized. For staining of surface antigens, tissues were incubated with 0.3 % Triton / PBS for 30 minutes at 4˚C and for nuclear and cytoplasmic antigens tissues were microwaved in antigen unmasking solution (VectorLab) for 20 minutes. Tissues were then cooled down at room temperature, washed 3 times in PBS and blocked with 3 % BSA/PBS for 30 minutes to avoid unspecific binding of the antibody. Primary antibody coupled with a fluorophore was incubated overnight at 4˚C. Next day, tissues were washed 3 times with PBS and then covered with DAPI conservation medium (ProLong Gold, Invitrogen) for counter staining of the nucleus. Tissues were left for 30 minutes at 4˚C and then used for imaging.

2.2.4 RNA Analysis

RNA isolation from cells and tissues

RNA from tissues or cells was obtained using the RNeasy Kit (Qiagen). Frozen tissue samples or pelleted cells were directly placed in RLT buffer containing 1 % β-mercaptoethanol and homogenized either using electronic homogenizer (for tissues) or pistils (for cells). The procedure of RNA isolation with Qiagen RNeasy Kit is described in the manufacturer's manual. RNA was eluted in RNAase free water and stored in -80˚C until use.

cDNA Synthesis

For the synthesis of the first complementary DNA strand was performed using oligo dT primer and reverse transcriptase. Upon isolation, purity and concentration of RNA was determined. Generally, 1 µg of RNA was used or less according to the RNA concentration.

RNA was incubated with 1 µl of Oligo dT (50 µM, Invitrogen) and 1 µl of dNTP-mix (10 mM, Invitrogen) and filled up to a total volume of 13 µl with RNase-free water for 5 minutes at 65˚C for annealing of the dT primers to mRNAs. The samples were then shortly spin-down and incubated on ice for 5 minutes. Master-mix (*Table 2:6*) of 7 µl was added in every sample to make 20 µl total volume and incubated at 42˚C for 1 hour. Finally, the samples were diluted 1:4 with RNase-free water and stored at -20˚C until use.

Master Mix (Invitrogen)	
5X buffer	4 µl
0.1 M DTT	1 µl
40 Units/µl RNase OUT	1 µl
200 Units/µl SuperscriptII	1 µl
Total volume	7 µl

Table 2:6 Reverse transcription master mix

qRT - PCR (quantitative - real time - polymerase chain reaction)

Primers specific for each gene were designed using the Primer Express™ software (*primer sequences are listed in Appendix A.4*). The lyophilized primers were reconstituted with dH_2O to a concentration of 100 µM and then combined to a final concentration of 20 µM to make a 10X solution. For the qRT-PCR reaction, SYBR Green (Roche) master mix (*Table 2:7*) was used with the following mixture for every sample:

SYBR Green Master Mix (Roche)	
dH_2O	9.5 µl
cDNA	0.5 µl
SYBR Green master mix	12.5 µl
10X solution Primer	2.5 µl
Total volume	25 µl

Table 2:7 Real-Time PCR master mix

The analysis of the reaction was performed on a standard program (*Table 2:8*):

Real-Time PCR standard program X 40 cycles	
50°C	2 minutes
95°C	10 minutes
95°C	30 seconds
60°C	1 minute
25 °C	maintain

Table 2:8 Real-Time PCR program

The reaction was done on StepOnePlus Real Time PCR system (Applied Biosystems) and the results were analyzed with StepOne Software v2.0.2 and normalized by the expression levels of the housekeeping gene *CyclophilinB*, as an internal control, with the following formula:

Expression = 2 ^ (CT (housekeeping) – CT (gene))

2.2.5 Protein Analysis

Protein extraction from IECs and total intestinal mucosa

Epithelial cell pellets removed from -80˚C and directly placed in liquid nitrogen, were lysed in 90-150 μl of ice-cold lysis buffer according to the amount of pelleted cells. The pellet was mechanically homogenized with a micro-pistill, as well as up and down pipetting, and left on ice for 15 minutes to ensure complete lysis. Subsequently, cell debris was removed by 15 minutes centrifugation at 13.3 Krpm at 4˚C and the proteins lysates were removed and placed to into 1.5 ml eppi and stored at -80˚C until further use.

For total mucosa samples the lysis was done with an electronic homogenizer within an appropriate lysis buffer (*Table 2:9*) according to the size of the frozen intestinal piece. The same procedure was followed also for the IEC isolation.

Protein Lysis Buffer (1X):	
NaCl (Sigma)	250 mM
Tris (pH 7.5) (Roth)	50 mM
EDTA (Roth)	30 mM
Sodiumpyrophosphate (Sigma)	25 mM
Triton-X 100 (Sigma)	1.00%
EGTA (Sigma)	30 mM
Glycerol (Merck)	10.00%
NP40 (Sigma)	0.50%
DTT (Sigma)	1 mM
β-glycerophosphate (Sigma)	50 mM
Sodium fluoride (Sigma)	25 mM
Sodium orthovanadate (Sigma)	5 mM
PMSF (Sigma)	2 nM

Table 2:9 Protein lysis buffer recipe

Measurement of protein concentration

Determination of protein concentration was accomplished spectrophotometrically, at a wavelength of 595 nm using Bradford assay (Biorad) and BSA to prepare a standard curve. Protein samples were normalized based on their concentration, diluted in 1X laemmli buffer (*Table 2:10*) and boiled for 5 minutes at 95˚C.

Laemmli Buffer (5X):	
Glycerol (Merck)	40% (v/v)
Tris-HCl (pH 6.8) (Roth)	200 mM
SDS (Roth)	8% (v/v)
Bromophenole blue (Sigma)	0.01% (w/v)
β-mercaptoethanol (Sigma)	5% (v/v)

Table 2:10 Laemmli buffer recipe

Western blot analysis

For immunoblot analysis 6-15% SDS resolving gels were prepared depending on the size of proteins to be analysed (*Tables 2:11-2:12*) and proteins were run in 1X running buffer (*Table 2:13*).

%	Acrylamide	Resolving Gel Buffer	dH_2O	10% APS
6	1.5 ml	2.51 ml	5.81 ml	50 µl
7	1.75 ml	2.51 ml	5.685 ml	50 µl
7.5	1.875 ml	2.51 ml	5.56 ml	50 µl
8	2 ml	2.51 ml	5.435 ml	50 µl
10	2.5 ml	2.51 ml	4.935 ml	50 µl
12	3 ml	2.51 ml	4.435 ml	50 µl
15	3.75 ml	2.51 ml	3.685 ml	50 µl
		for 10 ml resolving gel		

Table 2:11 Resolving gel recipes

Resolving Gel Buffer	Stacking Gel Buffer
27.23 g Tris	6 g Tris
80 ml dH_2O	60 ml dH_2O
pH:8.8	pH:6.8
6 ml 10% SDS	4 ml 10% SDS
dH_2O up to 150 ml	dH_2O up to 100 ml

Table 12:12 Resolving and stacking gel buffer recipes

10X Running Buffer	
Glycine	144 g
Tris	30.3 g
SDS	10 g
dH_2O	1 L

1X Running Buffer		
10X Running buffer	100 ml	
dH_2O	800 ml	for 1 L

Table 2:13 10X and 1X Running buffer recipes

The transfer of the protein gel was performed using the Mini-Trans-Blot cell system (Biorad) for the small gels (up to 15-well gels) or Criterion ™ Blotter system for the big gels (26-well gels) (Biorad) in 1X transfer buffer (*Table 2:14*) for 2 hours at 350 mA onto a PVDF membrane (Immobilion P, Zefa Laborservice), which previously has been activated for 1 minute in methanol (Merck). Following transfer, the PVDF membrane was air-dried for 5 minutes and then incubated in 3 % skim milk (Fluka)/PBST for 30 minutes at room temperature; a blocking step to minimize unspecific binding of the primary antibody. The membrane was incubated with the appropriate primary antibodies (*Appendix A.3.1*), then washed with PBST (PBS + 0.1 % Tween 20 (Sigma)) for 30 minutes, refreshing the buffer every 10 minutes and incubated with appropriate horseradish peroxidase (HRP)-conjugated secondary antibody for 30 minutes in 3% skim milk/PBST at room temperature. After incubation with the secondary antibody membrane was washed again for 30 minutes in PBST, refreshing the buffer every 10 minutes, dried on Whatman filter paper. The chemiluminescence reaction was accomplished by incubating the membrane for 3-5 minutes at room temperature with ECL solution Super Signal West Femto/Pico (Thermo Scientific) and signal was detected on an X-ray film (Thermo Scientific) for an appropriate period of time depending on the signal strength.

10X Transfer Buffer	
Glycine	144 g
Tris	30.3 g
dH_2O	1 L

1X Transfer Buffer		
Methanol	200 ml	
10X Transfer buffer	100 ml	
dH_2O	700 ml	for 1 L

Table 2:14 10X & 1X transfer buffer recipes

EMSA (3' DY682 infrared marker labeled oligonucleotide)

Evaluation of NF-κB binding activity, in a non-radioactive manner, was performed by using Odyssey Infrared EMSA Kit (LICOR) according to the manufacturers' instructions.

10-15 µg of proteins were incubated with 1 µM 3' DY682 labeled NF-κB consensus oligos (5'-GGA TCC TCA ACA GAG GGG ACT TTC CGA GGC CA-3') for 30 minutes at room temperature, protected from light. Then, samples were loaded in a 5 % acrylamide gel, run for 2 hours and finally bands were visualized with Odyssey Infrared imaging system (Li-COR Biosciences).

Co-immunoprecipitation

In order to identify protein-protein interaction co-immunoprecipitation was performed. 500 µg of total protein lysates were used to precipitate the protein of interest (X protein) with a specific antibody against it. The antibody of interest and total protein lysates were incubated in 500 µl PBS (low stringency buffer) total volume, overnight, rotating at 4˚C to allow for the possible complex to form. Next day, protein A sepharose beads (GE Healthcare) were washed 3 times in cold PBS and protein lysates with the antibody were applied to the beads. The above mixture was incubated at 4˚C, rotating, for 1 hour (not longer, as this might cause unspecific binding of the proteins to the beads). Beads-antibody-protein lysates were then washed 3 times with 1X lysis buffer (high stringency buffer, *Table 2:9*) and mixture was collected by 3 Krpm centrifugation for 5 minutes. Afterwards, 30 µl of laemmli buffer + 5 % mercaptoethanol was added to the precipitated beads, heated 10 minutes at 95˚C and centrifuged maximum at 13 krpm for 5 minutes. The supernatants were then subjected to immunobloting (as described above) for investigation of potential protein-protein interaction.

ELISA

For analysis of cytokines in the blood serum or cell culture supernatants enzyme-linked immunosorbent assay (ELISA) was used. The ELISA kits used are listed in the *Appendix*

A.1. Briefly, ELISA plates coated with capture antibody were washed and blocked for 1 hour at room temperature. After blocking and washing steps, plate was incubated for 2 hours at room temperature with the samples and standards diluted in the dilution buffer. Then, plates were washed and incubated with the detection antibody, streptavidin and substrate mix. The colour reaction was detected by a spectrophotometer using a plate reader at 450 nm.

3. Results

3.1 IKKα is essential for mucosa healing after DSS-induced injury

Physiological levels of inflammation are protective, while extreme levels are deleterious and can be the cause of Inflammatory Bowel Disease (IBD), such as Crohn's Disease and Ulcerative Colitis. In several studies, IKKα has been shown to confer resolution of inflammation [62, 65]. To functionally investigate the role of IKKα in intestinal homeostasis a knock-in mouse model that lacks inducible kinase activity due to the presence of alanines instead of serines in the activation loop of IKKα was used [61]. Mice homozygous for the mutated allele, *Ikkα*$^{AA/AA}$ knock-in mice, were subjected to acute tissue injury and colitis by adding 3.5% dextran sulphate sodium (DSS) in the drinking water for 5 days, followed by 4 days of recovery with normal drinking water (*Figure 3.1 A*). In sharp contrast to *Ikkα*$^{wt/wt}$ mice, which recovered once DSS was omitted, *Ikkα*$^{AA/AA}$ mutants showed increased susceptibility to the treatment and suffered from continued body weight loss, diarrhea and rectal bleeding, on day 7 until day 9 (*Figure 3.1 B*). Due to the severe weight loss of *Ikkα*$^{AA/AA}$ mice and to ethical reasons both groups had to be sacrificed on day 9. Hematoxylin & eosin (H & E)-stained colon sections from both genotypes were evaluated for histological changes. Histolopathological alterations were observed in DSS-treated colons from both *Ikkα*$^{wt/wt}$ and *Ikkα*$^{AA/AA}$ mice, characterized by crypt loss, ulceration and infiltration of leukocytes (*Figure 3.1 C-D*). In marked contrast to *Ikkα*$^{wt/wt}$ mice, which showed signs of re-epithelialisation, *Ikkα*$^{AA/AA}$ mutants displayed severe signs of injury and defects in epithelial reconstruction. The *Ikkα*$^{AA/AA}$ mutant epithelium was characterized by few if any crypts left throughout the entire colon, extensive ulceration resulting in complete destruction of the normal architecture of the tissue and massive infiltration of immune cells in the lamina propria and submucosa

(*Figure 3.1 C*). Notably, scoring of these histological parameters confirmed that colitis and number of ulcers in *Ikkα*$^{AA/AA}$ mice were significantly elevated compared to DSS-treated *Ikkα*$^{wt/wt}$ animals (*Figure 3.1 E-F*). Collectively, these results demonstrate that IKKα-dependent signaling is essential in maintaining intestinal tissue integrity during DSS-induced acute colitis

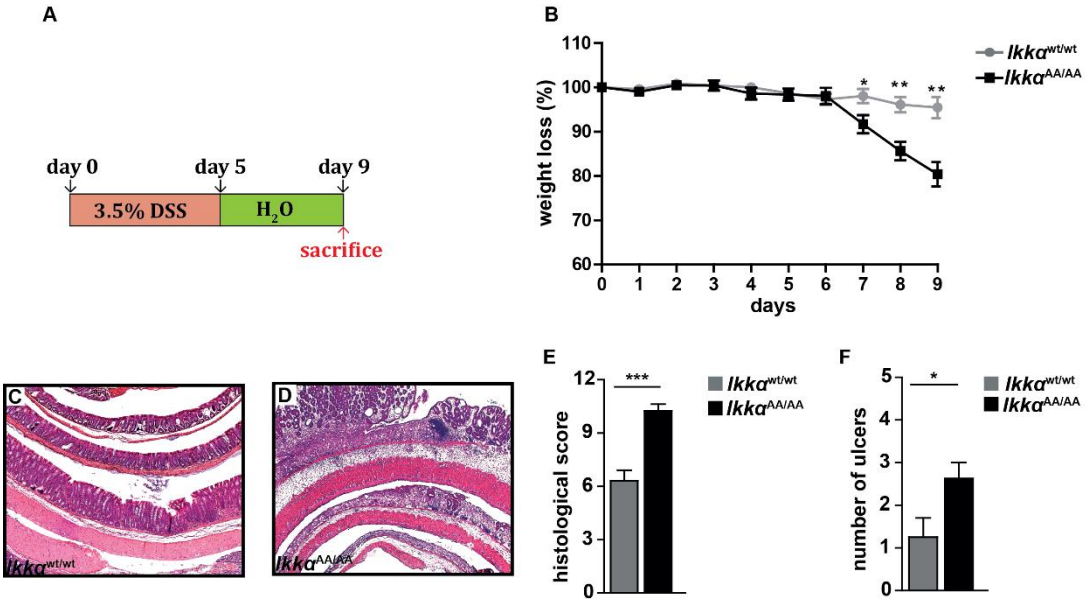

Figure 3.1: Increased epithelial damage and infiltration of immune cells in Ikkα$^{AA/AA}$ colons after DSS challenge. ***(A)*** *Schematic overview of the acute DSS-induced model. 3.5% DSS was given in the drinking water for 5 days and then changed to normal water for additional 4 days.* ***(B)*** *Weight loss during DSS (3.5%) colitis in Ikkα$^{wt/wt}$ and Ikkα$^{AA/AA}$ mice. Representative histologies from H&E-stained colons of Ikkα$^{wt/wt}$* ***(C)*** *and* ***(D)*** *Ikkα$^{AA/AA}$ mice 4 days after termination of DSS administration.* ***(E)*** *Histological scoring based on loss of crypts, infiltration of immune cells into the mucosa, submucosa and muscle layer.* ***(F)*** *Number of ulcers. Data are expressed as mean ± SEM; n≥6; * p<0.05, *** p<0.0001 by t test.*

3.1.1 Increased inflammation in the colons of *Ikkα*$^{AA/AA}$ mice

To obtain further evidence of this inflammatory phenotype in the *Ikkα*$^{AA/AA}$ mutants, given the significant increases in histological inflammation obtained above, RNA was isolated from whole colonic mucosa on day 9 after initiation of DSS administration and real-time

PCR was performed to examine the expression levels of proinflammatory genes including, *Il1β*, *Tnfα*, *Il6*, *Cxcl1*, *Cxcl2* and *Ccl2*. Consistent with the histological parameters discussed above, whole mucosa from *Ikkα*$^{AA/AA}$ treated colons contained higher mRNA levels coding for IL-1β, TNFα, IL-6, CXCL1, CXCL2 and CCL2 compared to the *Ikkα*$^{wt/wt}$ treated colons (*Figure 3.2 A*). Consistently, *Ikkα*$^{AA/AA}$ DSS-treated mice presented enhanced expression of COX-2 and matrix metalloproteinase-9 (MMP-9) (*Figure 3.2 B*). Thus, the above data demonstrate the fundamental role of IKKα activation in hindering excessive inflammatory responses upon DSS-induced injury.

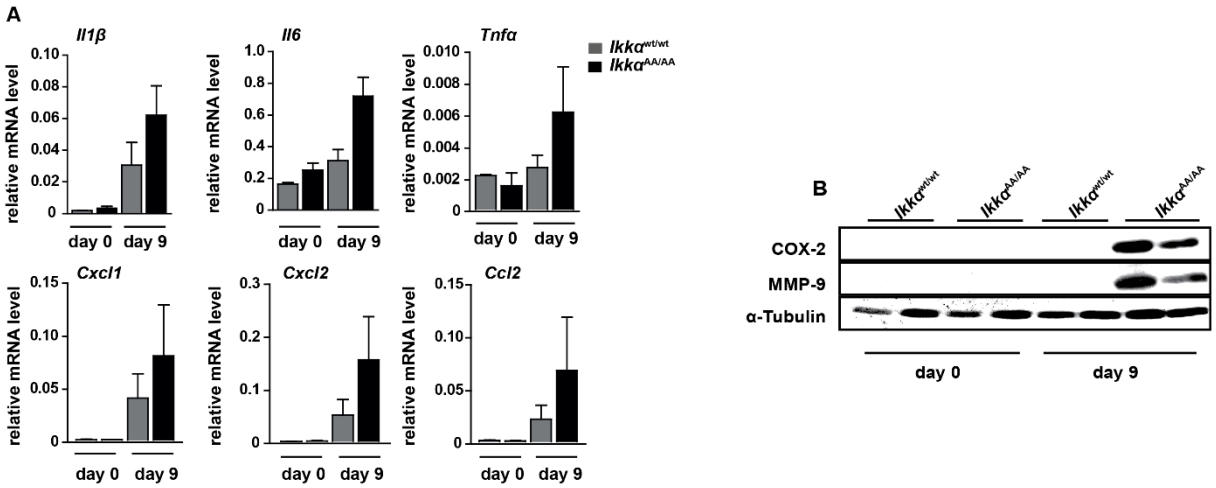

Figure 3.2: Enhanced inflammation in the colons of Ikkα$^{AA/AA}$ mice. (A) *Expression of inflammatory genes. Relative mRNA expression levels were quantified in whole colonic mucosa tissue of mice on day 0 and 9 of DSS regimen. The mRNA levels were quantified by real-time PCR and normalized to the level of cyclophilinB mRNA (n ≥ 4).* ***(B)*** *COX-2 and MMP-9 expression in whole colonic extracts on day 0 and 9 of DSS regimen. COX-2 and MMP-9 expression were determined by western blot (WB).*

3.2 IKKα signaling in IECs is crucial for tissue repair

In order to distinguish whether IKKα functions in IEC or hematopoietic cells to control DSS-induced tissue damage adoptive transfer experiments were performed (*Figure 3.3 A-B*). *Ikkα*$^{wt/wt}$ and *Ikkα*$^{AA/AA}$ bone marrow was transplanted into *Ikkα*$^{wt/wt}$ and *Ikkα*$^{AA/AA}$

lethally irradiated recipients. Eight weeks after bone marrow transplantation, mice were subjected to DSS treatment, as shown above (*Figure 3.1 A*), and colons were assessed for signs of histopathology in H & E-stained colon tissue sections. In line with the previous results (*Figure 3.3 A*), *Ikkα*$^{AA/AA}$ mice receiving *Ikkα*$^{AA/AA}$ bone marrow displayed significantly worse symptoms of colitis compared to *Ikkα*$^{wt/wt}$ mice receiving *Ikkα*$^{wt/wt}$ bone marrow (*Figure 3.3 A-B*). Severity and incidence of colitis was greater in *Ikkα*$^{AA/AA}$ mice receiving *Ikkα*$^{wt/wt}$ bone marrow compared to *Ikkα*$^{wt/wt}$ mice that received *Ikkα*$^{wt/wt}$ bone marrow, suggesting that IKKα activation in a non-hematopoietic compartment, likely the epithelium, is critical for protection against colitis. In contrast, *Ikkα*$^{wt/wt}$ mice transplanted with *Ikkα*$^{AA/AA}$ bone marrow presented with less severe symptoms of colitis compared to *Ikkα*$^{wt/wt}$ mice receiving *Ikkα*$^{wt/wt}$ bone marrow or *Ikkα*$^{AA/AA}$ mice receiving *Ikkα*$^{AA/AA}$ bone marrow (*Figure 3.3 A-B*), further suggesting that IKKα signaling in non-hematopoietic cells rather in the immune cells is essential for protection.

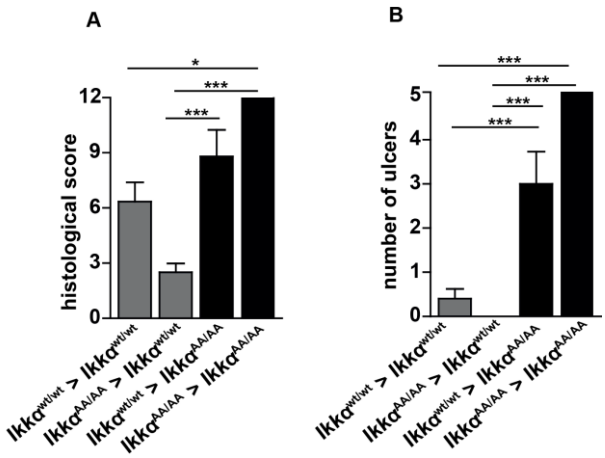

Figure 3.3: Impaired IKKα activation in IECs mediates the severe pathology. (A-B) *Four groups of bone marrow chimera mice for IKKα were generated and subjected to the DSS regimen.* ***(A)*** *Histological scoring based on loss of crypts, infiltration of immune cells into the mucosa, submucosa and muscle layer.* ***(B)*** *Number of ulcers. Data are expressed as mean ± SEM; n≥5; * p<0.05, ** p<0.001, *** p<0.0001 by ANOVA followed by Bonferroni post hoc test for multiple data sets.*

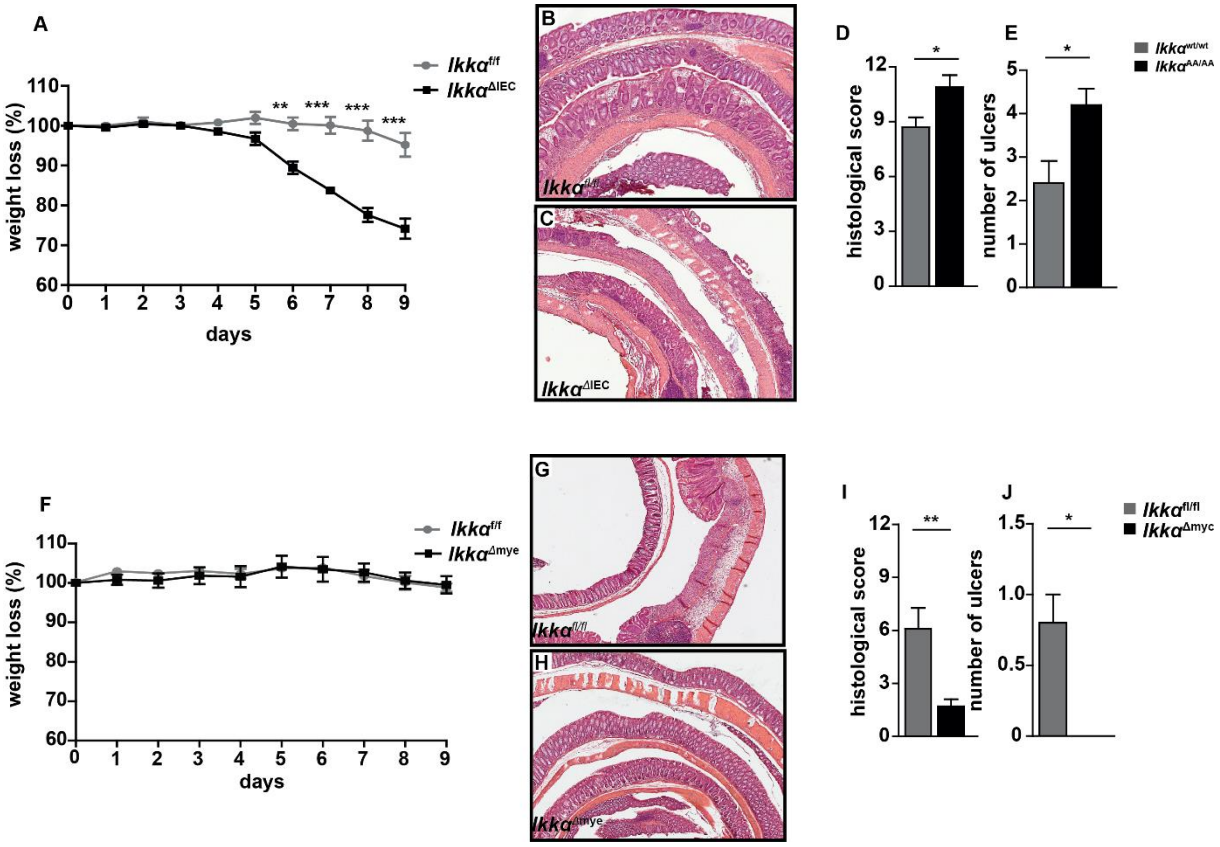

Figure 3.4: IKKα activation in IECs protects against colitis. (A) *Weight loss during DSS (3.5%) colitis in Ikkα$^{fl/fl}$ and Ikkα$^{\Delta IEC}$ mice. Representative histologies from H&E-stained colons of* ***(B)*** *Ikkα$^{f/f}$ and* ***(C)*** *Ikkα$^{\Delta IEC}$ mice 4 days after termination of DSS administration.* ***(D)*** *Histological scoring based on loss of crypts, infiltration of immune cells into the mucosa, submucosa and muscle layer.* ***(E)*** *Number of ulcers.* ***(F)*** *Weight loss during DSS (3.5%) colitis in Ikkα$^{fl/fl}$ and Ikkα$^{\Delta mye}$ mice. Representative histologies from H&E-stained colons of Ikkα$^{f/f}$* ***(G)*** *and* ***(H)*** *Ikkα$^{\Delta mye}$ mice 4 days after termination of DSS administration.* ***(I)*** *Histological scoring and* ***(J)*** *number of ulcers in Ikkα$^{fl/fl}$ and Ikkα$^{\Delta mye}$ 4 days after challenge with DSS (3.5%). Data are expressed as mean ± SEM; n≥5; * p<0.05, ** p<0.001, *** p<0.0001 by t test.*

To further confirm that IKKα signaling in non-hematopoietic cells is essential for protection, mice lacking *Ikkα* specifically in the intestinal epithelial cells (*Ikkα*$^{\Delta IEC}$) and myeloid cells (*Ikkα*$^{\Delta mye}$) were challenged with the same DSS regimen as in *Figure 3.1 A.* Mice deficient for IKKα in the IECs (*Ikkα*$^{\Delta IEC}$), displayed significant more body weight loss compared to *Ikkα*$^{fl/fl}$ littermate controls (*Figure 3.4 A*) and consistently, they exhibited increased sensitivity to the treatment reaching statistical significance on day 9 of DSS

challenge (*Figure 3.4 B-E*). On the contrary, yet in agreement with the transplantation experiments, deficiency of *Ikkα* in myeloid cells ($Ikk\alpha^{\Delta mye}$) resulted in comparable weight loss with the $Ikk\alpha^{fl/fl}$ mice *(Figure 3.4 F*) and showed improvement in clinical manifestations of colitis (*Figure 3.4 G-J*). Therefore, the above experiments demonstrate that activation of IKKα in IECs is critical for protection against DSS-induced colitis.

3.3 Severity of colitis is independent of alternative NF-κB activation

IKKα, contrary to IKKβ, comprises part of both canonical and alternative NF-κB pathways [144]. Activation of the alternative or noncanonical pathway relays on specific signals and involves processing of the NF-κB2 precursor protein, p100 [145].

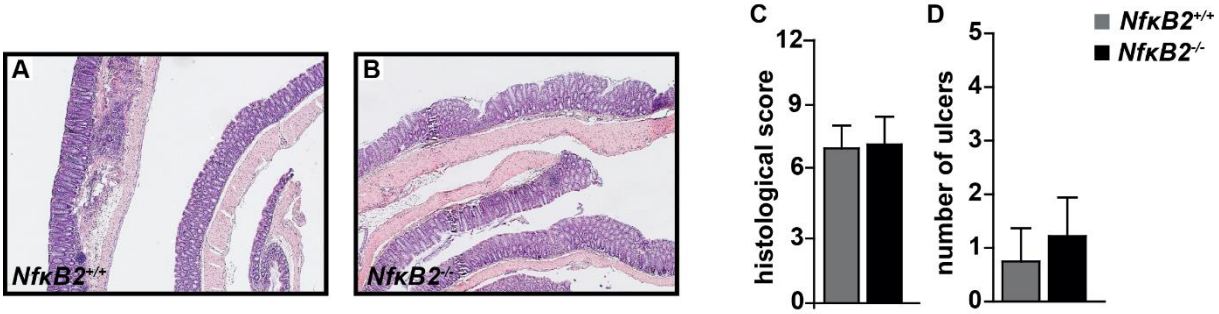

Figure 3.5: IKKα protects the intestinal epithelium from DSS-induced colitis independent of the alternative NF-κB activation*. Representative histologies from H & E-stained colons of* ***(A)*** *$NfκB2^{+/+}$ and* ***(B)*** *$NfκB2^{-/-}$ mice 4 days after termination of DSS (2.5%) administration.* ***(C)*** *Histological scoring and* ***(D)*** *number of ulcers in $NfκB2^{+/+}$ and $NfκB2^{-/-}$ mice 4 days after challenge with DSS (3.5%). Data are expressed as mean ± SEM; n≥5.*

To functionally examine the involvement of IKKα in the alternative pathway, *NfκB2* knockout mice were fed with 2.5% DSS (as they belong to different background) for 5 days and 4 days of regular water. Loss of NF-κB2/p100 did not affect disease severity induced by DSS as no differences could be observed upon histological examination (*Figure 3.5 A-B*). Both *NfκB2* deficient and proficient mice showed same colitis score (*Figure 3.5*

C) and number of ulcers (*Figure 3.5 D*). These results suggest that the colitis phenotype in *Ikkα*$^{AA/AA}$ mutants is not due to defective alternative NF-κB activation.

3.3.1 *Ikkα*$^{AA/AA}$ IECs display defective NF-κB activation

As the above experiments demonstrated that IKKα acted independently of the alternative NF-κB activation, its involvement in the canonical pathway was studied. Hence, intestinal epithelial cells were examined for the main events that govern canonical NF-κB activation, such as phosphorylation of IκBα or RelA/p65 subunit. In the DSS regimen the earliest alterations observed are loss of crypts and separation of the crypt base from the muscularis mucosa, which develop by day 3 post-administration of DSS [146]. Therefore, day 3 was chosen as an early time-point to elucidate the mechanism behind the severe acute colitis observed in *Ikkα*$^{AA/AA}$ mice.

Both IKKα and IKKβ have been shown to phosphorylate IκBα at serine 32 [147] and absence of IKKα resulted in diminished IκB degradation and p65 phosphorylation [148, 149]. Consistently, DSS-treated intestinal epithelial cells from *Ikkα*$^{AA/AA}$ mice displayed reduced phosphorylation of IκBα at serine 32, indicating that ubiquitin-dependent proteasomal degradation step was blocked (*Figure 3.6 A*). Moreover, RelA/p65 phosphorylation and NF-κB DNA binding activity were as well reduced in DSS-treated *Ikkα*$^{AA/AA}$ IECs compared to *Ikkα*$^{wt/wt}$ treated IECs, further suggesting that NF-κB activation was blocked (*Figure 3.6 A-B*). Taken together, IECs defective in IKKα activation exhibit weakened NF-κB activity, suggesting that IKKα comprises part of the canonical NF-κB pathway in this model.

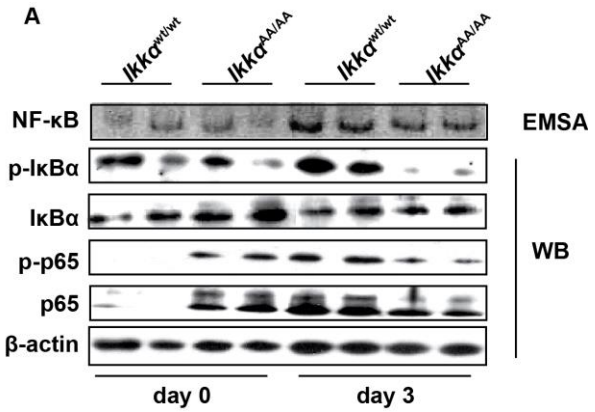

Figure 3.6: DSS activates NF-κB in Ikkα$^{wt/wt}$ but not in Ikkα$^{AA/AA}$ IECs. (A) *Colonic enterocytes were analyzed on day o and 3 post DSS (3.5%) by EMSA, using a non-radioactive probe corresponding to κB consensus sequence. Intestinal epithelial cell extracts of Ikkα$^{wt/wt}$ and Ikkα$^{AA/A}$ mice were analyzed on day 0 and day 3 post DSS (3.5%) application by immunoblotting for expression of phospho-IκBα, IκBα phospho-p65/RelA, p65/RelA and β-actin was used as loading control.*

3.4 Impaired IKKα activation enhances IECs cell death

DSS induces epithelial barrier dysfunction, allowing translocation of commensal bacteria to submucosa which eventually trigger the inflammatory response. Once DSS is omitted from the water the colonic epithelium can regenerate and inflammation resolves [150]. To address whether the delayed mucosa regeneration occurs due to enhanced epithelial cell death, *Ikkα*$^{wt/wt}$ and *Ikkα*$^{AA/AA}$ DSS-treated colons were stained for deoxynucleotidyl transferase-mediated dUTP nick end labeling (TUNEL). As shown in *Figure 3.7 A* DSS-treated *Ikkα*$^{AA/AA}$ colons displayed higher number of TUNEL-positive cells compared to *Ikkα*$^{wt/wt}$ mice. This could be also confirmed by the quantification of TUNEL-positive cells (*Figure 3.7 B*), indicating that IKKα signaling is required to protect against DSS-induced cell death.

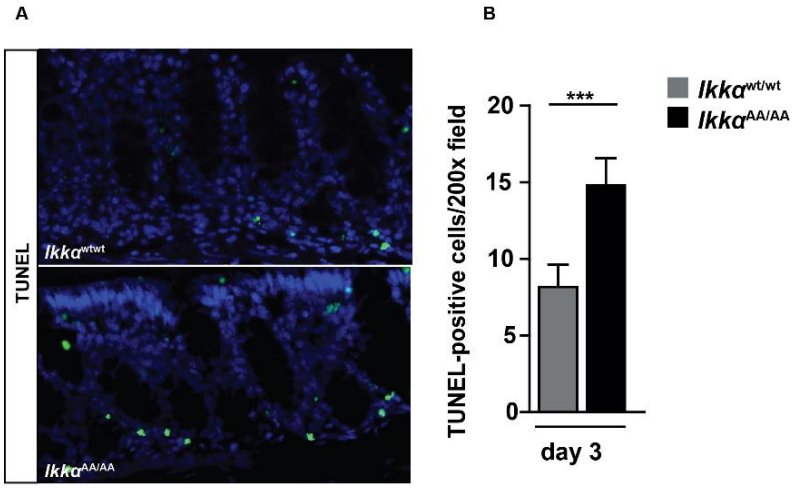

Figure 3.7: Massive cell death in Ikkα$^{AA/AA}$ mutant intestinal epithelium. (A) *TUNEL staining of colons of Ikkα$^{wt/wt}$ and Ikkα$^{AA/AA}$ on day 3 post DSS (3.5%).* ***(B)*** *Quantification of TUNEL-positive epithelial cells per 200x. Data are expressed as mean ± SEM; n>3, *** p<0.0001 by t test.*

3.5 IKKα mutant IECs display enhanced caspase-12 activation

Given the above results and considering that TUNEL staining detects DNA fragmentation and does not distinguish between apoptotic and necrotic cell death, to examine whether apoptosis was activated immunohistochemistry for cleaved caspase-3 (marker for apoptosis) was performed. Surprisingly, cleaved caspase-3 staining did not reveal any differences between the two genotypes on day 3 of DSS administration (*Figure 3.8 A*). Furthermore, the intrinsic apoptotic pathway was not affected, as no difference was observed for the pro-apoptotic caspase-9 and anti-apoptotic Bcl-xL in isolated enterocytes from both genotypes, whereas the anti-apoptotic Bcl-2 was moderately reduced in *Ikkα*$^{AA/AA}$ IECs (*Figure 3.8 B*).

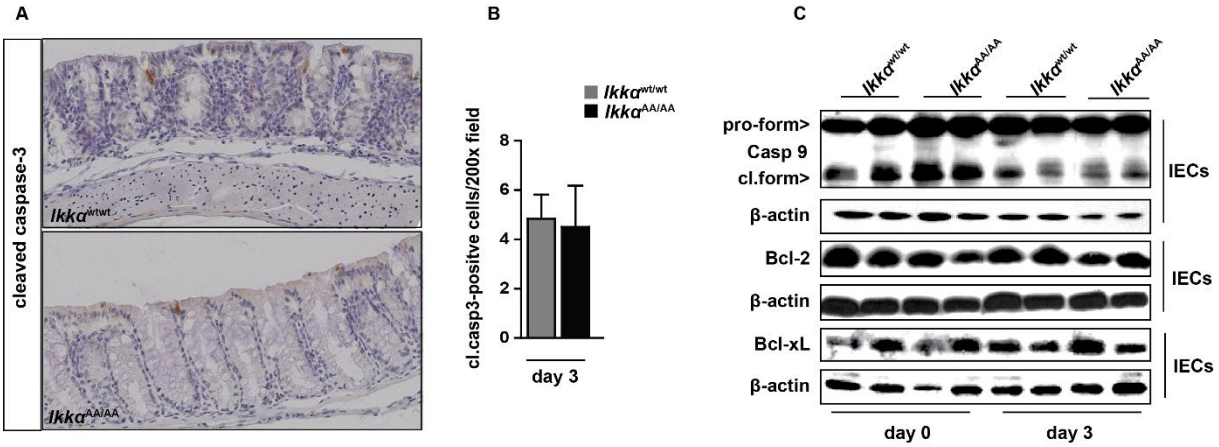

Figure 3.8: Increased epithelial cell death is independent of the intrinsic apoptotic pathway. ***(A-B)*** *Immunohistochemistry for cleaved caspase-3.* ***(A)*** *Representative sections stained with anti-cleaved caspase-3 antibody of colons from both genotypes on day 3 of DSS (3.5%) regimen.* ***(B)*** *Quantification of cleaved caspase-3 epithelial positive cells per 200x field. Data are expressed as mean ± SEM; n≥3.* ***(C)*** *Caspase-9, Bcl-2 and Bcl-xL levels in isolated epithelial cells of mice on day 0 and day 3 of DSS (3.5%) treatment were determined by western-blot. B-actin was used as loading control.*

To get a better insight into the cell death mechanism, IECs were analyzed for the expression of various caspases. Real-time PCR analysis revealed elevated expression of the pro-inflammatory caspases, caspase-11 and caspase-12 and the pro-apoptotic caspase-7 in DSS-treated *Ikkα*$^{AA/AA}$ IECs (*Figure 3.9 A*). However, when IKKα was targeted specifically in IECs the expression levels of caspase-7 and caspase-11 remained unchanged (*Figure 3.9 B*). On the other hand, the significant increased expression of caspase-12, seen in *Ikkα*$^{AA/AA}$ IECs challenged with DSS, persisted (*Figure 3.9 B*). Therefore, activation (cleavage) of caspase-12 was further examined by immunoblotting. Consistent with the real-time PCR results, *Ikkα*$^{AA/AA}$ IECs displayed a robust activation (cleavage) of caspase-12 upon DSS challenge (*Figure 3.9 C*), suggesting a potential role of this caspase in the IKKα mutant phenotype.

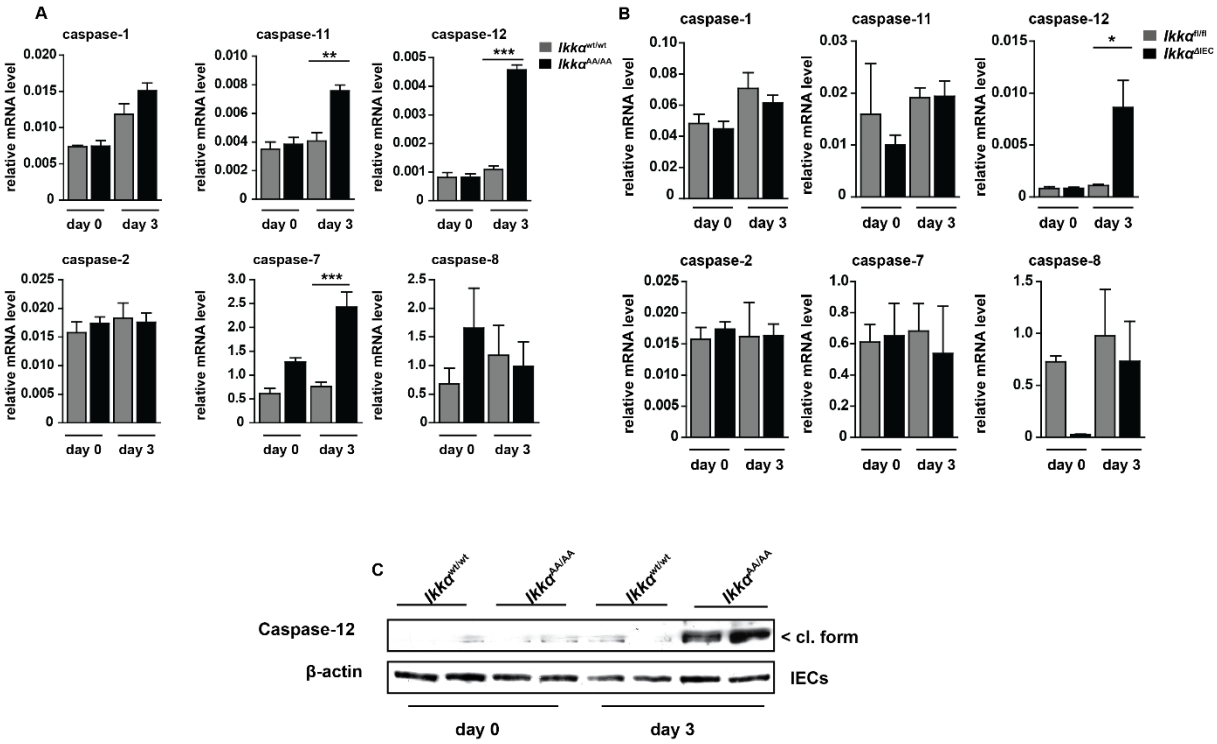

Figure 3.9: Caspase-12 is activated in Ikkα$^{AA/AA}$ IECs after DSS administration. (A-B) *Expression of caspase genes.* ***(A)*** *Relative mRNA expression levels were quantified in IECs of Ikkα$^{wt/wt}$ and Ikkα$^{AA/AA}$ mice on day 0 and 3 of DSS regimen.* ***(B)*** *Relative mRNA expression levels were quantified in IECs of Ikkα$^{fl/fl}$ and Ikkα$^{\Delta IEC}$ mice on day 0 and 3 of DSS regimen. The mRNA levels were quantified by real-time PCR and normalized to the level of cyclophilinB mRNA. Data are expressed as mean ± SEM; n=3; * p<0.05, ** p<0.001, *** p<0.0001 by ANOVA followed by Bonferroni post hoc test for multiple data sets.* ***(C)*** *Caspase-12 expression in IECs of Ikkα$^{wt/wt}$ and Ikkα$^{AA/AA}$ mice on day 0 and 3 of DSS (3.5%) regimen was determined by WB. B-actin was used as loading control. Intestinal epithelial cells (IECs), western-blot (WB).*

3.6 *Ikkα*$^{AA/AA}$ mutants display decreased IL-18 serum levels

Caspase-12 was reported to exert a dominant-negative effect on caspase-1 [127] and caspase-1 activation downstream of the NLRP3 and/or NLRP6 inflammasomes is required for the maturation of the related cytokines IL-1β and IL-18 [107, 112, 121]. Thus, in order to investigate the molecular basis of the impaired epithelial regeneration in *Ikkα*$^{AA/AA}$ mutants and given the substantial induction of caspase-12 in intestinal epithelial cells at both mRNA (*Figure 3.9 A-B*) and protein levels (*Figure 9.C*), serum levels of both IL-1β and IL-18 in *Ikkα*$^{wt/wt}$ and *Ikkα*$^{AA/AA}$ mice were examined. Although there was no

difference in IL-18 serum levels between the untreated genotypes, IL-18 was highly induced in the serum of *Ikkα*$^{wt/wt}$ animals upon DSS challenge compared to untreated *Ikkα*$^{wt/wt}$ and DSS-treated *Ikkα*$^{AA/AA}$ mutants (*Figure 3.10 A*). That was also similar for the knockout animals with specific deletion of *Ikkα* in the intestinal epithelial cells, *Ikkα*$^{\Delta IEC}$ (*Figure 3.10 B*). Unlike IL-18, IL-1β levels were highly elevated in the serum of DSS-treated *Ikkα*$^{AA/AA}$ knock-in (*Figure 3.10 C*) and *Ikkα*$^{\Delta IEC}$knockout mice (*Figure 3.10 D*).

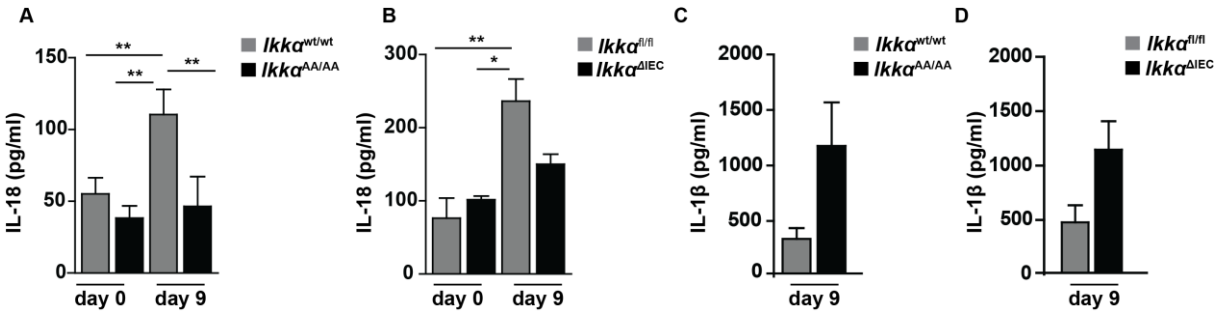

Figure 3.10: DSS-challenged Ikkα$^{AA/AA}$ mice fail to secrete active IL-18. (A-D) *IL-18 and IL-1β production in the serum was determined by ELISA. IL-18 was determined in the serum of* ***(A)*** *Ikkα$^{AA/AA}$ and* ***(B)*** *Ikkα$^{\Delta IEC}$ on day 0 and day 9 of the DSS (3.5%) regimen. Data are expressed as mean ± SEM; n≥4; * p<0.05, ** p<0.001, by ANOVA followed by Bonferroni post hoc test for multiple data sets. IL-1β was determined in the serum of* ***(C)*** *Ikkα$^{AA/AA}$ and* ***(D)*** *Ikkα$^{\Delta IEC}$ on day 9 of the DSS (3.5%) regimen. Data are expressed as mean ± SEM; n≥4.*

3.6.1 IL-18 mediates tissue repair after injury

Mice lacking inflammasome components such as *Caspase-1* [119], *Nlrp6* [112] or *Nlrp3* [107] were shown to have impaired epithelial regeneration attributed to decreased levels of IL-18 production by the intestinal epithelial cells. Furthermore, IL-18 and IL-18R knockout mice were presented to be highly susceptible to DSS-induced colitis [120]. The fact that IL-18 raised in the serum of *Ikkα*$^{wt/wt}$ mice upon DSS administration, suggested that IL-18 might be critical for tissue repair. To verify this hypothesis the role of exogenous administration of recombinant IL-18 (rIL-18) on disease progression in response to DSS was examined. Thus, *Ikkα*$^{AA/AA}$ mice, which displayed low IL-18 levels

upon DSS challenge, were injected intraperitoneally with 0.5 µg of rIL-18 or PBS as control, daily during the entire course of the DSS treatment. Remarkably, *Ikkα*$^{AA/AA}$ mice treated with rIL-18 lost significantly less body weight when compared to mice receiving PBS (*Figure 3.11 A*). Histologically, *Ikkα*$^{AA/AA}$ mice treated with rIL-18 exhibited signs of epithelial regeneration and reduced infiltration of immune cells into the mucosa, submucosa and lamina propria (*Figure 3.11 C*). In sharp contrast, *Ikkα*$^{AA/AA}$ mutants treated with PBS displayed severe transmural inflammation and extensive areas of ulceration (*Figure 3.11 B*). Semiquantitative scoring of these histological parameters confirmed that colitis (*Figure 3.11 D*) and number of ulcers (*Figure 3.11 E*) in the group receiving PBS was significantly higher than in the one receiving rIL-18. Meanwhile, attenuation of disease progression upon administration of rIL-18 was accompanied by decreased expression of mRNAs encoding IL-1β, IL-6, TNFα, Cxcl1, Cxcl2, and Ccl2 (*Figure 3.11 F*). Collectively, these data suggest that IL-18 can compensate for the loss of IKKα kinase activity upon acute injury of the intestinal epithelium.

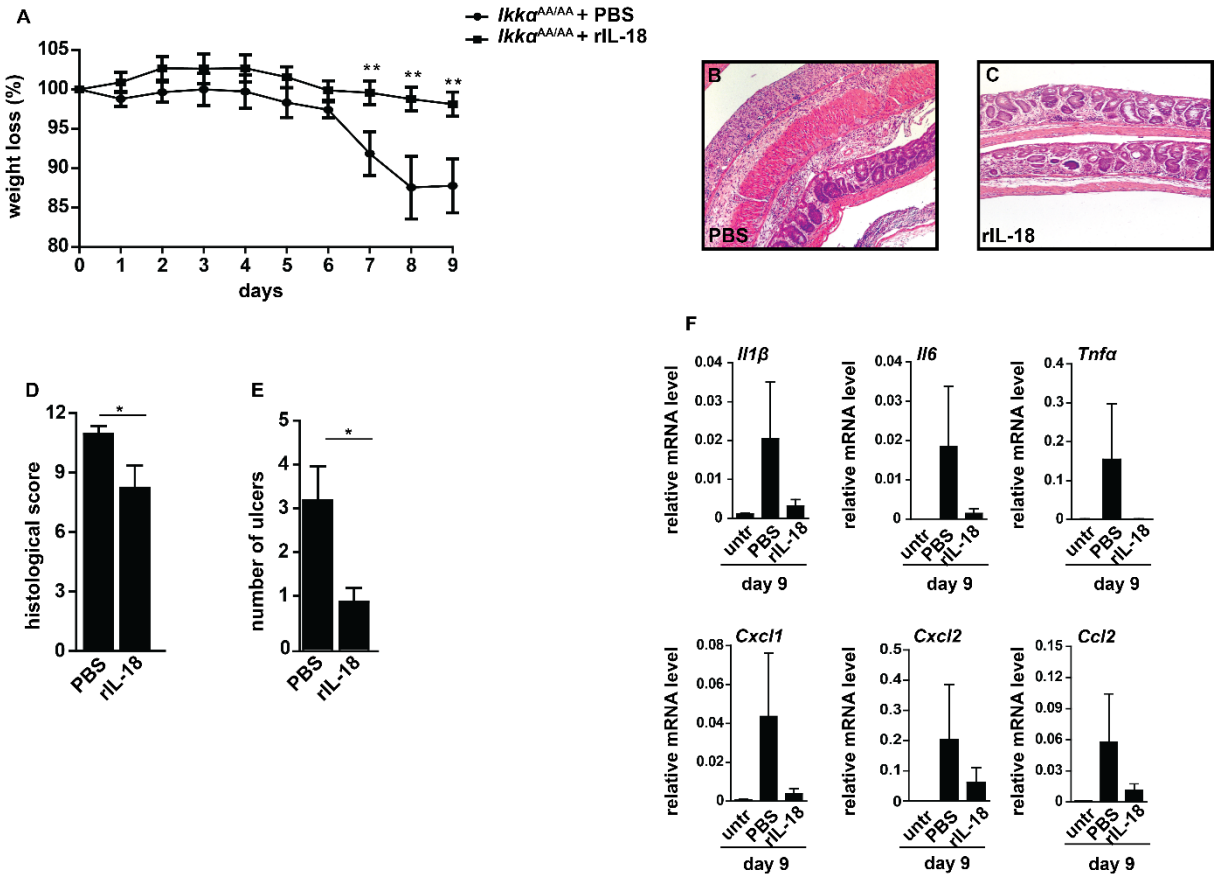

Figure 3.11: Administration of recombinant IL-18 rescues severity of colitis. (A) *Ikkα$^{AA/AA}$ mice were fed with 3.5% DSS for 5 days, followed by 4 days of regular drinking water. One group received intraperitoneal injections with 0.5 µg recombinant IL-18 (rIL-18) daily until the end of the DSS treatment, while the other control cohort received PBS instead. Data are expressed as mean ± SEM; n≥5, ** p<0.001 by t test. Representative histologies from H&E-stained colons of Ikkα$^{AA/AA}$ receiving PBS* ***(B)*** *and* ***(C)*** *rIL-18, on day 9 of the DSS treatment.* ***(D)*** *Histological scoring based on loss of crypts, infiltration of immune cells into the mucosa, submucosa and muscle layer and* ***(E)*** *number of ulcers on day 9 of DSS treatment. Data are expressed as mean ± SEM; n≥5; * p<0.05, by t test.* ***(F)*** *Expression of inflammatory genes. Relative mRNA expression levels were quantified in whole colonic mucosa tissue of mice on day 0 and 9 of DSS regimen. The mRNA levels were quantified by real-time PCR and normalized to the level of cyclophilinB mRNA (n ≥ 4).*

3.6.2 IECs comprise the main source of IL-18 production during DSS colitis

Contrary to IL-1β, which is mainly produced by hematopoietic cells, IL-18 has been identified in cells of both hematopoietic and non-hematopoietic origin and within the gut

mucosa is mainly produced by IECs [107, 112, 119, 151]. To investigate the cell population involved in IL-18 and IL-1β secretion, IECs and lamina propria immune cells were isolated from wild-type animals on day 5 of DSS treatment and cultured overnight, as previously described [119]. In agreement with previous studies [119], DSS-treated IECs secreted the highest amount of IL-18 (*Figure 3.12 A*), however, the main source of IL-1β were proven the immune cells (*Figure 3.12 B*).

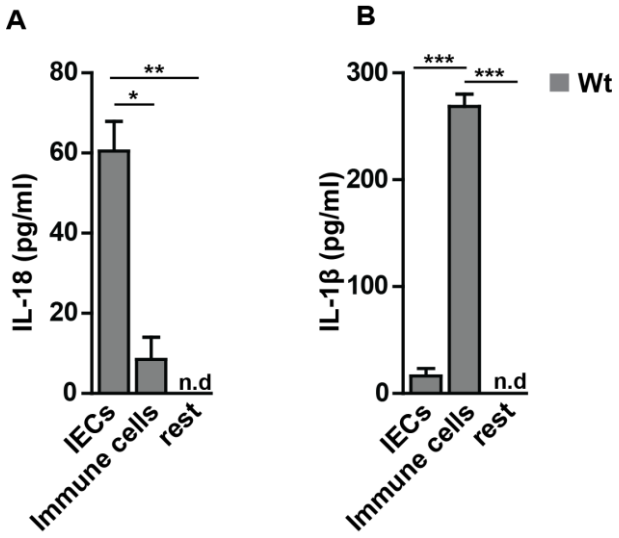

Figure 3.12: IECs produce IL-18 during DSS colitis. (A-B) *IL-18 and IL-1β secretion from the different cell populations was determined by ELISA on day 5 of DSS (3.5 %) treatment. The different cell populations were sorted according to CD45, EpCAM, CD11b and GR1 markers: IECs are defined as CD45$^-$, CD11b$^-$, GR1$^-$, EpCAM$^+$, immune cells as CD45$^+$, CD11b$^+$, GR1$^+$, EpCAM$^-$ and rest as CD45$^-$, CD11b$^-$, GR1$^-$, EpCAM$^-$. Data are expressed as mean ± SEM; n≥3; * p<0.05, ** p<0.001, *** p<0.0001 by ANOVA followed by Bonferroni post hoc test for multiple data sets. n.d, nondetected.*

Therefore, during DSS-induced colitis IECs is the main cell population contributing to IL-18 release, whereas IL-1β is mainly produced by immune cells. These data indicate that IL-18 is primarily produced by IECs and suggest a link between IKKα signaling and IL-18 production during DSS-induced colitis.

3.7 Deficiency of caspase-12 rescues the phenotype of *Ikkα*$^{AA/AA}$ mice

Caspase-12 deficiency has been associated with resistance to acute and chronic colitis induced by DSS [119] and with efficient clearance of systemic and abdominal bacterial infections [127, 138]. Based on the observation that *Ikkα*$^{AA/AA}$ DSS-treated IECs showed substantial activation of caspase-12 and reduced IL-18 production the role of caspase-12 during colitis was examined. Therefore, to investigate whether caspase-12 plays a role in the severe phenotype of *Ikkα*$^{AA/AA}$ mice, *casp12*$^{-/-}$*Ikkα*$^{AA/AA}$ double mutants were generated by crossing caspase-12 knockout mice (*casp12*$^{-/-}$) with *Ikkα*$^{AA/AA}$ mice. Notably, challenge of *casp12*$^{-/-}$*Ikkα*$^{AA/AA}$ mice with 2.5% DSS for 5 days and 4 additional days of regular water, revealed that the double mutants lost less weight compared to *Ikkα*$^{AA/AA}$ mutants reaching that of *casp12*$^{-/-}$ mice (*Figure 3.13 A*). In sharp contrast to *Ikkα*$^{AA/AA}$ (*Figure 3.13 B*), *casp12*$^{-/-}$*Ikkα*$^{AA/AA}$ (*Figure 3.13 C*) and *casp12*$^{-/-}$ (*Figure 3.13 D*) mice showed significant improvement at the end of the treatment and were capable of restricting mucosal damage and immune cell infiltration by inducing crypt regeneration. Histological scoring revealed significantly less tissue damage (*Figure 3.13 E*) and lower ulcer numbers (*Figure 3.13 F*) in *casp12*$^{-/-}$*Ikkα*$^{AA/AA}$ related to *Ikkα*$^{AA/AA}$ DSS-treated animals. No difference was observed between *casp12*$^{-/-}$*Ikkα*$^{AA/AA}$ and *casp12*$^{-/-}$ DSS-treated mice (*Figure 3.13 E-F*). Thus, the data indicate that deletion of caspase-12 ameliorates tissue damage and induces re-epithelialazation in *Ikkα*$^{AA/AA}$ mice.

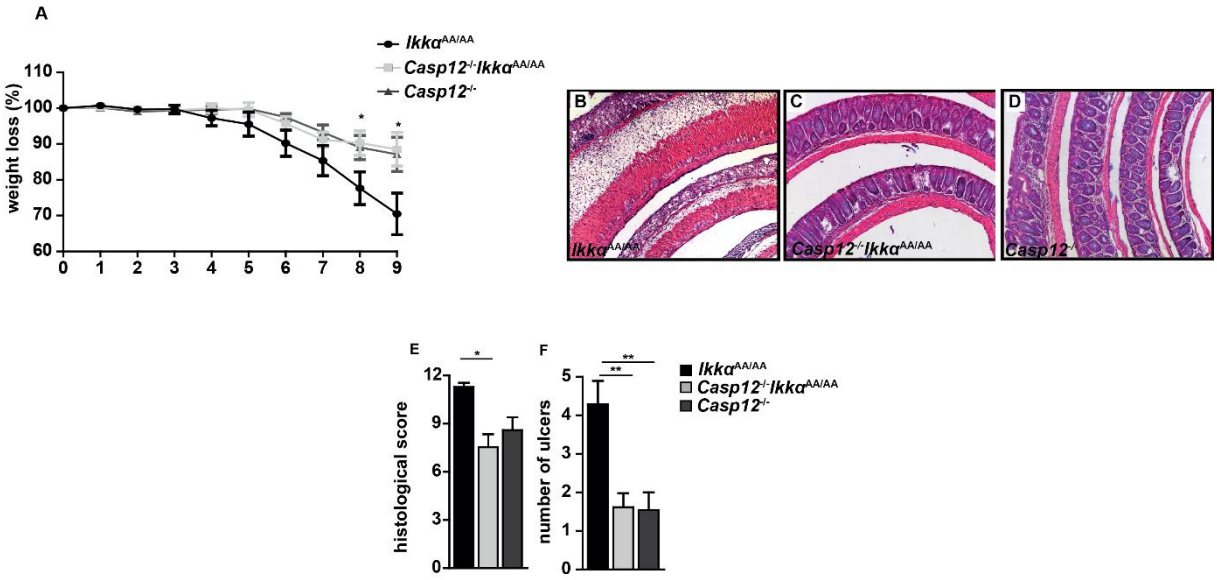

Figure 3.13: Caspase-12 deletion alleviates severity of colitis. (A) *Changes in body weight of Ikkα$^{AA/AA}$, casp12$^{-/-}$Ikkα$^{AA/AA}$ and casp12$^{-/-}$ during acute DSS-induced colitis. 2.5% DSS was administrated in the drinking water for 5 days, followed by a 4 day recovery of regular drinking water. Data are expressed as mean ± SEM; n≥5, * p<0.05 by t-test.* ***(B-D)*** *Representative hematoxylin & eosin-stained sections of colons from* ***(B)*** *Ikkα$^{AA/AA}$,* ***(C)*** *casp12$^{-/-}$Ikkα$^{AA/AA}$ and* ***(D)*** *casp12$^{-/-}$ mice on day 9 of DSS regimen.* ***(E)*** *Histological score and* ***(F)*** *number of ulcers in mice treated with 2.5% DSS. Data are expressed as mean ± SEM; n≥5, * p<0.05, ** p<0.001 by ANOVA followed by Bonferroni post hoc test for multiple data sets.*

3.7.1 Caspase-12 ablation attenuates colitis in *Ikkα*$^{AA/AA}$ mutants

Consistent with the significant alleviation of disease severity in the double and single caspase-12 mutants, expression of mRNAs encoding proinflammatory cytokines and chemokines in whole colonic mucosa, including IL-1β, IL-6, CxcL1, Cxcl2 and Ccl2, was as well reduced compared to *Ikkα*$^{AA/AA}$ kinase-dead mutants, however *Tnfα* levels were not much different between the groups (*Figure 3.14 A*). Furthermore, immunoblot analysis confirmed significant downregulation of COX-2 and MMP-9 in DSS-treated colonic mucosa from *casp12$^{-/-}$Ikkα*$^{AA/AA}$ and *casp12$^{-/-}$* compared to *Ikkα*$^{AA/AA}$ mutants (*Figure 3.14 B*). Collectively, the above data demonstrate that loss of caspase-12 reduced the massive

inflammatory response to an extent adequate to prevent DSS-induced mortality and morbidity observed in *Ikkα*$^{AA/AA}$ mice.

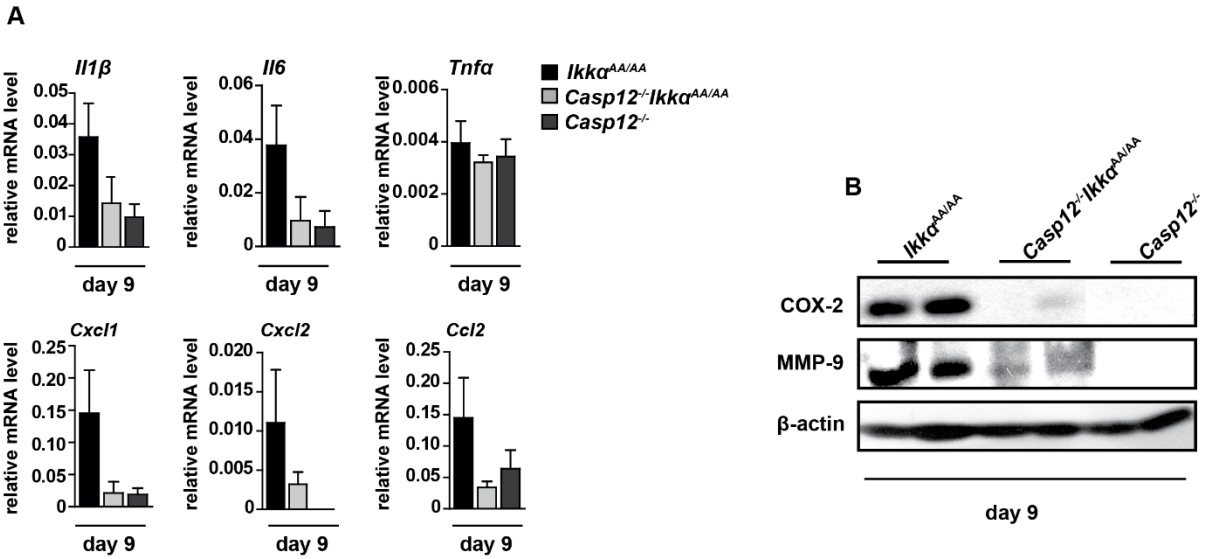

Figure 3.14: Deletion of caspase-12 reduces the expression of proinflammatory factors. (A) *Expression of inflammatory genes. Relative mRNA expression levels were quantified in whole colonic mucosa tissue of mice on day 0 and 9 of DSS regimen. The mRNA levels were quantified by real-time PCR and normalized to the level of cyclophilinB mRNA (n ≥ 4).* ***(B)*** *COX-2 and MMP-9 expression in whole colonic extracts on day 0 and 9 of DSS regimen. COX-2 and MMP-9 expression were determined by western blot (WB).*

3.8 Impaired IKKα activation results in enhanced ER stress

Based on the finding that the severe phenotype in *Ikkα*$^{AA/AA}$ mice was attributed to caspase-12, the mechanism by which caspase-12 is activated was further explored. Caspase-12 was found to localize at the cytoplasmic site of the endoplasmic reticulum (ER) [128] and has been suggested to be activated upon ER stress [126]. In notion of that, several ER stress markers, including IRE1α, XBP1, IRE1β, GRP78, GRP94, and CHOP were examined. Real-time PCR analysis revealed that the expression of *Ire1α* was significantly elevated in both untreated and DSS-treated *Ikkα*$^{AA/AA}$ IECs, while the expression of *Grp78* raised in *Ikkα*$^{AA/AA}$ enterocytes only upon DSS challenge (*Figure 3.15 A*). Also, the

expression of *Ire1β* and *Grp94* remained unchanged, whereas *Chop/Gadd153* was significantly down-regulated in DSS challenged *Ikkα*$^{AA/AA}$ epithelial cells (*Figure 3.15 A*). In line with the real-time PCR results, the ER chaperone, GRP78, was highly induced in *Ikkα*$^{AA/AA}$ mutant epithelial cells upon DSS treatment (*Figure 3.15 B*). Although IRE1α protein levels were elevated in *Ikkα*$^{AA/AA}$ untreated epithelial cells, DSS caused a further increase in *Ikkα*$^{AA/AA}$ compared to *Ikkα*$^{wt/wt}$ IECs, which displayed only a minor induction upon DSS treatment (*Figure 3.15 B*). ER stress-induced IRE1α overexpression and subsequent trans-autophosphorylation activates its RNase activity to cleave XBP1 mRNA resulting in the production of a potent transcription factor called XBP1s [152]. Consistently, DSS induced enhanced XBP1 splicing in *Ikkα*$^{AA/AA}$ DSS-challenged enterocytes compared to *Ikkα*$^{wt/wt}$ IECs (*Figure 3.15 B-C*). Furthermore, DSS treatment reduced substantially TRAF2 protein levels in the mutant enterocytes (*Figure 3.15 C*), consistent with studies which show that increased ER stress induces down-regulation of TRAF2 [73, 74] and subsequent release of caspase-12 [131]. Analysis of the PERK branch of the UPR demonstrated that during DSS challenge impaired IKKα activation resulted in lack of PERK phosphorylation and expression of its downstream target, CHOP [153] (*Figure 3.15 E*). Interestingly, untreated *Ikkα*$^{AA/AA}$ enterocytes were devoid of CHOP expression, implying that CHOP might be a direct target of IKKα. However, phosphorylation of eIF2α was not attenuated in DSS-treated *Ikkα*$^{AA/AA}$ IECs, thus implicating the possible involvement of other eIF2α kinases (*Figure 3.15 E*). Taken together, the above data indicate that impaired IKKα activation enhances ER stress in IECs through the IRE1α branch of the UPR leading to caspase-12 release and eventually activation.

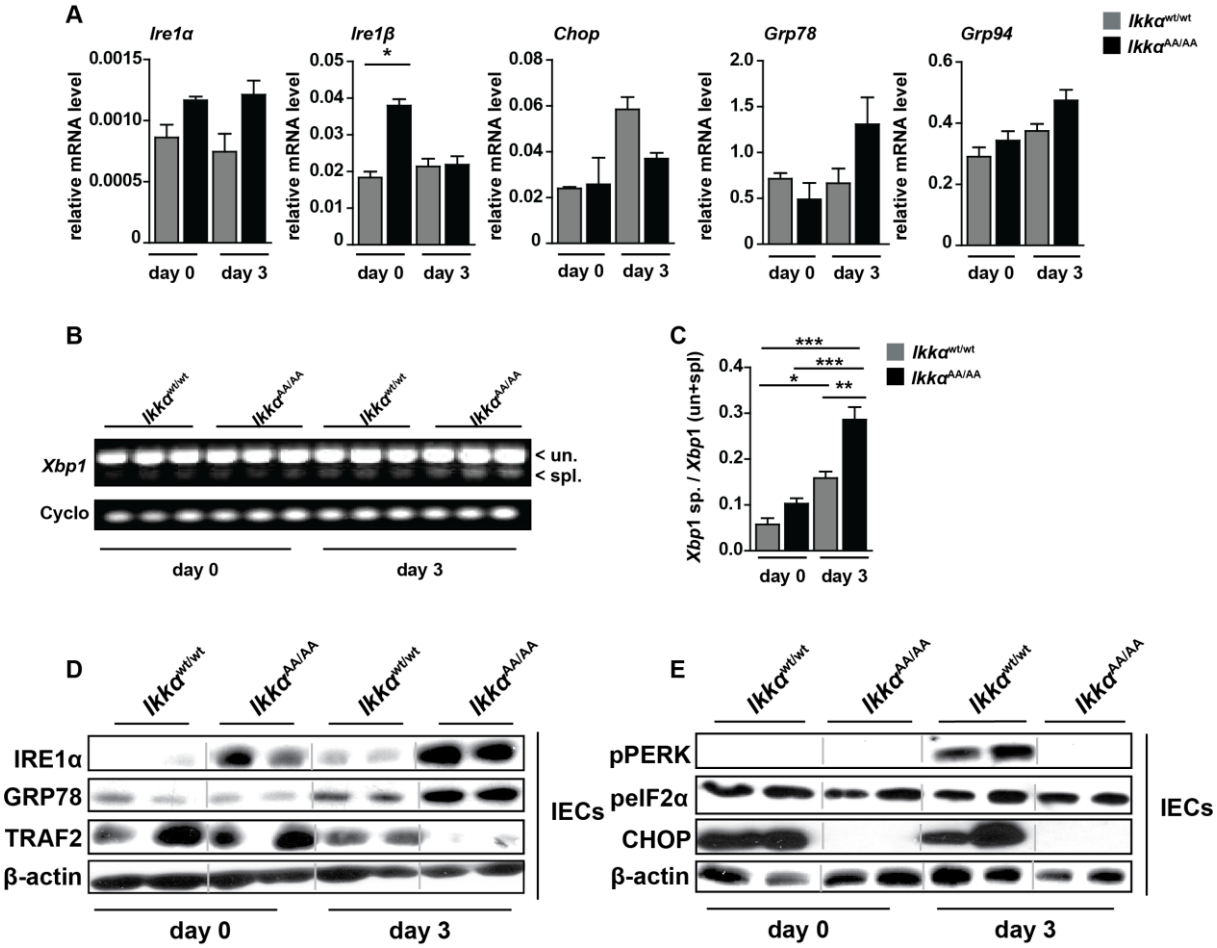

Figure 3.15: ER stress is aggravated in DSS-treated Ikkα$^{AA/AA}$ mice. (A) *Expression of ER stress markers. Relative mRNA expression levels were quantified in isolated intestinal epithelial cells of mice on day 0 and 3 of DSS (3.5%) regimen. The mRNA levels were quantified by real-time PCR and normalized to the level of cyclophilin B mRNA (n= 3).* ***(B)*** *Real time PCR analysis for XBP1 splicing.* ***(C)*** *Densitometry quantification of XPB1 splicing from 3% agarose gel. Data are presented as mean ± SEM; n=3, * p<0.05, ** p<0.001, *** p<0.0001 by ANOVA followed by Bonferroni post hoc test for multiple data sets.* ***(D)*** *IRE1α, GRP78, TRAF2 and* ***(E)*** *pPERK, peIF2α and CHOP expression in IEC extracts at day 0 and 3 of DSS (3.5%) regimen, were determined by WB. B-actin was used as loading control. Western blot (WB), intestinal epithelial cells (IECs).*

3.9 Caspase-12 ablation does not affect cell death

Caspase-12 activation triggered by ER stress has been proposed to induce apoptosis [129]. In light of the above results it was reasoned that ER stress-induced caspase-12 activation might be involved in the enhanced intestinal epithelial cell death observed in *Ikkα*$^{AA/AA}$ upon DSS treatment (*Figure 3.7 A-B*). To investigate the involvement of caspase-

12 activation in mediating cell death, *casp12*$^{-/-}$*Ikkα*$^{AA/AA}$ and *Ikkα*$^{AA/AA}$ mice were subjected to DSS treatment for 3 days and TUNEL staining was performed. TUNEL staining of DSS-treated colons revealed no difference in epithelial cell death upon caspase-12 ablation (*Figure 3.16 A*). This result is in agreement with recent studies which suggest that caspase-12 deficient cells are as prone to apoptosis induced by various stimuli as caspase-12 proficient cells [127, 133].

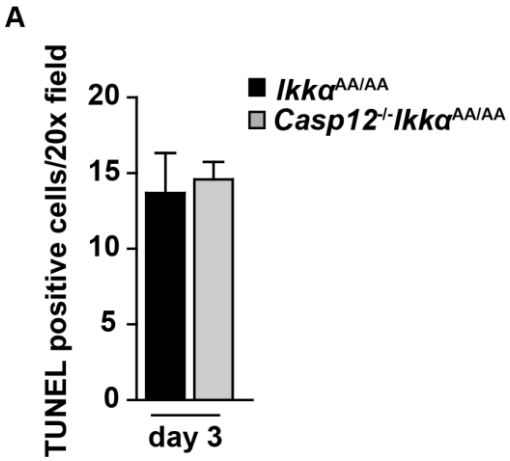

Figure 3.16: Caspase-12 deletion does not affect cell death. (A) *Quantification of TUNEL-positive intestinal epithelial cells of colons of Ikkα$^{AA/AA}$ and casp12$^{-/-}$Ikkα$^{AA/AA}$ mice on day 3 of DSS (2.5%) regimen. Data are expressed as mean ± SEM; n≥3.*

3.10 Defective IKKα activation impairs autophagy

Several lines of evidence highlight the close link between UPR and autophagy [75]. Furthermore, ER stress has been shown to be involved in autophagy induction [154]. In order to investigate whether ER stress triggered activation of autophagy, IECs isolated from *Ikkα*$^{wt/wt}$ and *Ikkα*$^{AA/AA}$ mice that were left either untreated or were challenged with DSS, were analysed for autophagic markers. LC3, the mammalian Atg8 homolog, undergoes proteolysis to produce the cytosolic LC3-I form, which is then lipidated to generate the LC3-II form. The LC3-II form is then attached to both faces of the

autophogosomal membrane [155]. Both *Ikkα*$^{wt/wt}$ and *Ikkα*$^{AA/AA}$ IECs exhibited obvious accumulation of LC3-II, consistent with the fact that basal, constitutive level of autophagy occurs many cells as a quality control mechanism [155] (*Figure 3.17 A*). However, in contrast to *Ikkα*$^{wt/wt}$, *Ikkα*$^{AA/AA}$ IECs subjected to DSS showed only a modest increase in LC3-I (*Figure 3.17 A*) indicating autophagosome formation. Quantification of the lipidated LC3-II form revealed that autophagosome formation was significantly elevated in *Ikkα*$^{AA/AA}$ DSS-treated IECs (*Figure 3.17 B*).

P62 acts as a receptor that binds ubiquitinated proteins and organelles targeting them into autophagosomes. Eventually, when autophagy completion occurs p62 is degraded within the lysosomes [156]. p62 accumulation occurs when autophagic protein degradation is blocked [85]. Interestingly, whereas p62 was decreased in *Ikkα*$^{wt/wt}$ treated IECs, *Ikkα*$^{AA/AA}$ DSS-treated IECs displayed accumulated p62 levels (*Figure 3.17 C*), indicating that autophagy was impaired. Moreover, ATG16L1 is an important autophagy protein in Paneth cells [14]. Given the recent association of, another ATG16L1 isoform, ATG16L2 with IKKα in pancreas, the potential interaction between ATG16L1 and IKKα in IECs was explored. Remarkably, mutant and wild-type IKKα interacted with ATG16L1 in unchallenged IECs, indicating that IKKα might be involved in the regulation of this autophagic protein in the colon. Although this interaction was maintained in DSS-treated *Ikkα*$^{wt/wt}$ IECs it was abrogated in the mutant IECs after DSS administration (*Figure 3.17 D*). Furthermore, the total levels of ATG16L1 decreased after DSS challenge and were further diminshed, in the mutant DSS-treated enterocytes (*Figure 3.17 E*), designating that in response to stress ATG16L1 was severely affected by the mutant IKKα. However the relevance of this interaction and the impact of IKKα on ATG16L1 remains still elusive. Taken together, these data suggest that defective IKKα activation might interfere with proper autophagic degradation thus leading to p62 accumulation.

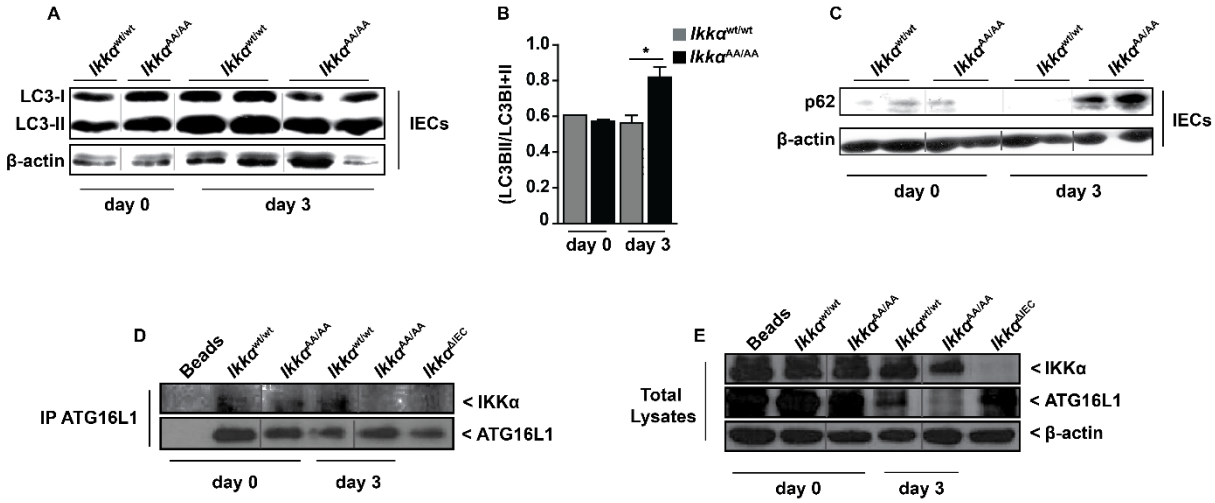

Figure 3.17: IKKa inactivation results in defective autophagic protein degradation and p62 accumulation. *Immunoblot analysis of IECs on day 0 and day 3 of DSS (3.5%) treatment for* ***(A)*** *LC3 and* ***(C)*** *p62. Real time PCR analysis for XBP1 splicing.* ***(B)*** *Densitometry quantification of LC3 conversion. Data are expressed as mean ± SEM; n≥4, * p<0.05 by ANOVA followed by Bonferroni post hoc test for multiple data sets.* ***(D-E)*** *Endogenous IKKa interacts with ATG16L1 in IECs. IEC lysates from wild-type and Ikkα$^{AA/AA}$ mice that remained untreated or were fed with DSS (3.5%) were immunoprecipitated with anti-ATG16L1 antibody.* ***(D)*** *The immunocomplexes and* ***(E)*** *total lysates were analysed by WB with the indicated antibodies. B-actin was used as loading control. Western blot (WB), intestinal epithelial cells (IECs).*

4. Discussion

IKKα, initially identified as a subunit of the IκB kinase complex that directly phosphorylates IκB, is an important protein kinase involved in numerous biological processes such as, cell survival, inflammation, development of secondary lymphoid organs and transcriptional regulation [145]. The fact that mice lacking IKKα die soon after birth [57] highlights its major significance during development and tissue homeostasis that cannot be substituted by other members of the IKK complex. Although its biological importance has been addressed in several human diseases the exact mechanisms remain still ill defined. This report here, provides important information for IKKα mode of action in maintaining intestinal homeostasis. Using *Ikkα*$^{AA/AA}$ mutants in a model of acute colitis this study provides strong evidence of a novel function of epithelial IKKα in suppressing excessive inflammatory responses in the large intestine, thus maintaining a fine balance between the intestinal epithelium and the host immune system.

4.1 Activation of IKKα suppresses inflammation in the large intestine

Given the fact that IBDs affect the quality of life of million people in the western world and its incidence has sharply enhanced since the early 1950's [157], identification of factors and singnaling pathways implicated in disease pathogenesis comprise an urgent need. One of the most commonly used model of IBD is by challenging mice with DSS salt. This model, which closely mimics UC in humans, induces inflammation in rodents that starts distally after about 5 days and is confined to the colonic mucosa [146]. The mechanism of action is by affecting directly the inner mucus layer and inducing death of IECs. IECs death disrupts the intestinal barrier and eventually allows bacterial translocation to the mucosa that induce a strong local inflammatory response [158].

Discussion

In the present study IKKα is proven a critical regulator of intestinal homeostasis. Is showed that mice engineered to express an inactive form of IKKα are unable to restrict excessive inflammatory responses when colon injury is induced by DSS. The colon of those mice is characterized by complete loss of crypts, massive infiltration of immune cells and large areas of ulceration (*Figure 3.1*). The enhanced inflammation seen in *Ikkα*$^{AA/AA}$ mutants is attributed to defective IKKα signaling in the intestinal epithelium (*Figure 3.3 and 3.4*). Interestingly, several studies have demonstrated that IKKα of epithelial origin is capable of suppressing enhanced inflammatory responses in various organs, including skin, lungs, pancreas and intestine [51, 66, 159-162]. In the skin and lungs impaired IKKα signaling enhances inflammation and macrophage recruitment and elevates the expression of cytokines and chemokines inducing tissue pathology [139, 159, 160], mirroring the events occurring in the intestine upon DSS-induced injury. The enhanced inflammatory phenotype seen in the skin and lung epithelia of mice defective in IKKα signaling is mainly attributed to elevated EGFR/ERK activities, which eventually lead to enhanced production of cytokines and chemokines allowing macrophages infiltration [139, 159, 160]. In the intestine, on the other hand, IKKα suppresses inflammation by inhibiting caspase-12 over-activation, most likely indirectly, thereby promoting inflammasome activation and downstream IL-18 production by the IECs. These findings suggest that impaired IKKα signaling orchestrates an inflammatory microenvironment which eventually triggers pathology in multiple epithelial organs, in both humans and mice. However, IKKα activation in the intestine limits the recruitment of IFNγ-producing M1-like polarized myeloid cells, thereby, promoting tumorigenesis in a nonautonomous manner [162]. Therefore, under inflammatory conditions cell autonomous IKKα signaling is essential for limiting exaggerated immune responses and to restore intestinal homeostasis. However, in circumstances where environmental triggers cause cell

mutagenesis, IKKα seems to act in a nonautonous manner to suppress recruitment of myeloid cells and to promote tumorigenesis. It seems that IKKα can act in many different ways, either in an autocrine or paracrine manner, depending on the external signals and pathways activated. This in turn results in differential contribution of IKKα in the final phenotype.

4.1.1 Pathology in *Ikkα*$^{AA/AA}$ mice is independent of the alternative NF-κB pathway

The canonical NF-κB pathway relies for its activation on the IκB kinase complex, which phosphorylates and marks the IκB inhibitors for proteasomal degradation. However, the alternative pathway is governed exclusively by IKKα and depends for its activation on the phosphorylation and partial degradation of the NF-κB2/p100 IκB-like inhibitor [144]. The data obtained here argue for the fact that IKKα acts independently of the alternative NF-κB activation, as deletion of the NF-κB2 precursor protein, p100, did not affect pathology induced by DSS (*Figure 3.5*). Nonetheless, this is not surprising since IKKα has been shown to have additional NF-κB-independent functions, including suppression of skin inflammation [159] and promotion of tumor cell proliferation in the intestine [162]. The alternative signaling seems to be mainly important for developmental processes, such as development of mammary gland [149] or secondary lymphoid organs [60, 67].

Defective IKKα activation results in diminished NF-κB activity (*Figure 3.6*), suggesting that it is involved in the canonical pathway. It has been shown that *Ikkβ* deletion in IECs renders mice susceptible to DSS-induced colitis [163], while simultaneous deletion of both *Ikkα* and *Ikkβ* kinases induces spontaneous colitis in mice [51]. This indicates that proper activation of NF-κB in the intestinal epithelium is required to maintain intestinal homeostasis. Inactivation of NF-κB upon defective IKKα signaling has been documented

in other studies as well [148, 149, 164]. On the contrary, IKKα has been as well reported to limit NF-κB activation in response to specific signals [62, 64]. The reason why in some tissues or cell types IKKα acts in different ways might depend on various factors such as, its expression, subcellular localization or interaction with different partners and on the specific signal.

4.2 IKKα activates inflammasome function and IL-18 production

Caspases are cysteine proteases that regulate tissue homeostasis, embryonic development, cell differentiation and removal of injured or harmful cells from many tissues in the body. Their activity is mainly regulated at the posttranslational level, allowing their rapid activation and response to cellular stress and pathogenic stimuli [165]. Some caspases, such as caspase-1, -5, -12 and -11 (-4 in humans), are activated during innate immune responses and control the inflammatory reaction by processing the pro-form of IL-1 family members (IL-18 and IL-1β) into their active forms, and therefore are called inflammatory caspases [165].

In the present study caspase-12 was of particular interest due to the significant activation (cleavage) found in IECs from DSS-treated *Ikkα*$^{AA/AA}$ animals (*Figure 3.9 C*). Nevertheless, the functional role of this activation remains still unidentified. The reason for that is the highly restricted substrate specificity and low catalytic efficiency of this enzyme, as it possesses proteolytic activity, which is, however, restricted to its self [133].

The importance of caspase-12 in the inflammatory phenotype of *Ikkα*$^{AA/AA}$ mice was supported by the rescue of *Ikkα*$^{AA/AA}$ animals upon deletion of this caspase. Abrogation of caspase-12 limited mucosal damage by promoting regeneration of crypts and surface epithelia (*Figure 3.13*), and inhibited production of proinflammatory factors (*Figure 3.14*).

Moreover, it is demonstrated that IL-18 levels are significantly downregulated in the serum of *Ikkα*$^{AA/AA}$ mice upon DSS treatment (*Figure 3.10*). The current data suggest that the phenotype of *Ikkα*$^{AA/AA}$ mice is ascribed to decreased IL-18 production, since administration of this recombinant cytokine induced epithelial regeneration and reduced inflammation in *Ikkα*$^{AA/AA}$ mutants treated with DSS (*Figure 3.11*). In agreement with former studies [107, 119], the data obtained here show that IEC comprise the major source of IL-18 during DSS colitis (*Figure 3.12*).

IKKα-dependent activation of the inflammasome seems to be cell-type specific, since IKKα was recently shown to limit inflammasome function in macrophages [166]. The authors reported that macrophages from *Ikkα*$^{AA/AA}$ and *Ikkα*^{K44A} (in which the ATP-binding domain of IKKα is mutated resulting in loss of kinase activity) hyperproduce IL-1β in response to stimuli that activate the inflammasomes [166]. In agreement with that the enhanced IL-1β serum levels seen in DSS-treated *Ikkα*$^{AA/AA}$ mice may have arrived from overactivation of the inflammasome in immune cells, as it is shown that IL-1β is mainly produced by the immune cells (*Figure 3.12 B*). Contrary to *Ikkα*$^{AA/AA}$ mice, mice lacking *Ikkα* specifically in the myeloid cells (*Ikkα*$^{\Delta mye}$) have less tissue damage than wild-type controls (*Figure 3.4 F-J*) and low IL-1β serum levels (not shown here), suggesting that IL-1β levels correlate with the extent of tissue damage. IL-1β has been shown to increase epithelial permeability [167] and increasing levels of this cytokine correlate with severity of intestinal inflammation in patients with CD and UC [168], which could explain how IL-1β contributes to tissue damage. Nevertheless, since IL-1β signaling was not profoundly explored in the present study it is still not well defined what the exact role of myeloid-derived IL-1β is in the absence of proper IKKα signaling.

The role of IL-18 is complex and its possible contribution to the maintenance of chronic inflammation in the intestine is unclear. Several studies have suggested that IL-18 could

be an effector cytokine in IBD, as circulating and local IL-18 levels have been associated with disease severity [116, 169, 170]. On the contrary, more recent investigations have shown that mice deficient in IL-18 production are more susceptible rather than resistant to DSS-induced colitis [107, 110, 112, 119, 171]. However, excessive production of IL-18 is pathogenic: inflammasome hyperactivation leads to increased IL-18 and IL-1β secretion by macrophages, thereby, resulting in increased DSS-induced colitis [87]. It appears that a dramatic shift in the cellular source of IL-18, from IECs to lamina propria macrophages and dendritic cells, occurs as the severity of disease progresses in patients with CD and UC [116, 151]. In the early phase of IBD injury of mucosa results in innate immune responses to environmental factors, such as commensal or pathogenic bacteria, that in turn may activate IECs to produce IL-18 [172]. However, in the later stages of chronic and severe inflammation the mucosa is infiltrated by lymphocytes, macrophages and other immune cells, which provide the cellular source of IL-18 and other cytokines (e.g IL-12) to mount a prototypic Th1-mediated immune response [151, 172].

Caspase-1 and *Asc* (the inflammasome adaptor) knockout mice develop severe colitis induced by DSS [107, 112, 119], while *Caspase-12* deficient mice are protected [119]. Furthermore, caspase-12 was shown to interact with caspase-1 and to inhibit its activation [127, 133]. The unique function of caspase-12 as a dominant-negative regulator of the inflammatory caspase cascade has been reported in both humans [136] and mice [119, 127]. Given the dominant negative effect of caspase-12 on caspase-1, the data propose that IECs unable to activate IKKα upon DSS treatment, display increased caspase-12 activation (*Figure 3.9 C*), which in turn acts as dominant negative regulator of caspase-1 and therefore, limits the production of the cytoprotective IL-18. As both NLRP6 [112, 171] and NLPR3 [107, 110] inflammasomes were shown to be required for IL-18 production *in vivo,* it remains still unknown whether IKKα signals through the NLRP3 or

NLRP6 inflammasome to induce IL-18 secretion. Likewise, the mechanism by which IL-18 production confers its protective effect on the colonic mucosa is not very clear yet and whether it acts directly or indirectly on the IECs remains a subject of investigation

4.3 Defective IKKα activation results in ER stress

ER stress has been genetically associated with both forms of IBD, Crohn's disease and Ulcerative colitis, through a candidate gene study of XBP1 [16]. The intestinal epithelium is highly sensitive, even to minor impairments in UPR signaling as can viewed by animal models that either lack or have mutated certain proteins of the UPR signaling. For instance, mice deficient in *Atf6a* and *p58^{IPK}* [78], *Ire1β* [77], *Arg2* [173], *Xbp1*[16] or bearing hypomorphic allele of the Site 1 protease (S1P)-encoding gene, *Mbtps1* [174] *or Xbp1*[16] develop severe colitis induced by DSS or in the case of *Arg2* and *Xbp1* spontaneous inflammation of the small intestine. Chemical chaperones such as TUDCA and PBA, which promote ER homeostasis and increase ER folding capacity, reduce ER stress in IECs and alleviate acute and chronic colitis in mice, further demonstrating the significance of proper UPR signaling in maintaining intestinal homeostasis [78].

It is demonstrated that activation of the UPR in the setting of impaired IKKα signaling, results in increased *Grp78*, *Ire1α* and *Xbp1* mRNA splicing (*Figure 3.15 A-D*). It has been shown that hypomorphic XBP1 function in the epithelium results in ER stress, manifested by an upregulation of GRP78 and profound induction of IRE1α [79]. Moreover, mice deficient in *Ire1β*, which is specifically expressed in the IECs, are susceptible to DSS [77], further emphasizes the importance of IRE1α-XBP1 axis in preserving homeostasis of the intestinal epithelium.

Previous studies have shown that ER stress induces the formation of IRE1α and IKK complex through TRAF2 [73, 175] and dissociation of TRAF2 from caspase-12 [131].

TRAF2 is also considered a protein sensitive to degradation and was shown to be reduced under ER stress conditions [73]. Moreover, *Traf2* knockout mice develop spontaneous colitis illustrating its crucial role in controlling homeostasis of the colon [176]. In this study it is shown that DSS-treated *Ikkα*$^{AA/AA}$ IECs display critically low levels of TRAF2 (*Figure 3.15 D*), which in agreement with these studies, underlie the importance of TRAF2 in maintaining colon physiology.

Examination of the PERK pathway revealed that it is significantly down-regulated (*Figure 3.15 A and E*), suggesting that IKKα loss induces enhanced ER stress that cannot be compensated by the other UPR pathways. Previous studies reported that loss of PERK/CHOP signaling cascade is linked to defects in cell death sensitivity and ROS-mediated ER stress [153]. PERK signaling is also required for proper differentiation of intestinal epithelial cells [79], delineating the importance of PERK pathway in the intestine. Thus, it seems that elevated IRE1α and reduced PERK signaling leads to increased sensitivity of the epithelium to environmental triggers, such as DSS, that further challenge the UPR and its compensatory pathways.

ER stress can be both a primary reason (as seen in *Xbp1* knockout mice [16]) and also a consequence of intestinal inflammation (as observed in *Il10* deficient mice). Several studies have proposed evidence of ER stress, based on increased *Grp78* and *Xbp1* splicing, in a significant proportion of UC and CD patients [27, 177], suggesting that ER stress is a consequence of inflammation. The present report proposes that caspase-12 activation, which occurs as a result of ER stress, is causing the massive inflammation seen in *Ikkα*$^{AA/AA}$ mice in response to DSS, suggesting ER stress as an upstream activator of inflammation (*chapters 3.7 and 3.7.1*). Nevertheless, based on these findings, the reverse order of events cannot be completely excluded and it should be further investigated.

Given the substantial caspase-12 activation found in *Ikkα*$^{AA/AA}$ IECs (*Figure 3.9 C*), it could be therefore assumed that in *Ikkα*$^{AA/AA}$ mutant IECs DSS triggers activation of the IRE1α/XBP1 branch of the UPR, down-regulation of TRAF2 and thus, dissociation from caspase-12. Caspase-12 in turn is activated causing an inflammatory environment in the colon that results in the severe pathology of *Ikkα*$^{AA/AA}$ mice (*Figure 3.13 and 3.14*).

4.4 IKKα controls autophagy

Perturbations in the function of autophagy-related proteins may contribute not only to increased susceptibility to infection, but also to chronic inflammatory diseases and autoimmune diseases. The only well-characterized link is between mutations in autophagy proteins and IBD, especially Crohn's disease [178]. The significance of autophagy in intestinal physiology can be seen in animal models lacking certain components of the autophagic machinery, such as *Atg16l1*, *Atg7* and *Atg5* [14, 86, 179-181]. These mice develop severe spontaneous Crohn's-disease-like transmural ileitis or DSS-induced colitis, due to inefficient autophagic clearance of enteric pathogens and aberrant immune priming that eventually act as a trigger for intestinal inflammation.

The IKK complex has been suggested a biological 'switch' for the rapid induction of autophagy. It was reported that IKK activation is able to effectively trigger autophagy and reversely, optimal induction of autophagy by several stimuli requires IKK activation [182, 183], supporting an intimate link between IKK complex and autophagy Here, it is shown that IECs unable to activate IKKα in response to DSS are defective in autophagy completion, which results in inefficient degradation and accumulation of p62 (*Figure 3.17*). LC3 conversion, which is used as a marker for autophagosome formation, is greatly elevated in *Ikkα*$^{AA/AA}$ IECs challenged with DSS, indicating that autophagy is activated. However, p62 is significantly increased, suggesting that alterations occur in the late stage

of the autophagic process. Loss of IKKα in pancreatic cells has been shown to impair autophagy, by means of increased LC3 conversion and p62 accumulation, and eventually to trigger inflammation [66]. It seems that IKKα, at least in some tissues, utilizes similar mechanisms to maintain homeostasis.

P62 has been suggested to regulate formation of protein aggregates and to be cleared out by autophagy [93]. Autophagy-deficient cells display elevated p62 levels and genetic ablation of *p62* suppresses the appearance of protein aggregates and rescues pathology caused by autophagy deficiency [66, 93-95]. P62 as an adaptor protein has been linked to IKK/NF-κB activation in response to diverse stimuli, such as IL-1 [96], RANK ligand [97] or nerve growth factor (NGF)[98]. Another report suggesting the existence of a signalling connection between IKK/NF-κB activation and p62 came from Duran *et. al* where they showed that p62 is essential for Ras-induced transformation of lung epithelial cells and IKK/NF-κB activation [184]. However, under conditions of stress, autophagy-defective cells accumulate p62, which suppress canonical NF-κB activation [185]. Specifically, under metabolic stress autophagy-deficient tumor cells preferentially accumulate p62 and fail to exert protein quality control, leading to enhanced ER stress and ROS production. This failure of autophagy-defective cells to eliminate p62 is sufficient to suppress NF-κB, impair survival and drive oncogenesis [185]. In a similar way is thought that inadequate IKKα signaling in IECs results in defective autophagy that causes p62 accumulation (*Figure 3.17 C*) and ER stress (*Figure 3.15 C*). It seems that under conditions where autophagy must be activated, IKK/NF-κB axis contributes to p62 degradation by inducing autophagy. Nevertheless, to connect the striking phenotype in $Ikk\alpha^{AA/AA}$ mutants and the relevance of p62 accumulation in disease outcome, it is essential to explore whether loss of p62 will resolve the inflammatory phenotype observed in $Ikk\alpha^{AA/AA}$ mice. The role of p62 ablation in $Ikk\alpha^{AA/AA}$ phenotype is currently under investigation.

Atg16l1 is an essential autophagy gene [87] and a candidate gene responsible for susceptibility to Crohn's disease [81]. Mice deficient in *Atg16l1* die within one day of delivery, indicating that is required for survival during neonatal starvation [87]. Importantly, IKKα is shown to interact with ATG16L1 (*Figure 3.17 D*) in IECs indicating that is somehow implicated in the regulation of this autophagy protein. This interaction, however, is abrogated when *Ikkα*$^{AA/AA}$ mutant IECs are challenged with DSS. Wild-type DSS-treated IECs show reduced ATG16L1 protein levels and intact ATG16L1-IKKα interaction (*Figure 3.17 E*), indicating that functional IKKα might be essential for inducing autophagy completion together with ATG16L1. Recently, it was reported that the Crohn's-disease-associated *Atg16l1* (*T300A*) risk variant is highly susceptible to proteolytic degradation resulting in defective autophagy, which in turn establishes a chronic inflammatory state [86, 181]. The critically low levels of ATG16L1 seen in the DSS-treated *Ikkα*$^{AA/AA}$ IECs and the lack of ATG16L1-*Ikkα*$^{AA/AA}$ interaction upon DSS challenge (*Figure 3.17 E*) presumably designates that under conditions of stress, mutant IKKα sensitizes ATG16L1 for degradation. As IKKα is a serine/threonine kinase it could be speculated that phosphorylation of ATG16L1 might be required to maintain this interaction with IKKα upon stress, as at resting state mutant IKKα is able to associate with ATG16L1 (*Figure 3.17 D*). It is possible that activation of IKKα is required to direct ATG16L1 to the autophagic process. Since it is claimed here that autophagy is compromised at later stages, ATG16L1 might function as an adaptor protein involved in autophagy completion, as suggested elsewhere [66]. Furthermore, ATG16L1 was required for Cullin-3 (an E3 ubiquitin ligase) activation and thus, for Cul-3-dependent ubiquitination and degradation of p62 [95]. This suggests a possible mechanism by which ATG16L1 regulates p62 degradation and thereby, limits inflammatory conditions. Nonetheless, whether IKKα is a kinase for

ATG16L1 and/or IKKα activation is essential to direct ATG16L1 to autophosomes and through which mechanism requires further examination.

The UPR and autophagy are integrally linked pathways. Not only may ER stress induce autophagy [83, 179, 186], but also vice versa, impaired autophagy can lead to ER stress [179, 185, 187]. In light of these findings and given the close relationship of ineffective autophagy with ER stress induction, it is likely that in the model of the present study impairment of autophagy might have triggered ER stress. Nonetheless, to suggest that further investigation is required and p62 ablation might shed light into this speculation.

Altogether, it is suggested that IKKα might control autophagy through the regulation of ATG16L1, a highly implicated protein in IBD. IECs in which IKKα is mutated cannot complete autophagy successfully, resulting in accumulation of p62. This in turn triggers ER stress and subsequently caspase-12 release, which compromises mucosal immunity and augments intestinal inflammation in the presence of DSS. Most likely this mucosal inflammation depends on the microbiome and proinflammatory cytokines and derives from increased IEC death, ER stress and caspase-12 activation, which are synergistically increased when autophagy is impaired.

5. Conclusion

Physiologic levels of inflammation are protective, while excessive inflammation is deleterious and is at the basis of IBD. One of the foremost inflammation-associated pathways is the NF-κB pathway, with IKKα being one of the central regulators of this pathway. IKKα is a protein kinase involved in inflammatory processes in various organs, yet, its specific function during acute inflammation of the colon has not been investigated to date.

The results presented in this study show that mice bearing an inactive form of IKKα are significantly more susceptible to DSS-induced colitis. The exacerbated inflammatory response is attributed to defective IKKα signaling in the IECs, suggesting that proper IKKα activation in local cells of the colonic mucosa is critical for protection against DSS-induced injury. The current model proposes that in response to environmental factors that can damage the intestinal mucosa, IKKα activation is essential to stimulate autophagy via the autophagy adaptor protein ATG16L1, resulting in efficient degradation of p62 and other ubiquitinated proteins. This in turn prevents ER stress and caspase-12 activation, thus, limiting the deregulated inflammatory responses in the colon (*Figure 5. A*).

On the other hand, absence of IKKα phospho-activation in the epithelial compartment, compromises the autophagic process, presumably by regulating ATG16L1. Inactivation of autophagy causes accumulation of p62 and other proteins and leads to ER stress, which in turn activates and releases caspase-12. Caspase-12 suppresses caspase-1 activity and downstream IL-18 production, which is required for epithelial regeneration and tissue repair. The failure of the injured epithelium to regenerate allows eventually bacterial products or commensals to penetrate into the mucosa and submucosa, where they stimulate resident immune cells through pattern recognition receptors. Enhanced

secretion of cytokines by activated immune cells results in IEC death and marked intestinal inflammation (*Figure 5. B*).

In conclusion, this study supports a mechanistic model for how defective IKKα signaling converts into a disease phenotype by integrating and impinging on three major pathways largely involved in IBD pathogenesis: autophagy, ER stress and bacterial sensing by the inflammasomes.

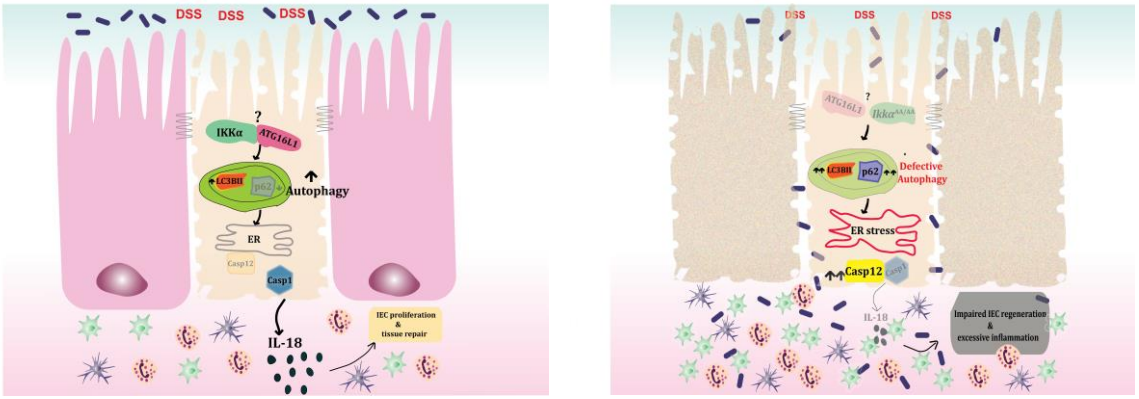

Figure 5.1: Summary of the suggested model depicting the function of IKKα in the colonic epithelium. (A) *IECs that have a fully functional IKKα kinase are able to react to the damage caused by DSS via inducing autophagy and preventing ER stress-dependent caspase-12 activation. This allows inflammasome-dependent caspase-1 activation and IL-18 production, which is required for compensatory proliferation and tissue repair.* ***(B)*** *When IKKα is inactive, autophagy is blocked leading to p62 accumulation and irremediable ER stress. In turn, ER stress triggers caspase-12 release, which inhibits the inflammasome and downstream IL-18 production, thus, resulting in excessive inflammation in the colon. IEC, intestinal epithelial cells.*

6. References

1. Liao, D.-H., *Gastrointestinal tract modelling in health and disease.* World Journal of Gastroenterology, 2009. **15**(2): p. 169.
2. Clevers, L.G.v.d.F.a.H., *Stem cells, self-renewal, and differentiation in the intestinal epithelium.* Annual Review of Physiology, 2009. **71**: p. 241-60.
3. Medema, J.P. and L. Vermeulen, *Microenvironmental regulation of stem cells in intestinal homeostasis and cancer.* Nature, 2011. **474**(7351): p. 318-26.
4. Barker, N., M. van de Wetering, and H. Clevers, *The intestinal stem cell.* Genes Dev, 2008. **22**(14): p. 1856-64.
5. Noah, T.K., B. Donahue, and N.F. Shroyer, *Intestinal development and differentiation.* Exp Cell Res, 2011. **317**(19): p. 2702-10.
6. Barker, N., et al., *Crypt stem cells as the cells-of-origin of intestinal cancer.* Nature, 2009. **457**(7229): p. 608-11.
7. Arthur Kaser, S.Z., and Richard S. Blumberg, *Inflammatory bowel disease.* Annual Review of Immunology, 2010. **28**: p. 573-621.
8. Zhang, Y.Z. and Y.Y. Li, *Inflammatory bowel disease: pathogenesis.* World J Gastroenterol, 2014. **20**(1): p. 91-9.
9. Wu, G.D., F.D. Bushmanc, and J.D. Lewis, *Diet, the human gut microbiota, and IBD.* Anaerobe, 2013. **24**: p. 117-20.
10. Yu, L.C., et al., *Host-microbial interactions and regulation of intestinal epithelial barrier function: From physiology to pathology.* World J Gastrointest Pathophysiol, 2012. **3**(1): p. 27-43.
11. Chassaing, B. and A. Darfeuille-Michaud, *The commensal microbiota and enteropathogens in the pathogenesis of inflammatory bowel diseases.* Gastroenterology, 2011. **140**(6): p. 1720-28.
12. Rance K. Sellon , S.T., Michael Schultz, Levinus A. Dieleman, Wetonia Grenther, Ed Balish, Donna M. Rennick and R. Balfour Sartor, *Resident Enteric Bacteria Are Necessary for Development of Spontaneous Colitis and Immune System Activation in Interleukin-10-Deficient Mice.* Infection and immunity, 1998. **66**(11): p. 5224–5231.
13. Gkouskou, K.K.D., C. Tsatsanis, C. Eliopoulos, A. G., *The gut microbiota in mouse models of inflammatory bowel disease.* Front Cell Infect Microbiol, 2014. **4**: p. 28.
14. Cadwell, K., et al., *A key role for autophagy and the autophagy gene Atg16l1 in mouse and human intestinal Paneth cells.* Nature, 2008. **456**(7219): p. 259-63.
15. Wehkamp, J., et al., *NOD2 (CARD15) mutations in Crohn's disease are associated with diminished mucosal alpha-defensin expression.* Gut, 2004. **53**(11): p. 1658-64.
16. Kaser, A., et al., *XBP1 links ER stress to intestinal inflammation and confers genetic risk for human inflammatory bowel disease.* Cell, 2008. **134**(5): p. 743-56.
17. Takeuchi, O. and S. Akira, *Pattern recognition receptors and inflammation.* Cell, 2010. **140**(6): p. 805-20.
18. Matam Vijay-Kumar, C.J.S., Rebekah T. Taylor, Amrita Kumar, Jesse D. Aitken, Shanthi V. Sitaraman, Andrew S. Neish, Satoshi Uematsu, Shizuo Akira, Ifor R. Williams and Andrew T. Gewirtz, *Deletion of TLR5 results in spontaneous colitis in mice.* The Journal of Clinical Investigation, 2007. **117**(12): p. 3909–3921.
19. Vijay-Kumar, M., et al., *Metabolic syndrome and altered gut microbiota in mice lacking Toll-like receptor 5.* Science, 2010. **328**(5975): p. 228-31.
20. Slack, E., et al., *Innate and adaptive immunity cooperate flexibly to maintain host-microbiota mutualism.* Science, 2009. **325**(5940): p. 617-20.
21. Shipra Vaishnava, C.L.B., Anisa S. Ismail, Lars Eckmann and Lora V. Hooper, *Paneth cells directly sense gut commensals and maintain homeostasis at the intestinal host-microbial interface.* PNAS, 2008. **105**(52): p. 20858-63.
22. Jan Wehkamp, N.H.S., Edith Porter, Sabine Nuding, Michael Weichenthal, Robert E. Petras,Bo Shen, Elke Schaeffeler, Matthias Schwab, Rose Linzmeier, Ryan W. Feathers, Hiutung Chu, Heriberto Lima, Jr., Klaus Fellermann, Tomas Ganz, Eduard F. Stange and

Charles L. Bevins, *Reduced Paneth cell alpha-defensins in ileal Crohn's disease.* PNAS, 2005. **102**(50): p. 18129-34.
23. Kuballa, P., et al., *Impaired autophagy of an intracellular pathogen induced by a Crohn's disease associated ATG16L1 variant.* PLoS One, 2008. **3**(10): p. e3391.
24. Johansson, M.E., et al., *The inner of the two Muc2 mucin-dependent mucus layers in colon is devoid of bacteria.* Proc Natl Acad Sci U S A, 2008. **105**(39): p. 15064-9.
25. Velcich, A., et al., *Colorectal cancer in mice genetically deficient in the mucin Muc2.* Science, 2002. **295**(5560): p. 1726-9.
26. Van der Sluis, M., et al., *Muc2-deficient mice spontaneously develop colitis, indicating that MUC2 is critical for colonic protection.* Gastroenterology, 2006. **131**(1): p. 117-29.
27. Chad K. Heazlewood, M.C.C., Rajaraman Eri, Gareth R. Price, Sharyn B. Tauro, Douglas Taupin,, C.W.P. David J. Thornton, Tanya L. Crockford, Richard J. Cornall, Rachel Adams, Masato Kato,, and N.A.H. Keats A. Nelms, Timothy H. J. Florin, Christopher C. Goodnow, Michael A. McGuckin, *Aberrant Mucin Assembly in Mice Causes Endoplasmic Reticulum Stress and Spontaneous Inflammation Resembling Ulcerative Colitis.* PLoS Medicine, 2008. **5**(3).
28. Brown, E.M., M. Sadarangani, and B.B. Finlay, *The role of the immune system in governing host-microbe interactions in the intestine.* Nat Immunol, 2013. **14**(7): p. 660-7.
29. Wehkamp, J., M. Schmid, and E.F. Stange, *Defensins and other antimicrobial peptides in inflammatory bowel disease.* Curr Opin Gastroenterol, 2007. **23**(4): p. 370-8.
30. Vaishnava, S., et al., *The antibacterial lectin RegIIIgamma promotes the spatial segregation of microbiota and host in the intestine.* Science, 2011. **334**(6053): p. 255-8.
31. Brandl, K., et al., *MyD88-mediated signals induce the bactericidal lectin RegIII gamma and protect mice against intestinal Listeria monocytogenes infection.* J Exp Med, 2007. **204**(8): p. 1891-900.
32. Hooper, L.V. and A.J. Macpherson, *Immune adaptations that maintain homeostasis with the intestinal microbiota.* Nat Rev Immunol, 2010. **10**(3): p. 159-69.
33. Suzuki, K.M., B. Doi, Y. Muramatsu, M. Chiba, T. Honjo, T. Fagarasan, S., *Aberrant expansion of segmented filamentous bacteria in IgA-deficient gut.* PNAS, 2004. **101**(7): p. 1981-6.
34. Harrington, L.E., et al., *Interleukin 17-producing CD4+ effector T cells develop via a lineage distinct from the T helper type 1 and 2 lineages.* Nature Immunology, 2005. **6**(11): p. 1123-32.
35. Bettelli, E., et al., *Reciprocal developmental pathways for the generation of pathogenic effector TH17 and regulatory T cells.* Nature, 2006. **441**(7090): p. 235-8.
36. Mangan, P.R., et al., *Transforming growth factor-beta induces development of the T(H)17 lineage.* Nature, 2006. **441**(7090): p. 231-4.
37. Takeda, H.K.K., *Regulation of Intestinal Homeostasis by Innate and Adaptive Immunity.* International Immunology, 2012. **24**(11): p. 673-680.
38. Yen, D., et al., *IL-23 is essential for T cell-mediated colitis and promotes inflammation via IL-17 and IL-6.* J Clin Invest, 2006. **116**(5): p. 1310-6.
39. Hue, S., et al., *Interleukin-23 drives innate and T cell-mediated intestinal inflammation.* J Exp Med, 2006. **203**(11): p. 2473-83.
40. Peter J. Mannon, M.D., M.P.H., Ivan J. Fuss, M.D., Lloyd Mayer, M.D., et al., *Anti–Interleukin-12 Antibody for Active Crohn's Disease.* The New England Journal of Medicine, 2004. **351**(120).
41. Ralf Kühn, J.L., Donna Rennick, Klaus Rajewsky, and Werner Müller, *Interleukin-10 Deficient Mice Develop Chronic Enterocolitis.* Cell 1993. **75**: p. 263-274.
42. M Shull, I.O., A Kier, S Pawlowski, R Diebold, M Yin, R Allen, C Siedman, G Proetzel, D Calvin, N Annunziata and T Doetschman, *Targeted Disruption of the Mouse Transforming Growth Factor-β1 Gene Results in Multifocal Inflammatory Disease.* Nature, 1992. **359**.
43. Greten, M.K.a.F.R., *NF-kappaB: linking inflammation and immunity to cancer development and progression.* Nature Reviews Immunology, 2005. **5**(10): p. 749-59.
44. Grivennikov, S.I., F.R. Greten, and M. Karin, *Immunity, inflammation, and cancer.* Cell, 2010. **140**(6): p. 883-99.

45. Hayden, M.S. and S. Ghosh, *NF-kappaB, the first quarter-century: remarkable progress and outstanding questions.* Genes Dev, 2012. **26**(3): p. 203-34.
46. Sun, S.C., *Non-canonical NF-kappaB signaling pathway.* Cell Research, 2011.
47. Bollrath, J. and F.R. Greten, *IKK/NF-kappaB and STAT3 pathways: central signalling hubs in inflammation-mediated tumour promotion and metastasis.* EMBO Rep, 2009. **10**(12): p. 1314-9.
48. Rogler, G., et al., *Nuclear factor kappaB is activated in macrophages and epithelial cells of inflamed intestinal mucosa.* Gastroenterology, 1998. **115**(2): p. 357-69.
49. Neurath, M.F., et al., *Local administration of antisense phosphorothioate oligonucleotides to the p65 subunit of NF-kappa B abrogates established experimental colitis in mice.* Nat Med, 1996. **2**(9): p. 998-1004.
50. Eckmann, L., et al., *Opposing functions of IKKbeta during acute and chronic intestinal inflammation.* Proc Natl Acad Sci U S A, 2008. **105**(39): p. 15058-63.
51. Nenci, A., et al., *Epithelial NEMO links innate immunity to chronic intestinal inflammation.* Nature, 2007. **446**(7135): p. 557-61.
52. Kris A. Steinbrecher, E.H.-L., Raquel Sitcheran, and Albert S. Baldwin, *Loss of Epithelial RelA Results in Deregulated Intestinal Proliferative/Apoptotic Homeostasis and Susceptibility to Inflammation.* The journal of Immunology, 2008.
53. Egan, L.J., et al., *IkB-kinase -dependent NF-kB activation provides radioprotection to the intestinal epithelium.* Proceedings of the National Academy of Sciences, 2004. **101**(8): p. 2452-2457.
54. Greten, F.R., et al., *IKKbeta links inflammation and tumorigenesis in a mouse model of colitis-associated cancer.* Cell, 2004. **118**(3): p. 285-96.
55. Zaph, C., et al., *Epithelial-cell-intrinsic IKKbeta expression regulates intestinal immune homeostasis.* Nature, 2007. **446**(7135): p. 552-6.
56. Qiutang Li, D.V.A., Frank Mercurio, and I.M.V. Kuo-Fen Lee, *Severe Liver Degeneration in Mice Lacking the IB Kinase 2 Gene.* Science, 1999. **284**(5412): p. 321-325.
57. Qiutang Li, Q.L., Jason Y. Hwang, Dirk Buscher, Kuo-Fen Lee, and a.I.M.V. Juan Carlos Izpisua-Belmonte, *IKK1 deficient mice exhibit abnormal development of skin and skeleton.* Genes and Development, 1999. **13**: p. 1322–1328.
58. Takeda, K., *Limb and Skin Abnormalities in Mice Lacking IKK.* Science, 1999. **284**(5412): p. 313-316.
59. Yinling Hu, V.B., Mireille Delhase, Peilin Zhang,, M.E. Thomas Deerinck, Randall Johnson,, and M. Karin, *Abnormal Morphogenesis But Intact IKK Activation in Mice Lacking the IKK Subunit of IB Kinase.* Science, 1999. **284**(5412): p. 316-320.
60. Senftleben, U., et al., *Activation by IKKalpha of a second, evolutionary conserved, NF-kappa B signaling pathway.* Science, 2001. **293**(5534): p. 1495-9.
61. Yixue Cao, G.B., Tiffany N. Seagroves, Florian R. Greten, Randall Johnson, Emmett V. Schmidt, and Michael Karin, *IKKα Provides an Essential Link Between RANK Signaling and Cyclin D1 Expression During Mammary Gland Development* Cell, 2002.
62. Toby Lawrence, M.B., George Y. Liu, Victor Nizet and M. Karin, *IKKa limits macrophage NF-kB activation and contributes to the resolution of inflammation.* Nature, 2005.
63. Li, Q., et al., *Enhanced NF-kappaB activation and cellular function in macrophages lacking IkappaB kinase 1 (IKK1).* Proc Natl Acad Sci U S A, 2005. **102**(35): p. 12425-30.
64. Shembade, N., et al., *The kinase IKKalpha inhibits activation of the transcription factor NF-kappaB by phosphorylating the regulatory molecule TAX1BP1.* Nat Immunol, 2011. **12**(9): p. 834-43.
65. Liu, B., et al., *Proinflammatory stimuli induce IKKalpha-mediated phosphorylation of PIAS1 to restrict inflammation and immunity.* Cell, 2007. **129**(5): p. 903-14.
66. Li, N., et al., *Loss of acinar cell IKKalpha triggers spontaneous pancreatitis in mice.* J Clin Invest, 2013.
67. Giuseppina Bonizzi, M.B., Dennis C Otero, Kirsten E Johnson,Vroom, Yixue Cao, Don Vu, Anil G Jegga, Bruce J Aronow, Gourisankar Ghosh, Robert C Rickert and Michael Karin,

Activation of IKKa terget genes depends on recognition of specific kB binding sites by RelB-p52 dimers. The EMBO Journal, 2004. **23**.
68. Mancino, A., et al., *I kappa B kinase alpha (IKKalpha) activity is required for functional maturation of dendritic cells and acquired immunity to infection.* EMBO J, 2013.
69. Malhotra, J.D. and R.J. Kaufman, *The endoplasmic reticulum and the unfolded protein response.* Semin Cell Dev Biol, 2007. **18**(6): p. 716-31.
70. Lin, J.H., P. Walter, and T.S. Yen, *Endoplasmic reticulum stress in disease pathogenesis.* Annu Rev Pathol, 2008. **3**: p. 399-425.
71. Fumihiko Urano, X.W., Anne Bertolotti, Yuhong Zhang, Peter Chung, Heather P. Harding, David Ron, *Coupling of Stress in the ER to Activation of JNK Protein Kinases by Transmembrane Protein Kinase IRE1.* Science, 2000. **287**(5453): p. 664-666.
72. Masayuki Kaneko, Y.N., and Yasuyuki Nomura, *Activation Signal of Nuclear Factor-k B in Response to Endoplasmic Reticulum Stress is Transduced via IRE1 and Tumor Necrosis Factor Receptor-Associated Factor 2.* Biol. Pharm. Bull, 2003. **26**(7): p. 931-935.
73. Hu, P., et al., *Autocrine tumor necrosis factor alpha links endoplasmic reticulum stress to the membrane death receptor pathway through IRE1alpha-mediated NF-kappaB activation and down-regulation of TRAF2 expression.* Mol Cell Biol, 2006. **26**(8): p. 3071-84.
74. Mauro, C., et al., *Central role of the scaffold protein tumor necrosis factor receptor-associated factor 2 in regulating endoplasmic reticulum stress-induced apoptosis.* J Biol Chem, 2006. **281**(5): p. 2631-8.
75. Kaser, A. and R.S. Blumberg, *Autophagy, microbial sensing, endoplasmic reticulum stress, and epithelial function in inflammatory bowel disease.* Gastroenterology, 2011. **140**(6): p. 1738-47.
76. Zhang, K. and R.J. Kaufman, *From endoplasmic-reticulum stress to the inflammatory response.* Nature, 2008. **454**(7203): p. 455-62.
77. Anne Bertolotti, X.W., Isabel Novoa, Rivka Jungreis, Karni Schlessinger, and A.B.W. Judy H. Cho, and David Ron, *Increased sensitivity to dextran sodium sulfate colitis in IRE1b-deficient mice.* J. Clin. Invest, 2001. **107**: p. 585–593.
78. Cao, S.S., et al., *The unfolded protein response and chemical chaperones reduce protein misfolding and colitis in mice.* Gastroenterology, 2013. **144**(5): p. 989-1000 e6.
79. Heijmans, J., et al., *ER stress causes rapid loss of intestinal epithelial stemness through activation of the unfolded protein response.* Cell Rep, 2013. **3**(4): p. 1128-39.
80. Kaser, A. and R.S. Blumberg, *Endoplasmic reticulum stress and intestinal inflammation.* Mucosal Immunol, 2010. **3**(1): p. 11-6.
81. Hampe, J., et al., *A genome-wide association scan of nonsynonymous SNPs identifies a susceptibility variant for Crohn disease in ATG16L1.* Nat Genet, 2007. **39**(2): p. 207-11.
82. McCarroll, S.A., et al., *Deletion polymorphism upstream of IRGM associated with altered IRGM expression and Crohn's disease.* Nature Genetics, 2008. **40**(9): p. 1107-12.
83. Fritz, T., et al., *Crohn's disease: NOD2, autophagy and ER stress converge.* Gut, 2011. **60**(11): p. 1580-8.
84. Levine, B. and G. Kroemer, *Autophagy in the pathogenesis of disease.* Cell, 2008. **132**(1): p. 27-42.
85. Johansen, T. and T. Lamark, *Selective autophagy mediated by autophagic adapter proteins.* Autophagy, 2011. **7**(3): p. 279-296.
86. Murthy, A.L., Y. Peng, I. Reichelt, M. Katakam, A. K. Noubade, R. Roose-Girma, M. DeVoss, J. Diehl, L. Graham, R. R. van Lookeren Campagne, M., *A Crohn's disease variant in Atg16l1 enhances its degradation by caspase 3.* Nature, 2014. **506**(7489): p. 456-62.
87. Saitoh, T., et al., *Loss of the autophagy protein Atg16L1 enhances endotoxin-induced IL-1beta production.* Nature, 2008. **456**(7219): p. 264-8.
88. Jean-Pierre Hugot, M.C., Habib Zouali, Suzanne Lesage, Jean-Pierre Cezard, Jacques Belaiche, Sven Almerk, Curt Tysk, Colm A. O'Morain, Miquel Gassull, Vibeke Binder, Yigael Finkel, Antoine Cortot, Robert Modigliani, Pierre Laurent-Puig, Corine Gower-Rousseau, Jeanne Macrykk, Jean-Frederic Colombel, Mourad Sahbatou & Gilles Thomas, *Association*

of NOD2 leucine-rich repeat variants with susceptibility to Crohn's disease. Nature, 2001. **411**.
89. Homer, C.R., et al., *ATG16L1 and NOD2 interact in an autophagy-dependent antibacterial pathway implicated in Crohn's disease pathogenesis.* Gastroenterology, 2010. **139**(5): p. 1630-41, 1641 e1-2.
90. Travassos, L.H., et al., *Nod1 and Nod2 direct autophagy by recruiting ATG16L1 to the plasma membrane at the site of bacterial entry.* Nat Immunol, 2010. **11**(1): p. 55-62.
91. Bitto, A., et al., *p62/SQSTM1 at the interface of aging, autophagy, and disease.* AGE, 2014.
92. Moscat, J. and M.T. Diaz-Meco, *p62 at the crossroads of autophagy, apoptosis, and cancer.* Cell, 2009. **137**(6): p. 1001-4.
93. Komatsu, M., et al., *Homeostatic levels of p62 control cytoplasmic inclusion body formation in autophagy-deficient mice.* Cell, 2007. **131**(6): p. 1149-63.
94. Korolchuk, V.I., et al., *Autophagy inhibition compromises degradation of ubiquitin-proteasome pathway substrates.* Mol Cell, 2009. **33**(4): p. 517-27.
95. Lee, J.K., H. R. Quinley, C. Kim, J. Gonzalez-Navajas, J. Xavier, R. Raz, E., *Autophagy suppresses interleukin-1beta (IL-1beta) signaling by activation of p62 degradation via lysosomal and proteasomal pathways.* J Biol Chem, 2012. **287**(6): p. 4033-40.
96. Laura Sanz, M.a.T.D.-M., Hiroyasu Nakano and Jorge Moscat, *The atypical PKC-interacting protein p62 channels NF-κB activation by the IL-1-TRAF6 pathway.* The EMBO Journal, 2000. **19**(7): p. 1576–1586.
97. Angeles Dura´n, M.S., Michael Leitges, Juana M. Flores, Sylvain Picard, Jacques P. Brown, Jorge Moscat, and Maria T. Diaz-Meco, *The Atypical PKC-Interacting Short Article Protein p62 Is an Important Mediator of RANK-Activated Osteoclastogenesis.* Developmental Cell, 2004. **6**: p. 303–309.
98. Marie W. Wooten, M.L.S., Vidya Mamidipudi, Maria T. Diaz-Meco, Philip A. Barker and Jorge Moscat, *The atypical protein kinase C-interacting protein p62 is a scaffold for NF-kappaB activation by nerve growth factor.* J Biol Chem, 2001. **276**(11): p. 7709-12.
99. Wooten, M.W., et al., *The p62 scaffold regulates nerve growth factor-induced NF-kappaB activation by influencing TRAF6 polyubiquitination.* J Biol Chem, 2005. **280**(42): p. 35625-9.
100. Jin, Z., et al., *Cullin3-based polyubiquitination and p62-dependent aggregation of caspase-8 mediate extrinsic apoptosis signaling.* Cell, 2009. **137**(4): p. 721-35.
101. Lee, H.M., et al., *Mycobacterium abscessus activates the NLRP3 inflammasome via Dectin-1-Syk and p62/SQSTM1.* Immunol Cell Biol, 2012. **90**(6): p. 601-10.
102. Choe, J.Y., et al., *Enhanced p62 expression through impaired proteasomal degradation is involved in caspase-1 activation in monosodium urate crystal-induced interleukin-1beta expression.* Rheumatology (Oxford), 2014.
103. Chen, G.Y. and G. Nunez, *Inflammasomes in intestinal inflammation and cancer.* Gastroenterology, 2011. **141**(6): p. 1986-99.
104. Schroder, K. and J. Tschopp, *The inflammasomes.* Cell, 2010. **140**(6): p. 821-32.
105. Elinav, E., J. Henao-Mejia, and R.A. Flavell, *Integrative inflammasome activity in the regulation of intestinal mucosal immune responses.* Mucosal Immunol, 2013. **6**(1): p. 4-13.
106. Villani, A.C., et al., *Common variants in the NLRP3 region contribute to Crohn's disease susceptibility.* Nat Genet, 2009. **41**(1): p. 71-6.
107. Zaki, M.H., et al., *The NLRP3 inflammasome protects against loss of epithelial integrity and mortality during experimental colitis.* Immunity, 2010. **32**(3): p. 379-91.
108. Zaki, M.H., et al., *IL-18 production downstream of the Nlrp3 inflammasome confers protection against colorectal tumor formation.* J Immunol, 2010. **185**(8): p. 4912-20.
109. Allen, I.C., et al., *The NLRP3 inflammasome functions as a negative regulator of tumorigenesis during colitis-associated cancer.* J Exp Med, 2010. **207**(5): p. 1045-56.
110. Hirota, S.A., et al., *NLRP3 inflammasome plays a key role in the regulation of intestinal homeostasis.* Inflammatory Bowel Disease, 2011. **17**(6): p. 1359-72.
111. Bauer, C., et al., *Colitis induced in mice with dextran sulfate sodium (DSS) is mediated by the NLRP3 inflammasome.* Gut, 2010. **59**(9): p. 1192-9.

112. Elinav, E., et al., *NLRP6 inflammasome regulates colonic microbial ecology and risk for colitis.* Cell, 2011. **145**(5): p. 745-57.
113. Chen, G.Y., et al., *A functional role for Nlrp6 in intestinal inflammation and tumorigenesis.* Journal of Immunology, 2011. **186**(12): p. 7187-94.
114. Wlodarska, M., et al., *NLRP6 Inflammasome Orchestrates the Colonic Host-Microbial Interface by Regulating Goblet Cell Mucus Secretion.* Cell, 2014. **156**(5): p. 1045-1059.
115. Zhernakova, A., et al., *Genetic analysis of innate immunity in Crohn's disease and ulcerative colitis identifies two susceptibility loci harboring CARD9 and IL18RAP.* Am J Hum Genet, 2008. **82**(5): p. 1202-10.
116. Theresa T. Pizarro, M.H.M., Marcia Bentz, Jan Cominelli, Christopher A. Moskaluk, Stephen J. Bickston and Fabio Cominelli, *IL-18, a Novel Immunoregulatory Cytokine, Is Upregulated In Crohn's Disease: Expression and localization in Intestinal Mucosal Cells.* Journal of Immunology, 1999. **162**: p. 6829-6835.
117. Siegmund, B., et al., *IL-1 beta-converting enzyme (caspase-1) in intestinal inflammation.* Proc Natl Acad Sci U S A, 2001. **98**(23): p. 13249-54.
118. Kanai, T., et al., *Macrophage-derived IL-18-mediated intestinal inflammation in the murine model of Crohn's disease.* Gastroenterology, 2001. **121**(4): p. 875-888.
119. Dupaul-Chicoine, J., et al., *Control of intestinal homeostasis, colitis, and colitis-associated colorectal cancer by the inflammatory caspases.* Immunity, 2010. **32**(3): p. 367-78.
120. Takagi, H., et al., *Contrasting action of IL-12 and IL-18 in the development of dextran sodium sulphate colitis in mice.* Scand J Gastroenterology, 2003. **38**(8): p. 837-44.
121. Huber, S., et al., *IL-22BP is regulated by the inflammasome and modulates tumorigenesis in the intestine.* Nature, 2012. **491**(7423): p. 259-63.
122. Saleh, M. and G. Trinchieri, *Innate immune mechanisms of colitis and colitis-associated colorectal cancer.* Nat Rev Immunology, 2011. **11**(1): p. 9-20.
123. Martinon, F. and J. Tschopp, *Inflammatory caspases and inflammasomes: master switches of inflammation.* Cell Death Differ, 2007. **14**(1): p. 10-22.
124. Amal Nadiri, M.K.W.a.M.S., *The Inflammatory Caspases: Key Players in the Host Response to Pathogenic Invasion and Sepsis.* Journal of Immnunology, 2006. **177**: p. 4239-4245.
125. Heinz Fischer, U.K., Leopold Eckhart, and Erwin Tschachler, *Human caspase-12 has acquired deleterious mutations.* Biochemical and Biophysical Research Communications, 2002. **293**: p. 722–726.
126. Kalai, M., et al., *Regulation of the expression and processing of caspase-12.* J Cell Biol, 2003. **162**(3): p. 457-67.
127. Saleh, M., et al., *Enhanced bacterial clearance and sepsis resistance in caspase-12-deficient mice.* Nature, 2006. **440**(7087): p. 1064-8.
128. Rao, R.V., et al., *Coupling endoplasmic reticulum stress to the cell death program. Mechanism of caspase activation.* J Biol Chem, 2001. **276**(36): p. 33869-74.
129. Toshiyuki Nakagawa, H.Z., Nobuhiro Morishima, En Li, and B.A.Y.J.Y. Jin Xu, *Caspase-12 mediates endoplasmic reticulum-specific apoptosis and cytotoxicity by amyloid-β.* Letters to Nature, 2000. **6**.
130. Yuan, T.N.a.J., *Cross talk between two cystein protease families. Activation of caspase-12 by calpain in apoptosis.* The Journal of cell biology, 2000. **150**: p. 887–894.
131. Yoneda, T., et al., *Activation of caspase-12, an endoplastic reticulum (ER) resident caspase, through tumor necrosis factor receptor-associated factor 2-dependent mechanism in response to the ER stress.* J Biol Chem, 2001. **276**(17): p. 13935-40.
132. E Fujita, Y.K., A Jimbo, A Isoai, K Maruyama and T Momoi, *Caspase-12 processing and fragment translocation into the nuclei of tunicamycin treated-cells.* Cell Death and Differentiation 2002. **9**: p. 1108 ± 1114.
133. Roy, S., et al., *Confinement of caspase-12 proteolytic activity to autoprocessing.* Proc Natl Acad Sci U S A, 2008. **105**(11): p. 4133-8.
134. Di Sano, F., et al., *Endoplasmic reticulum stress induces apoptosis by an apoptosome-dependent but caspase 12-independent mechanism.* J Biol Chem, 2006. **281**(5): p. 2693-700.

135. Hiroshi Shiraishi, H.O., Akihiko Yoshimura and Hiroki Yoshida, *ER stress-induced apoptosis and caspase-12 activation occurs downstream of mitochondrial apoptosis involving Apaf-1.* Journal of Cell Science, 2006.
136. Maya Saleh, J.P.V., Rona K. Graham, Matthew Huyck,, et al., *Differential modulation of endotoxin responsiveness by human caspase-12 polymorphisms.* Nature, 2004. **429**(6987): p. 72-5.
137. Labbe, K., et al., *Caspase-12 dampens the immune response to malaria independently of the inflammasome by targeting NF-kappaB signaling.* J Immunol, 2010. **185**(9): p. 5495-502.
138. LeBlanc, P.M., et al., *Caspase-12 modulates NOD signaling and regulates antimicrobial peptide production and mucosal immunity.* Cell Host Microbe, 2008. **3**(3): p. 146-57.
139. Liu, B., Xia, X., Zhu, F., Park, E., Carbajal, S., Kiguchi, K., DiGiovanni, J., Fischer, S. M., Hu, Y., *IKKalpha is required to maintain skin homeostasis and prevent skin cancer.* Cancer Cell, 2008. **14**(3): p. 212-25.
140. Paxian, S., et al., *Abnormal organogenesis of Peyer's patches in mice deficient for NF-κB1, NF-κB2, and Bcl-3.* Gastroenterology, 2002. **122**(7): p. 1853-1868.
141. Madison, B.B., et al., *Cis elements of the villin gene control expression in restricted domains of the vertical (crypt) and horizontal (duodenum, cecum) axes of the intestine.* J Biol Chem, 2002. **277**(36): p. 33275-83.
142. Clausen, B.E., et al., *Conditional gene targeting in macrophages and granulocytes using LysMcre mice.* Transgenic Res, 1999. **8**(4): p. 265-77.
143. Moolenbeek, C. and E.J. Ruitenberg, *The "Swiss roll": a simple technique for histological studies of the rodent intestine.* Lab Anim, 1981. **15**(1): p. 57-9.
144. Hayden, M.S. and S. Ghosh, *Signaling to NF-kappaB.* Genes Dev, 2004. **18**(18): p. 2195-224.
145. Sun, S.-C., *The noncanonical NF-κB pathway.* Immunological Reviews, 2012. **246**: p. 125-140.
146. Shuji Kitajima, S.T.a.M.M., *Changes in colonic mucosal permeability in mouse colits induced with Dextran Sulfate Sodium.* Exp. Anim., 1999. **48**: p. 137-143.
147. Ben-Neriah, M.K.a.Y., *Phosphorylation Meets Ubiquitination: The Control of NF-kB Activity.* Annual Review of Immunology, 2000. **18**: p. 621-663.
148. Adli, M., et al., *IKKalpha and IKKbeta each function to regulate NF-kappaB activation in the TNF-induced/canonical pathway.* PLoS One, 2010. **5**(2): p. e9428.
149. Yixue Cao, G.B., F.R.G. Tiffany N. Seagroves, and E.V.S.a.M.K. Randall Johnson, *IKKα Provides an Essential Link between RANK Signaling and Cyclin D1 Expression during Mammary Gland Development.* Cell, 2001. **107**: p. 763-775.
150. Yan, Y., et al., *Temporal and spatial analysis of clinical and molecular parameters in dextran sodium sulfate induced colitis.* PLoS One, 2009. **4**(6): p. e6073.
151. Pizarro, B.K.R.a.T.T., *The role of the IL-18 system and other members of the IL-1R/TLR superfamily in innate mucosal immunity and the pathogenesis of inflammatory bowel disease: friend or foe?* Eur J Immunol, 2004. **34**(9): p. 2356-64.
152. Marcella Calfon, H.Z., Fumihiko Urano, Jeffery H. Till, and H.P.H. Stevan R. Hubbard, Scott G. Clark & David Ron, *IRE1 couples endoplasmic reticulum load to secretory capacity by processing the XBP-1 mRNA.* Nature, 2002. **415**.
153. Verfaillie, T., et al., *PERK is required at the ER-mitochondrial contact sites to convey apoptosis after ROS-based ER stress.* Cell Death Differ, 2012. **19**(11): p. 1880-91.
154. Watanabe, T., et al., *NOD2 is a negative regulator of Toll-like receptor 2-mediated T helper type 1 responses.* Nat Immunol, 2004. **5**(8): p. 800-8.
155. Yang, Z. and D.J. Klionsky, *Mammalian autophagy: core molecular machinery and signaling regulation.* Curr Opin Cell Biol, 2010. **22**(2): p. 124-31.
156. Komatsu, M., S. Kageyama, and Y. Ichimura, *p62/SQSTM1/A170: physiology and pathology.* Pharmacol Res, 2012. **66**(6): p. 457-62.
157. Lakatos, P.L., *Recent trends in the epidemiology of inflammatory bowel diseases: Up or down?* World Journal of Gastroenterology, 2006. **12**(38): p. 6102-6108.

158. Malin E. V. Johansson, J.K.G., Karolina E. Sjöberg, Joel Petersson, Lena Holm, Henrik Sjovall, Gunnar C. Hansson, *Bacteria Penetrate the Inner Mucus Layer before Inflammation in the Dextran Sulfate Colitis Model.* Plos One, 2010. **5**: p. e12238.
159. B Liu, J.W.-B., S Liu, X Chen, SM Fischer and Y Hu, *IKKalpha represses a network of inflammation and proliferation pathways and elevates c-Myc antagonists and differentiation in a dose-dependent manner in the skin.* Cell Death Differ, 2011. **18**(12): p. 1854-64.
160. Xiao, Z., et al., *The pivotal role of IKKalpha in the development of spontaneous lung squamous cell carcinomas.* Cancer Cell, 2013. **23**(4): p. 527-40.
161. Park, E., et al., *Reduction in IkappaB kinase alpha expression promotes the development of skin papillomas and carcinomas.* Cancer Research, 2007. **67**(19): p. 9158-68.
162. Goktuna, S.I., et al., *IKKalpha Promotes Intestinal Tumorigenesis by Limiting Recruitment of M1-like Polarized Myeloid Cells.* Cell Reports, 2014.
163. Greten, F.R., Eckmann, L., Greten, T. F., Park, J. M., Li, Z. W., Egan, L. J., Kagnoff, M. F., Karin, M., *IKKbeta links inflammation and tumorigenesis in a mouse model of colitis-associated cancer.* Cell, 2004. **118**(3): p. 285-96.
164. Yumi Yamamoto, U.N.V., Shashi Prajapati, Youn-Tae Kwak and R.B. Gaynor, *Histone H3 phosphorylation by IKKa is critical for cytokine-induced gene expression.* Nature Letters, 2003.
165. Sokolovska, A., et al., *Activation of caspase-1 by the NLRP3 inflammasome regulates the NADPH oxidase NOX2 to control phagosome function.* Nature Immunology, 2013. **14**(6): p. 543-53.
166. Martin, B.N., et al., *IKKalpha negatively regulates ASC-dependent inflammasome activation.* Nature Communications, 2014. **5**: p. 4977.
167. Rana Al-Sadi, D.Y., Karol Dokladny, and Thomas Y. Ma, *Mechanism of IL-1β-Induced Increase in Intestinal Epithelial tight junction permeability* J Immunol, 2008. **180**(8): p. 5653–5661.
168. H.C. Reinecker, M.S., T. Witthoeft, I. Pflueger, S. Schreiber, and R.P.M.A. Raedler, *Enhanced secretion of tumour necrosis factor-alpha, IL-6, and IL-1 beta by isolated lamina propria mononuclear cells from patients with ulcerative colitis and Crohn's disease.* Clin Exp Immunol, 1993. **94**: p. 174-181.
169. Dinarello, C.A., *Interleukin-18 and the pathogenesis of inflammatory diseases.* Semin Nephrol, 2007. **27**(1): p. 98-114.
170. P V Sivakumar, G.M.W., S Kanaly, K Garka, T L Born, J M J Derry, J L Viney, *Interleukin 18 is a primary mediator of the inflammation associated with dextran sulphate sodium induced colitis: blocking interleukin 18 attenuates intestinal damage.* Gut, 2002. **50**: p. 812–820.
171. Normand, S., et al., *Nod-like receptor pyrin domain-containing protein 6 (NLRP6) controls epithelial self-renewal and colorectal carcinogenesis upon injury.* Proc Natl Acad Sci U S A, 2011. **108**(23): p. 9601-6.
172. Siegmund, B., *Interleukin-18 in intestinal inflammation: friend and foe?* Immunity, 2010. **32**(3): p. 300-2.
173. Zhao, F., et al., *Disruption of Paneth and goblet cell homeostasis and increased endoplasmic reticulum stress in Agr2-/- mice.* Dev Biol, 2010. **338**(2): p. 270-9.
174. Brandl, K., et al., *Enhanced sensitivity to DSS colitis caused by a hypomorphic Mbtps1 mutation disrupting the ATF6-driven unfolded protein response.* Proc Natl Acad Sci U S A, 2009. **106**(9): p. 3300-5.
175. Masayuki Kaneko, Y.N., and Yasuyuki Nomura, *Activation Signal of Nuclear Factor-k B in Response to Endoplasmic Reticulum Stress is Transduced via IRE1 and Tumor Necrosis Factor Receptor-Associated Factor 2.* Biol. Pharm. Bull., 2003. **26**(7): p. 931-935.
176. Piao, J.H., et al., *Tumor necrosis factor receptor-associated factor (TRAF) 2 controls homeostasis of the colon to prevent spontaneous development of murine inflammatory bowel disease.* J Biol Chem, 2011. **286**(20): p. 17879-88.
177. Shkoda, A., et al., *Interleukin-10 blocked endoplasmic reticulum stress in intestinal epithelial cells: impact on chronic inflammation.* Gastroenterology, 2007. **132**(1): p. 190-207.

178. Levine, B., N. Mizushima, and H.W. Virgin, *Autophagy in immunity and inflammation.* Nature, 2011. **469**(7330): p. 323-35.
179. Adolph, T.E., et al., *Paneth cells as a site of origin for intestinal inflammation.* Nature, 2013. **503**(7475): p. 272-6.
180. Cadwell, K., et al., *Virus-plus-susceptibility gene interaction determines Crohn's disease gene Atg16L1 phenotypes in intestine.* Cell, 2010. **141**(7): p. 1135-45.
181. Lassen, K.G., et al., *Atg16L1 T300A variant decreases selective autophagy resulting in altered cytokine signaling and decreased antibacterial defense.* Proc Natl Acad Sci U S A, 2014.
182. Criollo, A., et al., *The IKK complex contributes to the induction of autophagy.* EMBO J, 2010. **29**(3): p. 619-31.
183. Criollo, A., et al., *Autophagy is required for the activation of NFkappaB.* Cell Cycle, 2012. **11**(1): p. 194-9.
184. Duran, A., et al., *The signaling adaptor p62 is an important NF-kappaB mediator in tumorigenesis.* Cancer Cell, 2008. **13**(4): p. 343-54.
185. Mathew, R., et al., *Autophagy suppresses tumorigenesis through elimination of p62.* Cell, 2009. **137**(6): p. 1062-75.
186. Fujita, E., et al., *Two endoplasmic reticulum-associated degradation (ERAD) systems for the novel variant of the mutant dysferlin: ubiquitin/proteasome ERAD(I) and autophagy/lysosome ERAD(II).* Hum Mol Genet, 2007. **16**(6): p. 618-29.
187. Yang, L., et al., *Defective hepatic autophagy in obesity promotes ER stress and causes insulin resistance.* Cell Metab, 2010. **11**(6): p. 467-78.

Appendix

A.1 Chemicals, Reagents & Kits

Chemical	Company	Catalog Number
Antigen Unmasking Solution	VectorLab	H-3300
ApoAlert (TUNEL)	Clontech	630107
Collagen type I	BD	354236
DAPI	Invitrogen	P36931
DNase	Roche	4716728001
dNTP mix	Invitrogen	18427-088
DSS	MPI	160-110
DTT	Sigma	43815
Eosin Y	Sigma	230251
Hematoxylin	VectorLab	H-301
Liberase TL	Roche	5401020001
mouse IL-18 ELISA kit	MBL	7625
mouse IL-1β ELISA kit	R&D systems	DY-401
Odyssey Infrared EMSA Kit	LI-COR	829-07910
oligo (dT) primer	Invitrogen	AM5730G
Paraformaldehyde	EMS	15710
Percoll	GE Healthcare	17-5445-02
Protein A sepharose beads 6MB	GE Healthcare	17-0469-01
QIAshredder kit	Qiagen	79656
recombinant mouse IL-18 protein	MBL	B004-5
RNaseOUT	Invitrogen	10777-019
RNeasy Mini kit	Qiagen	74104
Streptavidin/Biotin Blocking Kit	VectorLab	SP-2001
SuperScriptII Reverse Transcriptase	Invitrogen	18064-014
SuperSignal West Femto Substrate	Thermo Scientific	34095
SuperSignal West Pico Substrate	Thermo Scientific	34080
SYBR Green Master (Rox)	Roche	79656
VectaMount Mounting Medium	VectorLab	H-5000
VECTASTAIN Elite ABC kit	VectorLab	PK-6100

A.2 Genotyping of mice

***Cre* Genotyping PCR**

Primers 5'->3'	Temperature °C	Time (seconds)	Cycles
ACCTGAAGATGTTCGCGATTATCT	94	30	35
ACCGTCAGTACGTGAGATATCTT	58	30	
	72	30	

***Ikkα*$^{AA/wt}$ Genotyping PCR**

Primers 5'->3'	Temperature °C	Time (seconds)	Cycles
GGA TCC GAT ATC TGC ATG AAA AC	94	30	40
CAA TGT TCC CAC AAA CGC TGT ACA GAG CGC	58	30	
CAA TGT TCC CAC AAA AGA TGT ACA GAG ACT	72	90	

***Ikkα* floxed Genotyping PCR**

Primers 5'->3'	Temperature °C	Time (seconds)	Cycles
GGA ATT AGT TCT CCT CCT CTC ATA TGG	94	30	35
TTA AAT TGT TGA AAT ATC TGT AAA GGA AGG	58	30	
	72	30	

***Caspase-12* Genotyping PCR**

Primers 5'->3'	Temperature °C	Time (seconds)	Cycles
CAG CTG TTC CTG GGA ATT GGC AAT G	94	45	45
GCC AGG AGG ACA CAT GAA AGA GAT C	65	60	
GGG TGG GAT TAG ATA AAT GCC TGC TCT	72	60	

A.3 Antibodies

A.3.1 Antibodies used for western blot

Primary Antibodies	Conditions	Company	Catalog Number
ATG16L1	1:1000 3% BSA 4°C ON	AbCam	ab47946
BCL-2	1:1000 3% Skim milk 4°C ON	BD	610539
BCL-xL	1:500 3% Skim milk 4°C ON	BD	556499
BiP/GPR78	1:1000 5% BSA 4°C ON	Cell Signaling	3177
Caspase-12	1:1000 5% Skim milk 4°C ON	Cell Signaling	2202
Caspase-9	1:1000 3% Skim milk 4°C ON	Cell Signaling	9504
CHOP	1:1000 5% BSA 4°C ON	Cell Signaling	2895
COX2	1:500 3% Skim milk 4°C ON	Cayman	160106
GADPH	1:3000 3% Skim milk 4°C ON	Santa Cruz	SC-32233
IKKα/IKK1	1:1000 3% BSA 4°C ON	Novus Biologicals	IMG136A
IRE1α	1:1000 5% BSA 4°C ON	Cell Signaling	3294
LC3B	1:1000 3% BSA 4°C ON	Cell Signaling	2775
MMP-9	1:1000 3% Skim milk 4°C ON	Santa Cruz	SC-6840
NF-κB p65	1:1000 3% BSA 4°C ON	Santa Cruz	SC-372
p62	1:1000 3% BSA 4°C ON	Progene	GP62-C
pelF2α	1:1000 5% BSA 4°C ON	Cell Signaling	3398
pIκBα	1:1000 3% BSA 4°C ON	Cell Signaling	2859
pNF-κB p65	1:1000 3% BSA 4°C ON	Cell Signaling	3033
pPERK	1:1000 5% BSA 4°C ON	US Biologicals	P3346-01
TRAF2	1:1000 5% BSA 4°C ON	Cell Signaling	4724
β-actin	1:3000 3% Skim milk 4°C ON	Sigma	A4700

Secondary Antibodies	Conditions	Company	Catalog Number
anti-Rabbit IgG-HRP conjugated	1:5000 3% Skim milk 30 min RT	GE HealthCare	NA9340V
anti-Mouse IgG-HRP conjugated	1:5000 3% Skim milk 30 min RT	GE HealthCare	NA931V
anti-Guinea Pig-HRP conjugated	1:5000 3% Skim milk 30 min RT	Sigma	SC-2020

A.3.2 Antibodies used for IHC/Immunofluorescence

Primary Antibodies	Working Conditions	Catalog Number	Company
Cleaved Caspase-3	1:400 3% BSA/PBS 4°C ON	9661	Cell Siganling
F4/80	1:200 3% BSA/PBS 4°C ON	MF480043	Invitrogen
Anti-Mouse Ly-6G (Gr-1) APC	1:100 3% BSA/PBS 4°C ON	17-5931	eBiosciences

Secondary Antibodies	Working Conditions	Catalog Number	Company
Biotinylated anti-rat IgG	1:1000 3% BSA/PBS 1 hr RT	BA-9400	Vector
Biotinylated anti-rabbit IgG	1:1000 3% BSA/PBS 1 hr RT	BA-1000	Vector

A.3.3 Antibodies used for cell sorting

Antibody	Working Conditions	Catalog Number	Company
Anti-Mouse Ly-6G (Gr-1) APC	1:100 in PBS/5% FCS	17-5931	eBiosciences
Anti-Mouse CD45 FITC	1:100 in PBS/5% FCS	11-0451	eBiosciences
Anti-Mouse CD11b APC	1:100 in PBS/5% FCS	17-0112	eBiosciences
Anti-Mouse CD326 (EpCAM) eFluor® 450	1:100 in PBS/5% FCS	48-5791	eBiosciences
Fixable Vialbility dye eFluor® 780	1:1000 in PBS/5% FCS	65-0865	eBiosciences
Human Fc Receptor Binding inhibitor Purified	1:100 in PBS/5% FCS	14-9161	eBiosciences

A.4 Real-time PCR primers

Target	Forward 5'-> 3'	Reverse 5'->3'
BiP/GRP78	ACAAAAAGCTCAAAGAGCGCA	ACCTCCCAGCTTTTCTTTATCTCC
Caspase-11	TGG AAG CTG ATG CTG TCA AG	GAG CCT CCT GTT TTG TCT CG
Caspase-12	GTCCTCAGACAGCACATTCCTG	CGGTGCTTCACCCCACAG
Caspase-2	TGACAATGCTAACTGTCCAA	GTCTCATCTTCATCAACTCC
Caspase-7	GGATCCGAACGATGACCGATGATCAG	AAGCTTGTGAGCATGGACACCATAC
Caspase-8	GGCATCTGCTTTCCCTTGTTC	ATCTTACGACGACTGCACTGC
CCL2	GGC TCA GCC AGA TGC AGT TAA	CCT ACT CAT TGG GAT CAT CTT GCT
CHOP	CCT AGC TTG GCT GAC AGA GG	CTG CTC CTT CTC CTT CAT GC
CXCL1	GCCAATGAGCTG CGCTGT	CCTTCAAGCTCT GGATGTTCTTG
CXCL2	ATC CAG AGC TTG AGT GTG ACG C	AAG GCA AAT TTT TGA CCG CC
Cyclophilin B	ATGGTCAACCCCACCGTGT	TTCTGCTGTCTTTGGAACTTTGTC
GRP94	CGG TTT TTA TTC TGC CTT CCT TG	ATT ACA GAG AAT TCA TTG GAG TCT GAT TC
IL-18	GCCATGTCAGAAGACTCTTGCGTC	GTACAGTGAAGTCGGCCAAAGTTGTC
IL-1β	GTG GCT GTG GAG AAG CTG TG	GAA GGT CCA CGG GAA AGA CAC
IL-6	ATGGTACTCCAGAAGACCAGAGGA	GTATGAACAACGATGCACTTG
IRE1α	GCCCCGGGAGTTTTGG	GGGTCGAGACAAACAACAAGGT
IRE1β	TTCCGAGGACAGTTTGAGGG	TCGCCGAACCAAGCCA
TNFα	ACT CCA GGC GGT GCC TAT G	GAG CGT GGT GGC CCC T
XBP1spilced	GAA CCA GGA GTT AAG AAC ACG	AGG CAA CAG TGT CAG AGT CC

Publications

1) Serkan I. Göktuna, Özge Canli, Julia Bollrath, Alexander A. Fingerle, David Horst, Michaela A. Diamanti, Charles Pallangyo, Moritz Bennecke, Tim Nebelsiek, Arun K. Mankan, Roland Lang, David Artis, Yinling Hu, Thomas Patzelt, Jürgen Ruland, Thomas Kirchner, M. Mark Taketo, Alain Chariot, Melek C. Arkan and Florian R. Greten. '*IKKα Promotes Intestinal Tumorigenesis by Limiting Recruitment of M1-like Polarized Myeloid Cells*. Cell Reports 2014; 7.

2) Martina E. Spehlmann, Carolin F. Manthey, Sara M. Dann, Elaine Hanson, Sukhman S. Sandhu, Linus Y. Liu, Farid K. Abdelmalak, Michaela A. Diamanti, Kristin Retzlaff, JürgenScheller, Stefan Rose-John, Florian R. Greten, Jean Y. J. Wang and Lars Eckmann. '*Trp53 Deficiency Protects against Acute Intestinal Inflammation'*. Journal of Immunology 2013; 191:837-847.